

**EMPIRICAL RULES FOR DEBRIS FLOW TRAVEL DISTANCE:
A COMPARISON OF FIELD DATA**

by

Matthias Busslinger

B.Eng. in Civil Engineering,
HSR University of Applied Sciences Rapperswil, 2006

A THESIS SUBMITTED IN PARTIAL FULFILLMENT OF
THE REQUIREMENTS FOR THE DEGREE OF

MASTER OF APPLIED SCIENCE

in

The Faculty of Graduate Studies

(Civil Engineering)

THE UNIVERSITY OF BRITISH COLUMBIA
(Vancouver)

August 2010

© Matthias Busslinger, 2010

ABSTRACT

Assessment of debris flow travel distance is an essential part of landslide risk management. Confidence in applying empirical rules in conditions different from their original study area is generally small. This research provides a systematic, quantitative approach to assess the utility of an empirical-statistical tool (UBCDFLOW), originally developed for the Queen Charlotte Islands, in the Kootenay area with different geo-bio-climatic conditions.

High quality ground-based debris flow volume measurements are essential for this research. A systematic traversing method is described and illustrated for two example events. It is particularly useful to analyse volume change processes (entrainment, deposition), quantify volume magnitudes and examine travel distances. Data gathered can be used to compare debris flow inventories and run a variety of empirical or dynamic analysis tools.

Compared to the Queen Charlotte Islands (QCI) the Kootenay study area has different geo-bio-climatic conditions, with larger event magnitudes and travel distances. Similarities were found for dominant volume change processes as a function of slope angles. Average yield rates in the Kootenays (2 to $3\text{m}^3/\text{m}$) are significantly smaller than on the QCI (12 and $23\text{m}^3/\text{m}$). Applicability of UBCDFLOW in the Kootenay area is evaluated based on three quantitative measures for simulation success regarding volume change process, magnitude and travel distance. The empirical rules capture the volume change process (entrainment, deposition) correctly for 80% of the lengths in the Kootenay inventory and therefore appear to be portable from the QCI location. However the regression equations overestimate the magnitude of volume change. In total, 15 out of 22 simulations terminate within 89 and 110% of the observed travel distance; the remaining 7 simulations exceed it by more than 110%.

Concerns that UBCDFLOW is sensitive to variations in slope angle input ($\pm 2^\circ$) are addressed in a Monte Carlo type analysis. For 13 (of 22) events, simulation of process is found sensitive, and 11 (of 22) experience considerable uncertainty in volume estimation, which ultimately yields uncertainty of travel distance estimate. Based on

confidence limits for volume estimates and travel distance exceedance probability, the Monte Carlo simulation output allows more informed decision making.

TABLE OF CONTENTS

Abstract	ii
Table of contents	iv
List of tables	viii
List of figures	ix
Acknowledgements	xiii
Co-authorship statement	xiv
1 Introduction.....	1
1.1 Debris flow classification and terminology.....	1
1.1.1 Debris flow classification.....	1
1.1.2 Debris flow terminology.....	2
1.2 General debris flow risk management aspects.....	3
1.2.1 Landslides in a global perspective	3
1.2.2 Debris flow practices in British Columbia.....	4
1.2.3 Concept of risk.....	6
1.3 Quantification of spatial impact.....	8
1.3.1 Empirical tools	8
1.3.2 Mechanics-based tools	12
1.3.3 Instrumented laboratory and field studies	14
1.4 Scope and hypothesis	16
1.5 References.....	23
2 Field traversing of debris flow volumes.....	29
2.1 Outline.....	29
2.2 Traversing of debris flows in British Columbia.....	30

2.3	Objectives.....	31
2.4	Field traversing methodology	32
2.4.1	Recommended procedure	33
2.4.2	Discussion of procedure	35
2.5	Illustrative traverse examples.....	36
2.5.1	Blueberry Creek event	36
2.5.2	Hummingbird Creek event	37
2.6	Summary remarks	39
2.7	Acknowledgement	40
2.8	References.....	47
3	Utility of empirical-statistical rules from the Queen Charlotte Islands for debris flow simulation in the Kootenay Region	49
3.1	Outline.....	49
3.2	Introduction.....	50
3.2.1	Classification of debris flows.....	50
3.2.2	Concept of risk and spatial impact of debris flows	51
3.2.3	Empirical rules for debris flow travel distance.....	52
3.2.4	Methodology	57
3.3	Study areas and field investigation.....	58
3.3.1	Field investigation	58
3.3.2	Characteristic topographies, geologies, climates and vegetation	59
3.3.3	Logging and road construction methods.....	61
3.3.4	Landslide densities and frequencies.....	61
3.3.5	Characteristics of debris flow events.....	63
3.4	Findings from inventory examination.....	64

3.4.1	Processes	64
3.4.2	Debris flow magnitudes and yield rates	66
3.4.3	Travel distances.....	67
3.5	Simulation of the Kootenay inventory	67
3.5.1	The UBCDFLOW model	67
3.5.2	Quantitative simulation success indicators	69
3.6	Results of simulation	70
3.6.1	Simulation algorithm	70
3.6.2	Example volume balances	70
3.6.3	Key results of the Kootenay inventory simulation	72
3.7	Discussion.....	72
3.7.1	Patterns and attributes of inventories.....	72
3.7.2	Simulation vs. observation	75
3.8	Summary and conclusions	76
3.9	References.....	95
4	A sensitivity analysis to slope angle of debris flow volume change processes.....	99
4.1	Outline.....	99
4.2	Introduction.....	100
4.2.1	Sources of uncertainties in debris flow analysis.....	100
4.2.2	Study objectives.....	102
4.3	Methodology.....	102
4.3.1	Monte Carlo simulation	103
4.3.2	Simulation output	104
4.4	Results	106

4.4.1	Example events	106
4.4.2	Analysis of the Kootenay dataset.....	109
4.5	Discussion.....	110
4.6	Summary and conclusions	112
4.7	References.....	121
5	Conclusions and recommendations.....	123
5.1	Research objectives	123
5.2	Conclusions.....	123
5.2.1	Field traverse methodology.....	123
5.2.2	Utility assessment of empirical rules.....	124
5.2.3	Sensitivity analysis to slope angle	126
5.3	Recommendations	127
5.4	References.....	130
Appendix A:	Notes landslide inventory project.....	131
Appendix B:	Blank landslide profile data card.....	147
Appendix C:	Blueberry Creek data.....	148
Appendix D:	Hummingbird Creek data.....	150
Appendix E:	Simulation success indicators.....	152
Appendix F:	Data interpretation for simulation.....	155
Appendix G:	UBCDFLOW: step-like vol. estimates	158

LIST OF TABLES

Table 3.1	a) Kootenay inventory overview by event type. Total travel distance along path L, length of terminal deposition zone I and yield rate Y. b) QCI inventory overview by event type (data from Fannin and Rollerson 1993).	79
Table 3.2	Simulation results.	80
Table 3.3	Characteristic slope angles from literature.	81
Table 4.1	Simulation results.	113

LIST OF FIGURES

Figure 1.1	Flow chart for landslide risk management after Fell et al. (2005). © Taylor & Francis, AT Balkema, Amsterdam. Reproduced with permission.	20
Figure 1.2	Overview: Decision support tools for simulation of debris flow travel distance.....	21
Figure 1.3	Organization of thesis.....	22
Figure 2.1	Aerial view on initiation zone in clear-cut of Blueberry Creek debris flow..	41
Figure 2.2	Plot of mapped volume changes along the path. Bars; volume change in each reach (dV). Dashed line; cumulative volume. Labels are reach ends; 1 = point of termination.....	41
Figure 2.3	Reach 17-18 of Blueberry Creek; a reach of confined flow.	42
Figure 2.4	Orthophoto of Hummingbird Creek: Dashed line in zoom box indicates approximate centerline, numbers indicate reach ends. (Picture edited from: FORREX Compendium of Forest Hydrology and Geomorphology in British Columbia. In press).	43
Figure 2.5	Field personnel standing at head scarp of Hummingbird Creek debris avalanche.	44
Figure 2.6	Looking up from point 4 in the debris avalanche path.	44
Figure 2.7	Looking down from point 5. Debris avalanche enters confined channel of Hummingbird Creek (flow from right to left).....	45
Figure 2.8	Plot of mapped volume changes along the path. Bars; volume change in each reach (dV). Dashed line; cumulative volume. Labels indicate reach ends. Debris enters Hummingbird Creek at end of avalanche.	46
Figure 3.1	Location map: Queen Charlotte Islands on the coast of British Columbia and Kootenay study area in the interior. Points indicate location of weather/hydrometric stations.	82

Figure 3.2	Precipitation in Kootenays (Kaslo R.) is significantly smaller, with a considerable portion of snow, compared to QCI (Pallant Ck.). Runoff regime in Kootenays (Kaslo R.) is strongly related to snowmelt, whereas it is controlled by precipitation on QCI.....	83
Figure 3.3	Example of event type 1: Revelstoke (Bigmouth) 11. Solid line indicates path profile, bars are volume changes in each reach.....	84
Figure 3.4	Example of Type 1 event Revelstoke Bigmouth 11. a) from point 10, looking down the path of the open slope event. b) main deposit in reach 2-end (geomorphologist for scale).....	85
Figure 3.5	Example of event type 2: Airy Creek 3017. Solid line indicates path profile, bars are volume changes in each reach.....	86
Figure 3.6	Example of Type 2 event Airy Creek 3017. a) looking up into unconfined path (reach 14-15) before the flow becomes confined (mapper for scale). b) Looking down the path of the confined channel (reach 10-11), average width 15m.....	87
Figure 3.7	Example of event type 3: Blueberry Creek 2037. Solid line indicates path profile, bars are volume changes in each reach.....	88
Figure 3.8	Example of Type 3 event Blueberry Creek 2037. a) Photo taken from air. b) looking down the confined channel (from point 17).	89
Figure 3.9	Volume behaviour occurrence Kootenay.....	90
Figure 3.10	Volume behaviour occurrence QCI.	91
Figure 3.11	Schematic plan view of a debris flow path.....	92
Figure 3.12	Conceptual framework used in UBCDFLOW. Starting with an initial volume, flow behaviour and slope angle determine how the simulation changes volume along the path. The event terminates in the reach where the volume becomes zero.	93

Figure 3.13	Comparison of volume balance along the path for a) Type 1: Revelstoke (Bigmouth) 11, b) Type 2: Airy Creek 3017 and c) Type 3: Blueberry Creek 2037.	94
Figure 4.1	Flow chart for Monte Carlo simulation.	114
Figure 4.2	Looking up into the path of East Kootenay (Dewan) 5000 event. The event occurred on an open slope and traveled down on an unconfined path. ...	115
Figure 4.3	Simulation results East Kootenay (Dewan) 5000: a) dotted line = observed volume balance; grey solid lines = confidence limits; black solid line = mode of simulations; reach endpoints are indicated on top. b) histogram of simulated volumes at the observed point of termination. c) Probability of travel distance exceedance ($P_{Ex,i}$) along the path. d) Comparison of deterministic result and mode of Monte Carlo simulation.	116
Figure 4.4	Looking up into the lower part of the confined path of event Revelstoke Bigmouth 5 before terminal deposition started. Further above the event travelled through a gully in mature forest.	117
Figure 4.5	Simulation results Revelstoke Bigmouth 5: a) dotted line = observed volume balance; grey solid lines = confidence limits; black solid line = mode of simulations; reach endpoints are indicated on top. b) histogram of simulated volumes at the observed point of termination. c) Probability of travel distance exceedance ($P_{Ex,i}$) along the path. d) Comparison of deterministic result and mode of Monte Carlo simulation.	118
Figure 4.6	Photo taken from air on upper part of event Blueberry Creek 2037. The event initiated in a cut-block and entered a confined gully.	119
Figure 4.7	Simulation results Blueberry Creek 2037: a) dotted line = observed volume balance; grey solid lines = confidence limits; black solid line = mode of simulations; reach endpoints are indicated on top. b) histogram of simulated volumes at the observed point of termination. c) Probability of travel distance exceedance ($P_{Ex,i}$) along the path. d) Comparison of deterministic result and mode of Monte Carlo simulation.	120

Figure 5.1 Conceptual overview of overall success in simulation of Kootenay events using UBCDFLOW129

ACKNOWLEDGEMENTS

I wish to express my sincere gratitude to my research supervisor, Dr. Jonathan Fannin, for his continued guidance and kind support throughout the course of this study. His “big picture” perspective greatly influenced my way of thinking and seeking for truth in the world of science. I also wish to thank Dr. Peter Jordan, Research Geomorphologist from the Ministry of Forests and Range BC in Nelson, for kindly providing the Kootenay debris flow inventory and his kind inputs and clarifications on the data in several telephone conference calls and e-mails. I further want to thank Dr. Jonathan Fannin, Dr. Peter Jordan and Pat Kailey (PhD Candidate, University of Canterbury, NZ) for the valuable time we spent field traversing at Hummingbird Creek.

I am grateful for the valuable inputs of my supervisory committee member Dr. Elisabeth Bowman, senior lecturer at the University of Canterbury NZ. Her kind suggestions and constructive comments improved the manuscript.

My thanks are extended to the graduate students in the geotechnical and mining group for their friendship and encouragement. I'm thankful for all the contributions from faculty and graduate students during the geotechnical seminars.

I am very grateful for the Leica scholarship and financial support from Natural Sciences and Engineering Research Council (NSERC). I am thankful for the Faculty of Applied Science Graduate Award (UBC) and additional support by the Swiss Association for Road and Transportation Experts (VSS), Alfred und Bertha Zangger-Weber Stiftung, Hilfsgesellschaft in Zürich, August Weidmann Fürsorge-Stiftung, Familien Vontobel Stiftung, and the Gemeinnützige Gesellschaft Meilen.

CO-AUTHORSHIP STATEMENT

The content of this thesis comprises three proposed manuscripts (Chapters 2, 3, and 4, respectively). For the first manuscript (Chapter 2) on debris flow traversing I carried out the literature review and distilled a “best practice”. The recommendations are based on field traversing experiences at Hummingbird Creek and discussions with Dr. Peter Jordan (Ministry of Forest and Range BC). Dr. Peter Jordan provided the raw data set of the Kootenay debris flow inventory for the second manuscript (Chapter 3). I was responsible for novel revisions, characterization and data reduction. I performed the simulations and carried out the analysis and interpretation of results. The third manuscript (Chapter 3) addresses sensitivity of the simulation to variable slope angles. I performed the simulations and carried out the analysis and interpretation of results. Preparation of all three manuscripts, including the contents, figures and tables, has been solely my responsibility.

Dr. R.J. Fannin reviewed all the manuscripts, gave feedback on technical content, assisted with the formulation of my ideas, and made suggestions for clarity of presentation. Accordingly, Dr. R.J. Fannin is a co-author on all three manuscripts. In recognition of Dr. Peter Jordan’s kind provision of the Kootenay inventory, his mentoring during the Hummingbird Creek survey and his technical review of the manuscripts, he is included as a co-author of the first and second manuscript.

1 INTRODUCTION

Debris flows are one of the most devastating landslide sub-types. High flow velocities, significant impact forces and long travel distances make debris flows very destructive. Temporal prediction of events is very difficult and consequently prediction of spatial impacts is of particular importance in debris flow risk management. Spatial impact is governed by travel distance, from the point of origin down-slope to the point of terminal deposition.

This thesis addresses the simulation of debris flow travel distance using empirical-statistical rules. The introduction starts with a few important definitions. A global overview of landslides is followed by a brief summary of debris flow risk management practices in British Columbia, before giving a brief literature review of spatial evaluation of debris flow movement. Finally, the scope and hypotheses examined in this thesis are outlined.

1.1 Debris flow classification and terminology

1.1.1 Debris flow classification

Cruden and Varnes (1996) proposed a landslide classification based on the type of material and type of movement. Hungr et al. (2001) introduced a more detailed classification for flow-like landslides by material type, water content, velocity and special conditions: Flow-like landslides often begin as *debris slides*. Before internal distortion occurs, the initial volume starts to slide along a forming rupture surface, and then gradually develops a distorted flow- or avalanche-like character. *Debris flow* is defined as a very rapid to extremely rapid flow (typically 1 to 20m/s) of saturated non-plastic debris in a steep channel. A debris flow event may occur in a series of surges which are separated by flood-like intersurge flow. According to Hungr et al. (2001) the presence of lateral confinement helps to maintain flow depth and facilitates longitudinal sorting (i.e. coarser material in the front) and surge development. The channel carries surface water which is incorporated into the debris flow surges, yielding an increased water content. *Debris avalanche* is a very rapid to extremely rapid (typically 1 to 20m/s) shallow flow of

partially to fully saturated debris on a steep slope, without confinement in an established channel. While debris avalanches typically travel in a partially saturated state, they may enter creeks and mix with water and gradually become flow-like. To avoid confusion when referring to events in general, *the term debris flow is meant to be inclusive of landslides that would otherwise be classified as debris avalanches or debris slides*. For discussion of particular details of an event the terms slide or avalanche may be used. *Debris flood* is a very rapid, surging flow of water, heavily charged with debris, in a steep channel with flow velocities similar to a water flood. Strictly, a debris flood is not a landslide but a mass transport phenomenon.

In contrast to these rather phenomenological descriptions, Iverson (1997) describes debris flows from a mechanical point of view: debris flows occur when masses of poorly sorted sediment, agitated and saturated with water, surge down slopes in response to gravitational attraction. Both solid and fluid forces vitally influence the motion, distinguishing debris flows from related phenomena such as rock avalanches (mainly solids) and sediment-laden water floods. Debris flows are largely saturated with water but differ from surging water floods in which sediment is held in suspension almost exclusively by fluid mechanical phenomena (e.g. viscous drag, buoyancy, turbulences). At the opposite extreme, debris flows have solid concentrations (i.e. void ratio) comparable to those of rock avalanches. But in rock avalanches the grains interact almost exclusively through solid-contact phenomena (e.g. collisions, adhesion, friction), perhaps mediated by inter-granular air. The degree of solid-liquid interaction may vary between debris flows (Iverson, 2005).

1.1.2 Debris flow terminology

Cruden and Varnes (1996) described *debris* as an aggregate of solid particles, generally of soil, rocks, and organic material, that contains a significant proportion of coarse material; 20 to 80% of the particles are larger than 2mm, and the remainder are less than 2 mm. Hungr et al. (2001) defined debris as loose unsorted material of low plasticity that may contain a significant portion of organic material such as logs, tree stumps and organic mulch.

The term *entrainment* refers to a process adding volume (or mass) to a debris flow event, whereas *deposition* describes a process of volume loss. Volume change process or simply process is used to refer to entrainment or deposition of material along the path of an event. In this thesis, processes are generally analyzed as net volume changes of entrainment or deposition. In order to describe reaches wherein both entrainment and deposition occur and play a significant role, the term *dual-mode of flow* is used (cf. Fannin and Wise, 2001). According to Hungr et al (1984), debris flow *magnitude* is defined as total volume transported into the terminal deposition zone. Spatial impact of debris flows depends on the volume change processes along the path, rather than the runout distance of a released mass (e.g. rock avalanche). The term runout distance, is therefore avoided in this thesis. Instead the term *travel distance* is used, referring to the distance along the path between point of origin and end of terminal deposition.

1.2 General debris flow risk management aspects

1.2.1 Landslides in a global perspective

In some countries, socioeconomic losses due to landslide activity are great, and apparently growing, as human development expands into unstable hillslope areas under the pressure of increasing populations. The United States leads other American nations in economic losses with estimated total annual losses (direct and indirect) of about US\$2 billion per year (Schuster and Lynn, 2001).

There is little doubt that global inventories on fatalities caused by landslides greatly underestimate the impact of landslides, mainly because disasters are often classified by trigger (e.g. earthquake, storm precipitation) rather than mechanism (e.g. debris flow, rock fall). Therefore the International Landslide Centre initiated a global landslide data base, which has identified the following patterns (Petley et al., 2005): In terms of fatalities, landslide disasters are focused upon less economically developed countries especially in mountainous regions experiencing tropical cyclones and monsoons. A majority of rainfall-induced landslides occur in China and South Asia during the northern hemisphere summer. A second peak occurs in the annual cycle during December and

January as heavy rains induce extensive landslides along the Indonesian archipelago. The annual number of global landslide fatalities probably exceeds 5000 per annum.

In the extreme, 20,000 fatalities occurred in the 1970 Huascarán debris avalanche in Peru, approximately 25,000 people died in the 1985 Nevado del Ruiz debris flow disaster in Colombia, and as many as 30,000 people were killed as a result of the 1999 landslides and floods in northern Venezuela (Schuster and Lynn, 2001).

These extreme numbers of landslide fatalities should not mislead from the fact that in many areas the landslide subtype debris flows is a high-frequency low-magnitude phenomenon. The focus of this thesis addresses the latter case, namely the many small events that occur, through data for the steep forest-landscapes in British Columbia.

1.2.2 Debris flow practices in British Columbia

In their historical perspective on terrain stability mapping in British Columbia forest lands, Schwab and Geertsema (2010) report an increase in landslide frequency from roads, and within cut-blocks, after forest harvesting advanced onto relatively steeper slopes, in the 1970s. In response, the BC Forest Practices Code was introduced in 1995 (Fannin et al., 2005). The code demanded safe, productive and environmentally sound forest management practices in landslide-prone terrain and accordingly the Terrain Stability Mapping (TSM) method (BCRIC 1996) was developed. The Forest Practice Board (2005) examined the influence of TSM guidelines and found that fewer landslides occurred after the code was implemented, although forest development activities still caused higher numbers of landslides than occurred in unlogged terrain. TSM is somewhat narrowly focused on the hazard of landslide initiation. Polygons are rated for the likelihood of landslide initiation, but not the likelihood of landslide impact and related consequences.

Jordan (2003) compiled a landslide inventory and conducted a terrain attribute study between 1996 and 2002 in the Nelson Forest Region of south-eastern BC. The purpose of the study was to compile data on landslide frequency and to investigate landslide causes. Using statistical regression in a Geographic Information System (GIS), he determined statistical relations between landslide frequencies and terrain attributes. To analyse development-related landslides, polygons consisting of cut-blocks, roads and

areas down-slope from them were mapped. Landslide frequency increased 4 to 9 times as a result of forest development. Most development-related landslides (i.e. 80%) in the Nelson Forest Region are due to roads (fill failures, drainage diversion). Jordan found that terrain categories, such as the glaciofluvial and kame category, and the deep morainal category, are significant factors for distributions of landslides. Hence, Terrain Stability Mapping is a useful tool for predicting development related landslide hazard.

The BC Forest Practices Code introduced mandated that forest development activities occurred within “prescriptive” rules. If forest companies followed those rules they were normally able to transfer some or all of the liability for damage that might occur to forest resources. Instead, the BC government, in specifying mandatory practices, assumed some or all of this liability whenever practices had been correctly followed. In 2004 the legislation moved away from the “prescriptive” plan based regulation of the BC Forest Practices Code, to the results-based legislation of the current BC Forest and Range Practices Act (BCMOF, 2004; Fannin et al., 2005). Forestry activities must not cause a landslide, gully process or fan destabilisation that has a material adverse effect on soils, visual quality, timber, forage and associated plant communities, water, fish, wildlife, biodiversity, recreation resources, resource features, or cultural heritage resources. Terrain stability professionals are expected to ensure that licensees mitigate the potential effects of landslides effectively. Guidelines for terrain stability assessment in the forest sector, prepared by the Joint Practices Board (JPB, 2009) of Association of British Columbia Forest Professionals (ABCFP) and Association of Professional Engineers and Geoscientists of British Columbia (APEGBC), require terrain stability professionals carry out a partial risk analysis and evaluate existing and potential effects of forest development on slope stability.

Over the last few decades more infrastructure and residential development has encroached on zones endangered by landslide hazards. While simple avoidance of landslide prone terrain may be an appropriate management practice in the forest industry, public safety in urban areas depends on a detailed assessment of consequences of potential landslides. Land-use zonation in association with urban planning requires a rigorous landslide hazard assessment and landslide risk assessment (APEGBC, 2008).

Estimating the likely event magnitude (e.g. volume in terminal deposition area) of a future event is very difficult, because reliable historical records are often rare and data gathering is costly. Debris flow magnitudes are a function of the travel distance of an event and the volume change processes along the path (Hungri et al., 2008; Hungri, 2005). Jakob et al. (2005) point out that debris flow magnitude further depends on the recharge rates of a basin, and also supply limits in the path (e.g. shallow bedrock in channel). A good example of frequency-magnitude estimations for land development planning in a debris flow threatened area of British Columbia was presented by Jakob and Friele (2010). Their study on the Cheekye fan includes stratigraphic analyses combined with radiometric dating and dendrochronology to reconstruct a comprehensive picture of Holocene debris-flow activity as well as analysis of hydrological constraints. A mechanics-based model (DAN3D) for debris flow simulation is used to verify the distribution of volume estimates from stratigraphic analysis. However, frequency-magnitude relationships are difficult to establish because of post-event volume alterations and difficulties in event dating. Additionally, conditions (e.g. climate, seismic activity) in the future may differ from those in the sampling period. Nevertheless, frequency-magnitude relationships are fundamental in decision making in any natural hazard risk assessment.

1.2.3 Concept of risk

Effective management and mitigation of landslides require a framework for action, given by the concept of risk. Traditionally landslide risk assessment and management was typically carried out using “engineering judgment” by geotechnical engineers and engineering geologists. The management principles evolved from qualitative hazard zoning for urban planning (since 1970’s) into more quantitative methods in the 1990’s (Fell et al., 2005). In a very broad sense, risk could be explained as any undesirable effect. Wise et al. (2004) describe the concept of risk applied to forest development planning and operation in British Columbia. In its most simple form, risk (R) can be defined as the product of the probability of occurrence (P) and consequence (C):

$$[1] \quad R = P \cdot C$$

The specific risk $R(S)$ is the risk of loss or damage to a specific element, resulting from a specific hazardous landslide. Specific risk is mathematically expressed as:

$$[2] \quad R(S) = P(H) \cdot P(S:H) \cdot P(T:S) \cdot V(L:T)$$

Corresponding to Eq.1, $P(H)$ represents the probability of occurrence, whereas the remaining terms define the consequence. In more detail, $P(H)$ is the probability of occurrence of a specific landslide and that landslide being a hazard to an element. It is only a measure of hazard, and not risk, as it does not consider the effects of the landslide on an element. $P(S:H)$ is the probability that there will be a spatial effect, given that a specific hazardous landslide occurs. For example, in forestry risk analysis, this is the probability that an event will reach a fish habitat or a road. $P(T:S)$ is the probability that there will be a temporal effect, given that there is a spatial effect: For example, a fish habitat like a creek is permanent and accordingly the temporal probability is 1, however a truck driving on a road is a mobile element and the resultant probability is between 0 and 1. $V(L:T)$ is the vulnerability of an element, conditional on the element being at the site at the time of landslide occurrence. Taking for example a timber stand as element at risk, the vulnerability could be the probability of resource loss or damage.

Fell et al. (2005) discuss quantitative landslide risk management and provide a useful summary of general terminology. The risk management process is schematically outlined in Figure 1.1. The process starts with defining the scope and goal of risk management. Hazard analysis involves characterising the landslide (type, size, velocity, mechanics, location, travel distance) and the corresponding frequency (annual probability) of occurrence. Risk analysis looks at findings of the hazard analysis and combines it with a consequence analysis. Consequence analysis includes identifying and quantifying the elements at risk (e.g. property, infrastructure, persons), the temporal spatial probability (i.e. time exposure) and the vulnerability. Vulnerability is formulated either as conditional probability in the case of property damage, or as conditional probability of loss of life or injury. Risk assessment takes the outputs from a risk analysis and assesses them against value judgments and risk acceptance criteria. Risk management takes the output from risk assessment and looks at risk mitigation within the context of acceptable risk. Risk can be lowered by reducing the likelihood (e.g.

hazard zoning), or reducing the consequences (monitoring, warning, evacuation plans). Risk mitigation plans are established and implemented, risk outcomes are monitored and the feedback is used for further iterations in the risk management process. The iterative process should be updated periodically as more data become available. Landslide risk management involves a number of stakeholders including; owners, occupiers, affected public and regulatory authorities, geotechnical professionals and risk analysts. It is an integral part that estimated risks are compared to acceptance criteria. Geotechnical professionals are likely to be involved as risk analysts and may provide guidance, but do not define acceptable risks. Ultimately owners, regulators and governments decide whether calculated risks are acceptable or mitigation is required.

1.3 Quantification of spatial impact

Prediction of the spatial impact of debris flows (i.e. travel distance) is an essential part of the risk analysis. In land development and urban planning, various decision support tools are used to delineate hazard maps. In forestry risk management, estimation of debris flow travel distance is important for safety reasons (e.g. access roads, timber harvesting in steep terrain) or assessment of environmental impacts. A typical task is to establish if a debris flow, initiated by forestry activities, will reach a creek and damage fish habitat or reduce water quality. A wide portfolio of decision support tools for debris flow travel distance has been developed over the last few decades. This section gives an overview of the tools available. There are three main approaches to estimate travel distance of debris flows; empirical tools, primarily mechanics-based tools and instrumented field or laboratory studies (Figure 1.2). Each category has its own benefits and disadvantages.

1.3.1 Empirical tools

Empirical tools can be divided into three main categories; angle of reach models, area inundation models and mass or volume balance models (Figure 1.2). Angle of reach models use the total vertical distance h , between point of origin and end of deposition, and the empirically derived angle of reach α , to estimate the maximum horizontal travel distance l , where α is defined as:

$$[3] \quad \alpha = \arctan \left(\frac{h}{l} \right)$$

Scheidegger (1973) related α to the landslide volume and found that events with larger volumes travel further than smaller events. Corominas (1996) and Rickenmann (1999) compiled large inventories and proposed equations using volume and α for estimation of debris flow travel distance. Prochaska et al. (2008) apply the same principle but instead of using a point of origin as a reference point, they use a point midway down the path. These models are very easy to use but are gross simplifications of reality and yield a large variability. They rely on total volume of an event. Unlike other landslide types, volume magnitudes of debris flows are a function of the volume change processes along the path of an event. Rickenmann (1999) compared various angle of reach models and concluded that most of these relations can only give an order of magnitude estimate of some debris flow parameters, but that they cannot provide an accurate prediction of these values. Nevertheless, angle of reach methods are sometimes applied in preliminary risk assessments.

Inundation area models are based on the research by Iverson et al. (1998), who introduced semi-empirical equations to predict inundated valley cross-sectional areas (A) and planimetric areas (B) as functions of lahar volume (V) in the form of power laws:

$$[4] \quad A = \beta_A \cdot V^{2/3}$$

$$[5] \quad B = \beta_B \cdot V^{2/3}$$

Several researchers expanded the concept by using different β -coefficients to adapt the regression equations for debris flows. These regression equations are implemented into GIS applications using digital elevation models (DEM) to delineate inundation areas (Griswold and Iverson, 1998; Berti and Simoni, 2007; Scheidel and Rickenmann, 2010). The models require inputs like topography (DEM), regression coefficients, volume to be deposited (V), and a starting point for onset of deposition. The cross-sectional area A and the total inundated area B are derived using volume and empirical β -coefficients in Eq. 4 and 5. The area of interest is divided into elements and the flow of volume is routed through the cells. For every step in the flow routing procedure cells are filled up until the sum of their cross-sectional areas reaches A. Subsequently, the planimetric

area of the inundated cells is calculated. The flow is then routed into the next step, until the sum of planimetric areas of all inundated cells reaches the total planimetric area B. The inundated cells define a polygon of the depositional area of an event. Unfortunately these models are often limited by low resolutions of the DEM. However, GIS implementation makes these tools attractive for delineation of risk zones in land use planning.

Mass or volume balance approaches form another group of empirical tools. These tools account for volume change along the path of an event. Unlike dynamic models, empirical tools neglect the rheology of debris flows and instead use parameters like geometry or morphology that are easier to obtain. Hungr et al. (1984) introduced the yield rate concept. Yield rate (Y) is the rate of volume change per unit length. The magnitude (M) of a potential debris flow to be modeled is the volume transported into the terminal deposition zone, comprising the initial landslide volume ($V_{initial}$), any point sources (V_{point}) from any tributary landslides and the sum of a characteristic (i.e. constant) yield rate multiplied by the length along the entire entraining channel (Hungr et al., 2005):

$$[6] \quad M = V_{initial} + \sum V_{point} + \sum_{i=1}^n Y_i \cdot L_i$$

The magnitude divided by a typical deposition thickness gives the size of depositional area. Benda and Cundy (1990) proposed another empirical model to predict debris flow travel distance using empirically derived, constant yield rate (i.e. $8\text{m}^3/\text{m}$) for entrainment. Their model assumes deposition for slope angles gentler than 3.5° . Sharp channel bends are assumed to cause momentum loss. For slope angles between 3.5 and 20° deposition is assumed if the tributary junction angle (i.e. change in azimuth between previous and actual reach) is greater than 70° . Based on 26 debris flow events in Hawaii, Cannon (1993) proposed a single regression equation to predict deposition using an initial volume equal to scar volume, segment length, lateral confinement (i.e. radius of flow channel) and slope gradient. Starting with an initial volume the rate of volume change is calculated reach by reach in flow direction and termination is assumed where the flow volume reaches zero. Cannon's model accounts for deposition only, with a variable yield rate.

Fannin and Wise (2001) used a large debris flow inventory (449 events) from the Queen Charlotte Islands and proposed an empirical-statistical tool (UBCDFLOW) to simulate travel distance and flow volumes. The flow path is divided into reaches with uniform properties. Input parameters are initial volume, morphology (confined, unconfined and transition), slope angle, reach length, width, path azimuth. Termination is assumed at the end of the reach wherein the flow volume becomes zero. The model by Fannin and Wise (2001) is based on a much larger inventory than the other volume-based approaches discussed above. Three types of morphology characterize lateral confinement. Based on slope angle and morphology one of five regression equations is selected to quantify volume change processes. A bend-angle-function accounts for momentum loss in channel bends. UBCDFLOW accounts for entrainment and deposition with variable yield rates.

Empirical tools bring several advantages. Primarily, they are based on field evidence. Second, they are often very simple to use, requiring only a few input parameters. No speculation has to be made on rheology or boundary conditions. However, this also limits empirical tools to conditions similar to the origin of the data used for model development. Jakob et al. (2005) highlight that most empirical-statistical decision support tools for travel distance simulation (e.g. Fannin and Wise, 2001; Benda and Cundy, 1990; Cannon, 1993) neglect channel recharge rates. A debris flow occurring one year after the most recent event would have had the same predicted volume as its predecessor. Clearly, actual volumes will be significantly lower since the channel will likely have been scoured clear of debris by the earlier event. In a narrow sense these empirical-statistical models are therefore only applicable where debris-flow channels are in approximately the same state of recharge as the sample of channels used to develop the predictive model. This argument is logical but impractical, as an analysis is only carried out for the case that a basin has been recharged. A scenario of an event in a basin that has been recently discharged is of little practical significance. However, in supply-limited basins, both the timing and magnitude of debris flows depend on elapsed time, which in turn determine the recurrence interval for a given magnitude of event. This implies that calculated encounter probabilities as described by McClung (1999) will

lead to overestimates, especially when a debris flow has recently occurred in a supply-limited basin.

Larger debris flow inventories (e.g. more than 30 events) allow application of statistical methods (e.g. regression analysis) to establish rules regarding debris flow travel distance. However, it is difficult and costly to gather large, high quality inventories. Therefore landslide inventories are often built from remotely sensed data (e.g. air photo interpretation). Ground based observations (e.g. field traversing) require more effort but bring significantly higher quality and resolution. Regardless, one of the main challenges is caused by local patterns in the data sets. Within a small region debris flows may behave quite similarly (small variability) but often not enough data are available to establish rules. Using data from other regions (e.g. nearby mountain ranges) obviously increases the number of data points, however it often increases the variability for the combined dataset as well. Higher variability consequently reduces the significance of the rules. Experience from snow avalanches shows that a separate data set may be needed for each mountain range (McClung, 2000).

1.3.2 Mechanics-based tools

In addition to empirical tools, mechanics-based models have been developed over the last three decades. Increased computational efficiency has allowed development of complex models. Ironically, while mechanics-based tools use physical laws to simulate debris flows, many of the parameters required to run the models are calibrated or derived from empirical methods. This thesis focuses on empirical tools, but for the sake of completeness a brief overview about mechanics-based models is given here.

Mechanics-based approaches can be roughly divided into center of mass models and continuum based models (Figure 1.2). Center of mass or sliding block models reduce the debris flow to a single point of mass and solve the problem for velocity and travel distance (Heim, 1932; Scheidegger, 1973; Hungr et al., 2005).

Continuum mechanics models assume the debris flow as a deformable body. The interaction between solids and solids, solids and fluids and their interaction with boundaries is complex. Models can be categorized by the number of phases considered. Hungr (1995) simplifies the problem using lumped rheologies, whereas

Iverson (2005) separates stress contributions from solids and fluids. Hungr (1995) proposed the dynamic analysis model (DAN) using a Lagrangian algorithm to solve equations of motion for a variety of lumped rheologies. The model can be calibrated by modification of rheology parameters to obtain the best simulation of observed bulk behaviour of an event. Lumped rheologies have traditionally been used in various snow avalanche simulations and are appealing for their mathematical simplicity. A common type of model (Hungr, 1999; Gamma, 2000) has been adapted from snow avalanche simulations (Voellmy, 1955). Flow resistance is considered in two different terms. The first is basal friction and the second is a term accounting for drag due to turbulence. While general consensus exists for basal friction, turbulence drag is debated amongst experts; some (e.g. Iverson, 2005) argue that high solids concentrations suppress turbulence in debris flows. Goodings (1984) stated that in order to develop pore pressures, the flow regime must be laminar from a soil mechanics point of view. It seems possible that turbulent flow might theoretically occur at the debris flow front, however due to large particle sizes the debris is not saturated and consequently no positive pore pressures can occur. Resistance parameters in lumped rheology models are commonly calibrated by back-calculation of previous events and a variety of literature reports on calibration experience (Hungr and Evans, 1996; Koerner, 1976). However, Perla et al. (1980) point out that calibration success depends on the combination of friction parameters, rather than their absolute value.

Instead of using lumped rheologies, Iverson (2005) argues for an approach using representative volume elements (containing large numbers of solids and intergranular muddy fluid). He solves the problem using separate stress contributions of solids and fluids and their interaction. In principle the models are driven by gravity. Gravitational forcing is not necessarily constant, but depends on vertical velocity changes due to terrain breaks. For 2- and 3-D simulation, motion in horizontal directions is driven by stress gradients arising from reaction to gravitational forcing. Mass conservation as well as momentum conservation is used to solve for travel distance and velocity. Iverson (2005) theoretically accounts for mass changes due to erosion and deposition but neglects them in application, pointing out that more research is needed to appropriately account for external forces involved with mass change processes. He further argues

(see also Iverson, 2003) that separating the stress contributions facilitates the use of “standard testing” of each phase (fluid and solids), whereas no protocol exists to test rheologies of mixtures (i.e. lumped rheologies). The main fluid solid coupling parameter may be captured by the permeability tests used in soil mechanics. Separating stress contributions allows analysis of stress evolution.

Discrete particle models simulate “single discrete solids” in fluids. The benefit of discrete particle models is that the interaction between solids and fluid are calculated from so called “first principles” of physical laws. Such models require high computational power and are currently not popular in practical applications. However, more research and higher computational power may advance the development of discrete particle models in the future (Iverson, 2005).

In general, mechanics-based tools bring the advantage of a velocity output which is useful to estimate, for example, impact pressures on infrastructure or defensive works. In contrast to empirical tools, they are not area specific. While empirical tools are based on relatively large sets of direct field observations (high degree of experience) they are valuable in the area they are developed in, but their utility in different settings may be limited. Mechanics-based models are transferable between sites; however selection of the applicable rheology and corresponding resistance parameters is crucial and very complex. As mentioned above, back-calculation of a few events is often used to calibrate the models. Considering the intrinsic variability between single debris flow events such procedures require very careful evaluation. Nevertheless, mechanics-based tools are commonly used in practice. Clearly more research is needed to guide characterization of debris flow rheology and calibration procedures.

1.3.3 Instrumented laboratory and field studies

Field observations of debris flow events occurring are relatively few. Laboratory tests can aid our understanding of the mechanics of debris flows. In particular, parametric studies can be undertaken with relative ease in flume studies, helping to explain the significance of field observations (Fannin and Bowman, 2007). Laboratory studies offer a way to understand better and characterize the rheological behaviour of debris flows (O’Brien and Julien, 1988). They are commonly carried out at reduced scale, and

scaling laws have to be applied to extrapolate to field conditions. Laboratory studies are conducted for design of complex deflection dams, hydraulic structures, catchment basins or to verify numerical models. McDougall and Hungr (2004) used a laboratory scale model to verify a three dimensional extension of the DAN model. Iverson et al. (1992) carried out large scale flume tests in Oregon using a reinforced concrete channel 95 meters long, 2 meters wide, 1.2 meters deep that slopes 31 degrees. Up to 20 m³ of sediment can be released into the flume. Results were used to test and develop mathematical models, for interpreting and forecasting debris-flow behaviour and to develop improved technologies for mitigating the destructive effects of debris flows. Measured stresses at the base of debris flows changed rapidly, and the relative magnitude of stress fluctuations increased as the area of the measurement surface decreases. This indicates that individual grains or groups of grains and adjacent fluid interact dynamically with the flow boundary, and probably with one another. Measured basal fluid pressures indicated that heads of debris flow surges generally lack much fluid pressure, whereas the finer-grained tails of surges were nearly liquefied by high fluid pressure. Interior fluid pressures remained at near-liquefaction levels even during deposition, indicating that deposition results mainly from resistance at flow heads and margins (Iverson 1997).

Jordan (1995) investigated 25 debris flow events in the southern Coast Mountains of British Columbia. Field evidence suggested that fine-textured debris flows from Quaternary volcanic complexes were much more mobile than those originating in coarse-textured plutonic rocks. To verify these findings a flume was built; 4.9m long, and 95mm wide at the base with 60° side walls. Samples of about 20 litres were released down the flume. Observations showed that coarse-grained flows tend to have a clast supported surface layer and deposits are irregular in thickness. Fine-textured, volcanic-source, materials have no surface layer and deposit in generally uniform thickness. Accordingly Jordan recommends a Bingham flow model for simulation of fine-textured flows and a granular, or dilatants flow model for coarse-grained events. A clay content of about 4% in the matrix (sub-4mm) is a useful measure to distinguish between the two populations. Jordan further identified permeability of the debris and hence the rate of

consolidation to be important in controlling mobility. Volume of debris flow events was found to be the most significant factor controlling spatial impact.

Bowman et al. (2010) modelled volume change processes of debris flows in a geotechnical centrifuge at the Swiss Federal Institute of Technology (ETHZ). Experiments with unconsolidated material flowing over fixed and erodible bases verified previous observations that debris flow behaviour is governed mainly by friction and consolidation processes. The pioneering work in centrifuge testing by Bowman et al. (2010) showed that contact-dominated behaviour (Savage number) and high pore pressures (Pore pressure number) are closer to field scale observations compared to 1g flume experiments. Accordingly, centrifuge testing has the potential to complement experimental 1g studies.

Instrumented field studies measuring dynamic properties of natural debris flows in the field offer rare insights into debris flow behaviour. For example the channel of the Illgraben catchment, in south-western Switzerland, experiences several debris flows per year. The channel has been instrumented to monitor debris flows (McArdell et al., 2007). Their study confirmed the idea that excess pore-fluid pressures exist over considerable periods of time in debris flows, and therefore contribute to their mobility.

1.4 Scope and hypothesis

Debris flows are a highly mobile and very destructive subtype of landslides. While landslide risk management in the BC forestry sector focused on landslide hazard and avoidance of landslide prone terrain, recent work emphasizes more on consequences. Temporal occurrence is difficult to predict and therefore assessment of spatial impact becomes an essential part of debris flow risk management. In a quantitative risk assessment, estimation of debris flow travel distance is commonly done using either empirical or mechanics-based tools for decision support.

Empirical rules are relatively simple to use and often require only a few input parameters that can be measured in the field or obtained from a desk study. In contrast to mechanics-based tools, no speculation has to be made on rheologies and boundary conditions. Rheologies and boundary conditions are implicitly given by the data origin

used for model development. Flow behaviour is believed to be determined by terrain characteristics (e.g. slope angle, morphology). Therefore empirical decision support tools only apply in conditions similar to their origin. But should empirical rules just be limited to their original study area? Rickenmann (2005) states that experience in applying empirical-statistical methods in different settings is still limited; however potential exists for applying them in preliminary hazard assessments. The intended contribution of this research is to provide a quantitative approach to assess the utility of an empirical-statistical tool in conditions that differ from its original study area.

Figure 1.3 shows the conceptual organization of this thesis. The thesis is manuscript-based and contains an introduction and three manuscript chapters followed by a concluding chapter:

- The introductory chapter gives a global overview of landslides, followed by a more detailed description of debris flow practices in the British Columbia forestry sector. The concept of debris flows risk management is briefly introduced. Relevant research on prediction on the spatial impact of debris flows (e.g. travel distance, inundated area) is summarized, with an emphasis on empirical and mechanics-based tools for decision support. Empirical tools using a volume balance approach to simulate debris flow travel distance evolved from a simple yield rate approach (Hunggr et al., 1984). Benda and Cundy (1990) considerate slope angles and channel bends together with a constant yield rate. Using multiple regression analysis to account for initial volume and path confinement, Cannon (1993) proposed a relation for variable rates of deposition. Fannin and Wise (2001) applied multiple regression analysis accounting for initial volume, length, width, slope, morphology and azimuth, to propose five regression equations accounting for variable rates for entrainment and deposition. Whereas these empirical tools are very useful in the original study area, their utility in different regions needs to be tested. As outlined below, this thesis addresses characterization and comparison of study areas, the portability of empirical-statistical rules and the sensitivity of these rules.
- Good quality field data are crucial for testing the utility of empirical rules. Landslide inventories are most often compiled primarily on the basis of remote

sensing (e.g. airphotos). Ground-based data collection from field traverses offers much more detailed insights into debris flow behaviour. A systematic approach to traverse debris flows in the field is essential to assure good data quality and facilitate comparison between events or inventories. Over the last few decades several versions of 'Landslide Profile Data Cards' for debris flow traversing evolved in the British Columbia forestry sector. However no attempt was made to describe the methodology. Chapter 2 is a concise description of the BC traversing method. The BC traversing method is a descriptive, quantitative characterization of debris flow events with reference to volume change along the path. It facilitates characterization of volume change processes, magnitude and travel distance.

- The following hypothesis is tested in chapter 3; within certain limitations, empirical-statistical rules for debris flow travel distance simulation can be applied in conditions different from the original study area. Fannin and Rollerson (1993) described the Queen Charlotte Island (QCI) data base. Chapter 3 first characterizes the Kootenay study area (22 events). For both inventories the BC traversing approach (chapter 2) was used, facilitating various quantitative comparisons between the two data sets. From the original QCI data, Fannin and Wise (2001) established empirical-statistical rules for debris flow simulation and proposed the UBCDFLOW tool. This research tests the utility of these empirical-statistical rules for the Kootenay study area, which has different climate, topography, event sizes and travel distances than the QCI. The simulations are analyzed based on three quantitative success indicators for simulating the correct volume change process, volume magnitude and travel distance, respectively.
- The third manuscript (chapter 4) addresses concerns about the model architecture of UBCDFLOW itself, and tests the hypothesis that accounting for uncertainty in slope angles yields better-informed estimate of travel distance. The deterministic tool used in the second manuscript is extended into a Monte Carlo type analysis, with random slope angle input over a defined range, and then applied to the Kootenay data base. Results are compared to the deterministic version and sources for uncertainty are discussed.

- The concluding chapter summarizes the findings of this study, and relates them to the current state of research. Further recommendations for future research are made.

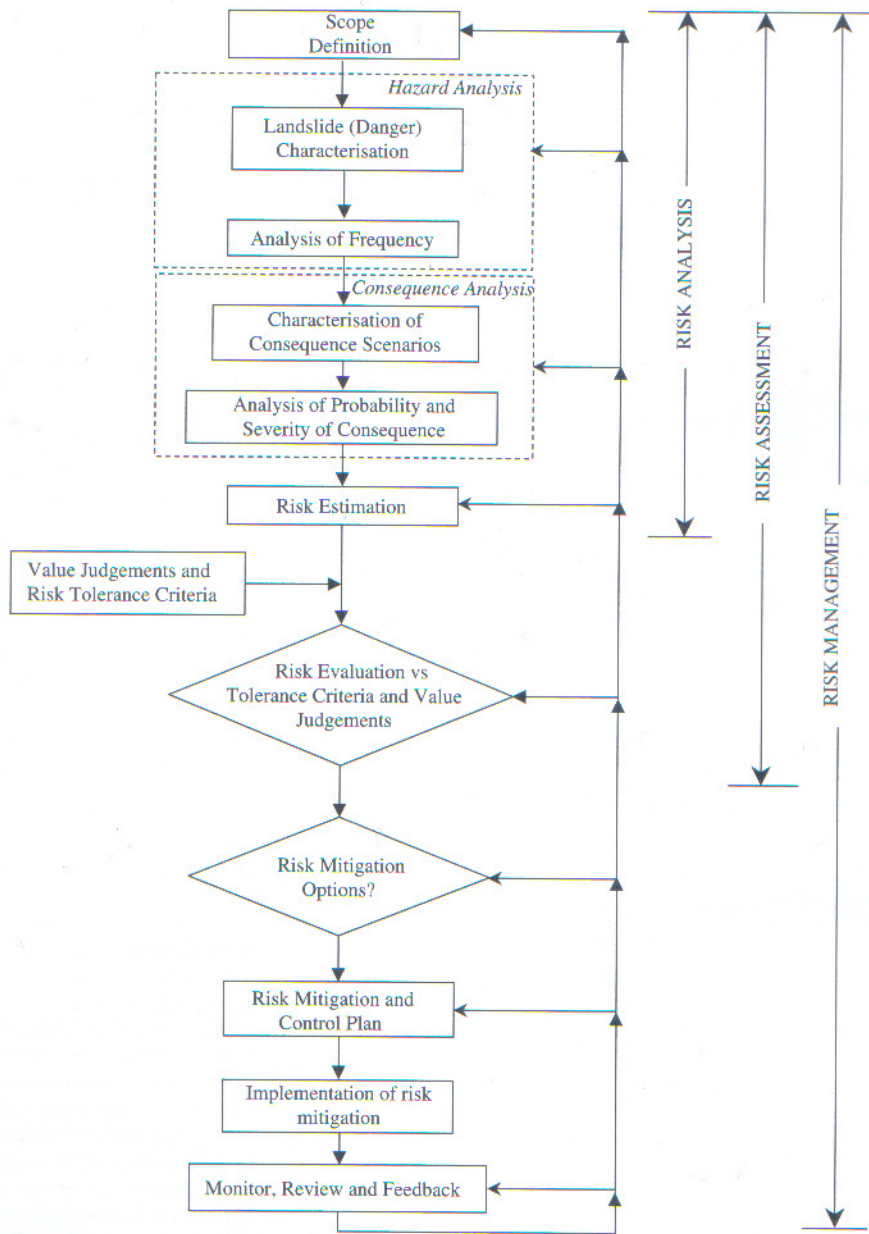


Figure 1.1 Flow chart for landslide risk management after Fell et al. (2005). © Taylor & Francis, AT Balkema, Amsterdam. Reproduced with permission.

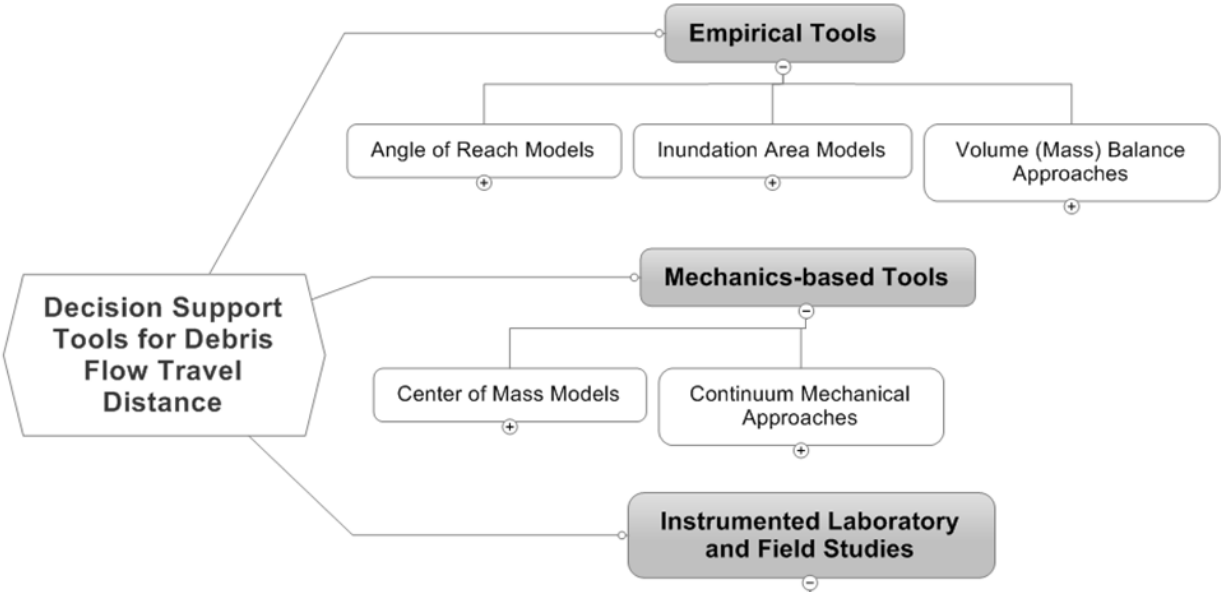


Figure 1.2 Overview: Decision support tools for simulation of debris flow travel distance.

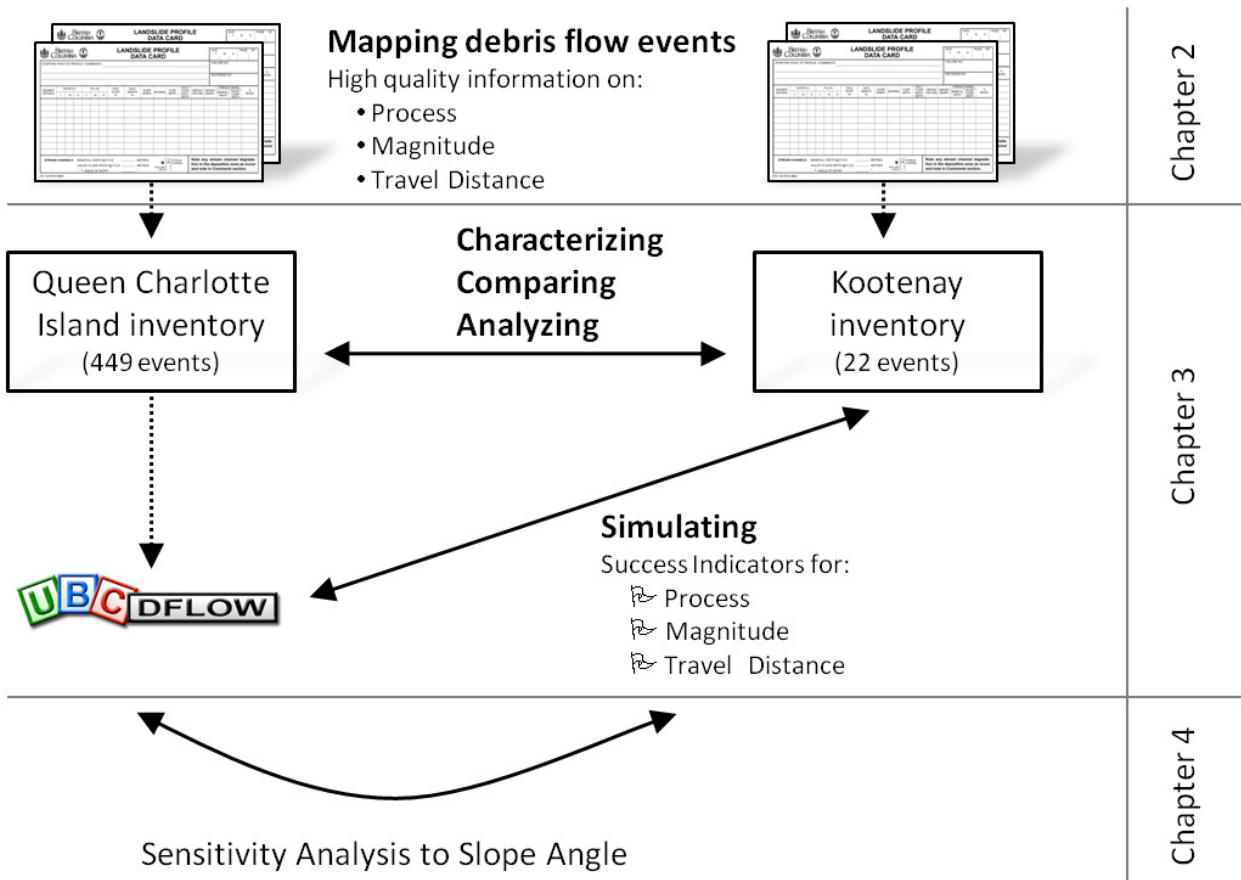


Figure 1.3 Organization of thesis.

1.5 References

- Association of Professional Engineers and Geoscientists of British Columbia (APEGBC), (2008). Guidelines for legislated landslide assessments for proposed residential development in British Columbia. Association of Professional Engineers and Geoscientists of British Columbia, Burnaby, Canada.
- Benda, L.E., and Cundy., T.W. 1990. Predicting deposition of debris flows in mountain channels, *Canadian Geotechnical Journal*, **27**(4): 409-417.
- Berti, M., and Simoni, A. 2007. Prediction of debris flow inundation areas using empirical mobility relationships. *Geomorphology*, **90**(1): 144–161.
- Bowman, E.T., Laue, J., Imre, B., and Springman, S.M. 2010. Experimental modelling of debris flow behaviour using a geotechnical centrifuge. *Canadian Geotechnical Journal*, **47**(7): 742-762.
- British Columbia Ministry of Forests (BCMOF), 2004. Forest and Range Practices Act. <http://www.for.gov.bc.ca/code/>, (last accessed 24. June, 2010).
- British Columbia Resources Inventory Committee (BCRIC), 1996. Guidelines and Standards to Terrain Mapping in British Columbia. Government of British Columbia, Victoria BC, Canada, http://www.env.gov.bc.ca/terrain/terrain_files/standards.html, (last accessed July 10, 2010).
- Cannon, S.H. 1993. Empirical model for the volume-change behavior of debris flows. *In* Proceedings of the National Conference on Hydraulic Engineering, July 25, 1993 - July 30, pp. 1768-1773.
- Corominas, J. 1996. The angle of reach as a mobility index for small and large landslides. *Canadian Geotechnical Journal*, **33**(2): 260-271.

- Cruden, D.M., and Varnes, D.J. 1996. Landslide types and processes. *In* Landslides Investigation and Mitigation. *Edited by* A.K. Turner and R.L. Schuster.: Transportation Research Board, US National Research Council, Special Report 247, Washington, DC, pp. 36-75.
- Fannin, R.J., and Bowman, E.T. 2007. Debris flows - Entrainment, Deposition and Travel Distance. *Geotechnical News* **25**(4): 3-6.
- Fannin, R.J., Moore, G.D., Schwab, J.W., and VanDine, D.F. 2005. Landslide risk management in forest practices. *In* Landslide Risk Management, Proceedings International Conference on Landslide Risk Management, Vancouver, Canada, May 1–June 3, 2005. O. Hungr, R. Fell, R. Couture, and E. Eberhardt (editors). A.A. Balkema Publishers. p 299-320.
- Fannin, R.J., and Rollerson, T.P. 1993. Debris flows: Some physical characteristics and behavior. *Canadian Geotechnical Journal*, **30**(1): 71-81.
- Fannin, R.J., and Wise, M.P. 2001. An empirical-statistical model for debris flow travel distance. *Canadian Geotechnical Journal*, **38**(5): 982-994.
- Fell, R., Ho, K.K.S., Lacasse, S., and Leroi, E. 2005. A framework for landslide risk assessment and management. *In*: Landslide risk management. *Edited by* O. Hungr, R. Fell, R. Couture, and E. Eberhardt. AT Balkema, Amsterdam, 3–25.
- Forest Practices Board. 2005. Managing Landslide Risk from Forest Practices in British Columbia. Special Investigation. FPB/SIR/14, <http://www.fpb.gov.bc.ca/WorkArea/DownloadAsset.aspx?id=2820>, (last accessed July 10, 2010).
- Gamma, P. 2000. dfwalk – Ein Murgang Simulationsprogramm zur Gefahrenzonierung. PhD Thesis, Philosophisch-naturwissenschaftliche Fakultät, Universität Bern, Switzerland.

- Goddings, D. 1984. Relationships for modelling water effects in geotechnical centrifuge models. *In: Proceedings of the Symposium on the Application of Centrifuge Modelling to Geotechnical Design*, Manchester, UK, 16-18 April 1984. Balkema Rotterdam, the Netherlands. pp. 1-23.
- Griswold, J.P., and Iverson, R.M. 2008. Mobility statistics and automated hazard mapping for debris flows and rock avalanches. USGS Scientific Investigations Report 2007-5276, 59 p.
- Heim, A. 1932. Bergsturz und Menschenleben. Vierteljahreszeitschrift der Naturforschenden Gesellschaft, Fretz & Wasmuth, Zürich, *Translated by* Skermer, N.A., 1989. Landslides and Human Lives. BiTech Publishers, Vancouver British Columbia.
- Hungr, O. 2005. Some methods of landslide hazard intensity mapping. *In: Landslide risk assessment. Edited by* D. Cruden, R. Fell, and R. Couture. Balkema. Rotterdam. ISBN 9054109149. pp: 215–225.
- Hungr, O. Corominas, J., and Eberhardt, E. 2005. Estimating landslide motion mechanism, travel distance and velocity. *In: Landslide risk management. Edited by* O. Hungr, R. Fell, R. Couture, and E. Eberhardt. AT Balkema, Amsterdam, 99–128.
- Hungr, O. and Evans, S.G. 1996. Rock avalanche runout prediction using a dynamic model. *Procs., 7th. International Symposium on Landslides*, Trondheim, Norway, 1:233-238.
- Hungr, O., Evans, S.G., Bovis, M.J., and Hutchinson, J.N. 2001. A Review of the Classification of landslides of the flow type. *Environmental and Engineering Geoscience*, **7**: 221–238.
- Hungr, O., Morgan, G.C., and Kellerhals, R. 1984. Quantitative analysis of debris torrent hazards for design of remedial measures, *Canadian Geotechnical Journal*, **21**(4): 663-677.

- Hungr, O., McDougall, S., and Bovis, M. 2005. Entrainment of material by debris flows. *Edited by M. Jakob and O. Hungr. Debris-flow Hazards and Related Phenomena*, Springer Praxis Publishing Ltd. Chichester, UK, pp. 135–158.
- Hungr, O., McDougall, S., Wise, M., and Cullen, M. 2008. Magnitude–frequency relationships of debris flows and debris avalanches in relation to slope relief. *Geomorphology* **96**: 355–365.
- Iverson, R.M. 1997. The physics of debris flows: *Reviews of Geophysics*, **35**, 245-296.
- Iverson, R.M. 2003. The debris-flow rheology myth. *In Debris-flow Hazards Mitigation: Mechanics, Prediction, and Assessment, V.1*, *Edited by D. Rickenmann and C.L. Chen*, Millpress, Rotterdam, 303-314.
- Iverson, R.M. 2005. Debris-flow mechanics. *In Debris-flow Hazards and Related Phenomena. Edited by Jakob, M. and Hungr*, Springer Praxis Publishing Ltd. Chichester, UK, pp. 105-134.
- Iverson, R.M., Costa, J.E., and LaHusen, R.G. 1992. Debris-Flow Flume at H.J. Andrews Experimental Forest, Oregon. USGS Open-File Report 92-483.
- Iverson, R.M., Schilling, S.P., and Vallance, J.W. 1998. Objective delineation of lahar-hazard zones downstream from volcanoes. *Geological Society of America Bulletin*, **110**: 972–984.
- Jakob, M., Bovis, M., and Oden, M. 2005. The significance of channel recharge rates for estimating debris-flow magnitude and frequency. *Earth Surface Processes and Landforms*, **30**: 755–766.
- Jakob, M., and Friele, P. 2010. Frequency and magnitude of debris flows on Cheekye River, British Columbia. *Geomorphology*, **114**: 382–395.
- Joint Practices Board (JPB) of ABCFP and APEGBC, 2009. Guidelines for Terrain Stability Assessments in the Forest Sector.

www.degifs.com/pdf/ABCPF%20APEGBC%20TSA%20Guidelines%20Oct%202009.doc, (last accessed 24. June, 2010).

Jordan, R.P. 1995. Debris flows in the southern Coast Mountains, British Columbia: dynamic behaviour and physical properties. PhD. Thesis. Department of Geography, University of British Columbia, Vancouver B.C. Canada.

Jordan, P. 2003. Landslide and Terrain Attribute Study in the Nelson Forest Region. FRBC Project Number: KB97202-0RE1, Final Report to Ministry of Forests Research Branch, Victoria B.C.

Koerner, H.I. 1976. Reichweite und Geschwindigkeit von Bergstürzen und Fliessschneelawinen. *Rock Mechanics*, **8**: 225-256.

McArdell, B., Bartelt, P. and Kowalski, J. 2007. Field observations of basal forces and fluid pore pressure in a debris flow. *Geophysical Research Letters*, Vol **34**: L07406.

McClung, D.M. 1999. The encounter probability for mountain slope hazards. *Canadian Geotechnical Journal*, **36**: 1195–1196.

McClung, D.M. 2000. Extreme avalanche runout in space and time. *Canadian Geotechnical Journal*, **37**: 161-170.

McDougall, S., and Hungr, O. 2004. A model for the analysis of rapid landslide runout motion across three- dimensional terrain. *Canadian Geotechnical Journal*, **41**: 1084-1097.

O'Brien, J.S., and Julien, P.Y. 1988. Laboratory analysis of mudflow properties. *Journal of Hydraulic Engineering*, **114**: 977-887.

Perla, R., Cheng, T.T., and McClung, D.M. 1980. A two-parameter model of snow-avalanche motion. *Journal of Glaciology*, **94**:197-207.

- Petley, D.N., Dunning, S.A., and Rosser, N.J. 2005. The analysis of global landslide risk through the creation of a database of worldwide landslide fatalities. *In: Landslide risk management. Edited by O. Hungr, R. Fell, R. Couture, and E. Eberhardt.* AT Balkema, Amsterdam, 367–374.
- Prochaska, A.B., Santi, P.M., Higgins, J.D., and Cannon, S.H. 2008. Debris-flow runout predictions based on the average channel slope (ACS). *Engineering Geology*, **98**: 29–40.
- Rickenmann, D. 1999. Empirical Relationships for Debris Flows. *Natural Hazards*, **19**: 47–77.
- Rickenmann, D. 2005. Runout prediction methods. *Edited by M. Jakob and O. Hungr.* Debris-flow Hazards and Related Phenomena, Springer Praxis Publishing Ltd. Chichester, UK, pp. 305–324.
- Scheidegger, A.E. 1973. On the prediction of the reach and velocity of catastrophic landslides, *Rock Mechanics*, **5**(4): 231-236.
- Scheidel, C., and Rickenmann, D. 2010. Empirical prediction of debris-flow mobility and deposition on fans. *Earth Surface Processes and Landforms*, **35**: 157–173.
- Schuster, R.L., and Highland, L.M. 2001. Socioeconomic and environmental impacts of landslides in the western hemisphere. USGS Open-File Report 01-0276.
- Schwab, J.W., and Geertsema, M. 2010. Terrain stability mapping on British Columbia forest lands: an historical perspective. *Natural Hazards* **53**(1):63-75.
- Voellmy, A. 1955. Über die Zerstörungskraft von Lawinen. *Schweiz. Bauzeitung* **73**: 212-285.
- Wise, M.P., Moore, G.D., and VanDine, D.F. (eds.) 2004. *Landslide Risk Case Studies in Forest Development Planning and Operations.* B.C. Ministry of Forests, Land Management Handbook 56, 119 p.

2 FIELD TRAVERSING OF DEBRIS FLOW VOLUMES¹

2.1 Outline

The results-based practice legislation in the British Columbia forestry sector requires terrain stability professionals to conduct a partial risk analysis to ensure forestry companies mitigate the potential effects of landslides effectively. Systematic collection of debris flow inventories is an essential part to fulfill that task. Field traversing procedures for debris flows in British Columbia have been used, and refined, over the last 35 years. While several versions of traversing sheets evolved, no attempt has yet been made to describe the traversing procedure. This article describes the BC debris flow traversing methodology and illustrates its application for two events. The systematic traversing approach is a quantified characterization of debris flows, combined with qualitative descriptions. It is particularly useful to describe volume change processes (entrainment, deposition), quantify debris flow volume magnitude, and measure travel distance. Data gathered can be used to compare debris flow inventories, and as input to a variety of empirical or dynamic analysis tools for debris flow travel distance.

¹ A version of this chapter will be submitted for publication. Busslinger, M., Fannin, R.J. and Jordan, P. (2010). Field traversing of debris flow volumes.

2.2 Traversing of debris flows in British Columbia

In a historical perspective on terrain stability mapping in British Columbia forest lands, Schwab and Geertsema (2010) report an increase in landslide frequency from roads and within cut blocks after forest harvesting advanced onto steep slopes in the 1970s. In response, the BC Forest Practices Code was subsequently introduced in 1995 and the Terrain Stability Mapping (TSM) method (BCRIC, 1996) was developed to guide forest management practice. The Forest Practice Board (2005) found that implementation of TSM guidelines reduced the amount of landslides caused by forestry activities. TSM is somewhat narrowly focused on the hazard of landslide initiation. Polygons are rated for the likelihood of landslide initiation, but not the likelihood of landslide impact and related consequences.

In 2004 the legislation moved away from the “prescriptive” plan based regulation of the BC Forest Practices Code, to the results-based legislation of the current BC Forest and Range Practices Act (Fannin et al., 2005; BCMOF 2004). Forestry activities must be safe, productive, and environmentally sound, and must not cause a landslide that has a material adverse effect on soils, visual quality, timber, forage, plant and wildlife communities, water and fish habitats, recreation or cultural heritage resources. Terrain stability professionals are expected to ensure the licensees mitigate the potential effects of landslides effectively. The guidelines for terrain stability assessments in the forest sector by the Joint Practices Board (JPB, 2009), of the Association of British Columbia Forest Professionals (ABCFP) and the Association of Professional Engineers and Geoscientists of British Columbia (APEGBC), require terrain stability professionals to carry out a partial risk analysis and evaluate existing and potential effects of forest development on slope stability. Compiling and comparing debris flow inventories are essential tasks to meet this goal. Understanding of debris flow volume change processes (i.e. entrainment and deposition) is fundamental to effectively manage debris flow risks. A systematic approach for traversing debris flows facilitates characterization and comparison of events.

Good quality of field data are crucial for testing the utility of empirical rules. Landslide inventories are often compiled primarily on the basis of remote sensing (e.g. airphotos).

Ground-based data collection from field traverses offer much more detailed insights into debris flow behaviour and more accurate measurements (Guthrie et al., 2010). For example, Robinson et al. (1999) compared field measurements of slope gradient with values obtained from Digital Elevation Models (DEM) with various resolutions (30m, 6m and 1m grid). They found that slope angles obtained from commonly available 30m DEM poorly correlated with field measurements. For DEMs with higher resolutions, effectiveness in providing accurate values could not be confirmed. In the BC forestry sector, field traversing procedures have been used and refined over the last few decades. The Land Use Planning Advisory Team (LUPAT) of MacMillan Bloedel Forestry Company compiled a large database of debris flows (449 events) on the Queen Charlotte Islands. The BC Ministry of Forests has an example of a Landslide Profile Data Card (BCMOF, 1996) available online. A copy of the card is attached in Appendix B. Details and qualitative attributes on the card may vary by region, but in essence the quantitative measurements of path geometry and volumes (columns 1 to 5 in Appendix B) are essentially the same. For instance, P. Jordan used a slightly different version of the card (Appendix C) to compile data for the landslide and terrain attribute study in the Nelson Forest Region (Jordan, 2002). The only difference in quantitative columns is that length of entrainment or length of deposition (i.e. columns 2 and 3) are not accounted for individually, but rather taken as the length of the reach.

2.3 Objectives

While several versions of Landslide Profile Data Cards evolved over the last few decades, no attempt was made to describe the traversing procedure. To compile a ground-based debris flow inventory, there is need for a systematic observation method facilitating comparison between events or inventories. This article is a concise description of the traversing method. The intent is to minimize inconsistent field records. The method is believed to be particularly well suited to characterize high frequency, low magnitude events.

Two example events are used to illustrate the utility of the field records. In particular insights into yield rates along the path help to better understand the competing processes of entrainment and deposition and further facilitate determination of the point

of onset of terminal deposition. Refined volume estimates from field traverses are likely closer to reality than estimates from desk studies (e.g. air photos). The quantitative data gathered are particularly useful to analyse volume change processes (i.e. entrainment, deposition), quantify volume magnitudes and spatial impact (i.e. travel distances or areas inundated). Field observations can be used as input to a variety of empirical or dynamic analysis tools for debris travel distance.

2.4 Field traversing methodology

This section describes the equipment and procedure used to traverse an event in the field, and record measurements and observations along the event path. The procedure involves measurements of distance and angles, together with qualitative observations. The following equipment is required to carry out the field traverses:

Special equipment:

- Hip-chains
- Inclinometer
- Compass
- Laser range finder
- Folding rule

General equipment:

- Digital photo camera
- Water resistant note book
- Maps and air photos
- Altimeter (optional)
- Binoculars
- GPS device (optional)
- Hand calculator (optional)
- Copies of Landslide Profile Data Cards (e.g. Appendix B, C)²
- Copies of Landslide Data Cards³
- Terrain Classification System Field Card of Codes (optional)⁴

² <http://www.for.gov.bc.ca/isb/forms/lib/fs123-1.pdf>

³ <http://www.for.gov.bc.ca/isb/forms/lib/fs123-1.pdf>

Traditionally hip-chains have been used to measure distances. Inclinometers with a typical resolution of $\pm 0.5^\circ$ are used to measure gradients. Azimuths are measured using a compass with similar resolution. Erosion depths are measured with a folding rule.

Recently laser range finders became more affordable and are gradually replacing analog devices. Laser range finders send a light beam to a target, and the time between emitting and receiving the reflected signal is used to derive the distance. A built-in inclinometer measures the angle of inclination to the horizontal, from which the horizontal and vertical distance between observer and target can be derived. This essentially substitutes hip-chain and analog inclinometer. The measurement accuracy depends on the quality of the reflected signal and therewith on the surface of the target. Under good conditions measuring resolutions are about $\pm 0.1\text{m}$. It should be noted that converted measurements of horizontal and vertical distances depend on the resolution of the built in inclinometer (typically around $\pm 1.0^\circ$) and the distance measured. As for any portable electronic device, laser range finders require power supply. Laser range finders particularly enhance the convenience for channel cross-section levelling, where all the measurements can be taken without crossing the channel. Some laser range finders are even available with a built in compass. However, it is recommended to bring an analog inclinometer and a hip-chain to test the laser range finder in the field and as a backup in case of an outage.

Today GPS reception in gullied channels is still limited and hence accuracy of GPS devices does not reach the level of the technique outlined above. However, carrying a GPS device and recording way-points along the path centerline (e.g. reach ends) is proving to be a useful quality control, by minimal effort.

2.4.1 Recommended procedure

Prior to traversing, a desk study of the debris flow area, and a safety assessment regarding the terrain stability professionals' exposure to any hazards in the area, are carried out. Topographic maps and aerial photographs assembled during the desk study are very valuable in the field. Access to the area and a time schedule should be carefully planned. Field traversing is best completed in teams of two people.

⁴ <http://archive.ilmb.gov.bc.ca/risc/pubs/teecolo/terclass/fieldcar.htm#anchor510868>

1. Start from a point of reference: The path is usually traversed from bottom to top, because post-event alterations of debris flow volumes are often most evident in the lower depositional areas.
2. Split the path into reasonably short reaches with uniform attributes. This is the key to a systematic traversing procedure. Reach ends are, for example, located at distinct terrain breaks, channel bends, creek junctions, changes in morphology or width, else changes in deposition or entrainment depth. Typical reach lengths should not exceed 100m. Mapping of longer segments requires experience, as volume change processes may vary. Channel bends may require relatively shorter reaches.
3. According to the Landslide Profile Data Card (Appendix B); measure length, gradient and azimuth of the centerline for each reach (i.e. column 1, 4 and 5 respectively). Lengths are typically approximated to the nearest meter. Width and depth should be measured for at least three characteristic cross-sections in a reach before a representative value is chosen. Very wide cross-sections with small depths require careful selection of depth. Depths are typically taken to approximately 0.1m. The resolution of widths depends on channel shape and should be higher for narrow channels. However, in narrow gullies practicalities may not allow a resolution greater than 10% of full width. Length, width and depth of scour and fill are noted in columns 2 and 3. Note that depth of scour or fill is measured perpendicular to the slope. Slope gradient is typically recorded to the nearest 0.5 to 1° (depending on resolution of inclinometer) and azimuth to the nearest 1°. These measurements are used to characterize the path centerline and volume change along the path.
4. Document additional attributes like slope morphology, gully floor width/depth, bank-full width and valley floor width to further characterize the topography of the path. Observations of trim-lines or bark damage on trees are used to infer flow depths. The Terrain Classification System for British Columbia (BCMOF, 1997) is used to characterize the entrained material, as well as the texture and morphology of the deposit. Comments about vegetation are also included. Depending on the purpose of the field survey some columns may be substituted

or replaced, for example columns may be added for supply limits of erodible material. However the systematic procedure of traversing the event in reaches with uniform attributes should be maintained.

5. Make a hand sketch of the plan view of the path in the notebook. It should indicate significant features. Label the location and direction of any photographs. The sketch should be updated continually in every reach.
6. Survey channel cross-sections at representative points and make a sketch in the notebook, including dimensions of the cross-section. The number of cross-sections to be measured depends on topography and purpose of the study. Field measurements of channel cross-sections are more accurate than data obtained from topographic maps.
7. Repeat steps 2 to 6 reach by reach until the crest of the landslide is reached (if traversing upslope).

More general landslide attributes, like trigger, failure type, drainage class, should be documented on the landslide data card (BCMOF, 1996) or similar forms like those used by Peter Jordan for the Nelson Forest Region landslide and terrain attributes study (Appendix A).

2.4.2 Discussion of procedure

It is recommended to map the profile of an event for a reasonable distance beyond the observed point of termination. This small extra effort greatly enhances the utility of the gathered data for calibration of numerical models, where simulations may exceed the observed point of termination.

The procedure depends on the determination of representative values for depths and widths of scour or fill. While the error in measuring reach lengths is relatively small, compared to its absolute value, errors in depth and width determination are more challenging because profiles may not be uniform. Where it is difficult to determine a representative depth or width it is recommended to use shorter reach intervals to assure good quality volume estimates.

Careful measurements of slope angles are particularly important where depositional processes become significant, and especially around the point of onset terminal

deposition (Hungry et al., 2005; Guthrie et al., 2010). These measurements are often used to establish or apply rules for spatial impacts of debris flows, and are important in some empirical tools for debris flow simulation (Benda and Cundy, 1990; Fannin and Wise, 2001).

Estimates of debris volume may be complicated when evidence of pre-event topography is gone. It should be appreciated that above-ground woody debris may add a substantial proportion to the total debris flow volume.

The method allows a quick check of the volume balance of an event. Large differences in total entrained versus deposited volumes may help to identify curious events in the field. Critical assessment of the data gathered requires judgment and detailed knowledge of the event, and should ideally be carried out right after a traverse has been completed.

2.5 Illustrative traverse examples

2.5.1 Blueberry Creek event

The Blueberry Creek debris flow event occurred in May 1993, 17km west-southwest from Castlegar BC (Fannin et al., 2006). Figure 2.1 is an aerial view of the upper part of the event. A small slide (130m^3) in an unconfined clear-cut slope was likely triggered by snowmelt. It entered a confined gully, entrained additional material, and terminated after 1450m of travel distance on an alluvial fan.

In Appendix C the field observations are noted on Landslide Profile Data Cards. Reach lengths vary between 18 and 185m with an average length of 58m. Widths range between 2 and 15m with erosion depths of up to 0.8m and deposition depths of up to 2.0m. Slope angles range between 6.5° and 33° . The event is mapped from end of deposition (i.e. point 1) to the landslide crown at the top (i.e. point 28) in a total of 27 reaches. In Figure 2.2 the volume change for each reach (bar) is calculated from the Landslide Data Cards in Appendix C and summed in flow direction (dotted line). The difference between cumulative volumes at point 27 and point 17 divided by the distance between the points results in an average yield rate of $1.5\text{m}^3/\text{m}$. An example of a typical confined reach in this part of the path is shown in Figure 2.3. Entering reach 16-17, the

channel widened from 9 to 16m and confinement changed from confined to slightly confined, likely causing the event to deposit 250m^3 before it entrained again with an average yield rate of $2.1\text{m}^3/\text{m}$ to a peak cumulative volume of 1760m^3 at point 10. After exiting the gully, the path widened and was only slightly confined, causing the flow to deposit. Over 95% of the total volume deposited occurred over a distance of 277m (or 14% of total travel distance) between point 10 and point 5.

Cumulative volume in the last few reaches is negative. Physically this makes no sense, because one would expect the volume to be zero at the end of deposition. This illustrates one of the challenges in traversing debris flow volumes. Changes in bulk density may occur; post-event hydrologic or mass-movement processes may significantly alter evidence of volume changes before the event is mapped. It is often relatively easy to judge whether entrainment or deposition occurred in a reach. However, estimating the magnitude is complicated by errors in depth or width estimation (i.e. small number) multiplied by the length (large number) yielding in significant inaccuracy. However, the systematic approach used in the BC traversing method causes the terrain stability professional to ask critical questions and increases the understanding of debris flow volume change processes. It is therefore recommended that the terrain stability professionals use their detailed knowledge of the event and experience to perform a quality check of the surveyed volumes, immediately after completion of a field traverse.

2.5.2 Hummingbird Creek event

The Hummingbird Creek debris flow event occurred on 11 July 1997 at Mara Lake, near Sicamous, and is reported as the largest non-volcanic debris flow in British Columbia with an estimated magnitude of $92,000\text{m}^3$. The event is well documented and analyzed in Jakob et al. (2000). The orthophoto (Figure 2.4) gives an overview of the path of the whole event. Note that the orthophoto was taken several years after the event, and a large portion of deposited material has since been removed and only volumes at onset deposition are evident in the field now. Rainfall and road diversion triggered a debris avalanche that entered Hummingbird creek. The event entrained material as it traveled

down the confined channel until it finally deposited on the fan, causing substantial damage to three buildings.

In July 2009 the BC traversing method was applied to the Hummingbird Creek debris flow event (Appendix D). The event was traversed from top down, rather than bottom up, due to practicalities discussed below. The findings are briefly reported herein to illustrate challenges and benefits of the method. It is suspected that evidence of volume change in the confined channel of Hummingbird Creek has been substantially altered mainly by hydraulic processes, and therefore no measurements of volume change were made in the channel of Hummingbird Creek. Furthermore, in the depositional area, debris was removed shortly after the event occurred. Therefore only volume changes for the initial debris avalanche are reported. This emphasizes the time window wherein traversing is most effective. Ideally traverses should be carried out as soon as the risk for the field personnel is acceptable and before the evidence is significantly altered.

Figure 2.5 was taken immediately above the head scarp, where the field personnel are standing, and width and depth ($w \times d = 10\text{m} \times 0.3\text{m}$) were noted on the field card (Appendix D). The initial failure took place in a till veneer, mostly down to the bedrock. Further down the path, trees that were up-rooted by the debris movement are evident. Figure 2.6 looks up the path from point 4 (see zoom box in Figure 2.4). The initially narrow path widens. The young tree growth illustrates a further challenge in traversing debris flow volumes, in this case 12 years after the event occurred. However in some cases, vegetation can also be a helpful indicator to date events. Figure 2.7 looks down from about point 5. The debris avalanche entered the confined channel of Hummingbird creek and traveled downhill. Superelevation and deposits on the opposite side of the creek are evident.

Based on the field measurements, the volume change for each reach was calculated in Figure 2.8; bars indicate volume changes in each reach and the dashed line represents cumulative volume changes along the path. In total, the debris avalanche entrained $6,800\text{m}^3$ between the head scarp and the point of entry into Hummingbird Creek. Jakob et al. (2000, Eq. 1) reported a debris avalanche volume of $25,000\text{m}^3$ based on an estimated average erosion depth of 0.77m times the surface area of the avalanche. While at that time conditions probably did not allow a field traverse to be made, this

comparison emphasizes the utility of the more detailed BC traversing method. At a reasonable extra effort it brings better estimates of volumes, allowing insights into volume change processes and debris flow behaviour. Guthrie et al. (2010) expect ground-based methods like the one described in here to be more accurate than any observation by any remote means (e.g. air photographs or remote sensing).

2.6 Summary remarks

Almost every tool used to evaluate the spatial impact of debris flows in a risk analysis relies on empiricism. Therefore, there is a tremendous role for compiling systematic inventories. This article is a concise description of the BC traversing method for characterisation of debris flow events. Data can be used for simple empirical methods (e.g. reach angle, yield rate) or for input in dynamic analysis. The path of a debris flow is surveyed as a series of reaches with uniform attributes. Reach-by-reach quantitative measurements on path geometry and volume changes are taken, together with qualitative descriptors of morphology and material. The quantitative data can be used to characterize volume change processes, magnitude and travel distance of an event and facilitate comparison between events or databases. The volume estimates along the path greatly improve the understanding of terrain attributes on volume change processes, the point of onset of terminal deposition and hence travel distance.

Field traversing in a systematic manner forces the terrain stability professional to ask critical questions. Field traversing gives a sense for proportions, geomorphology, other attributes and details not visible on maps and air photos. It requires experience and proper training. Compared to data obtained from desk studies, the BC traversing method provides for better estimates and more insights into volume change behaviour at a reasonable extra effort. Regardless, measuring errors occur in the field and a few common mistakes are highlighted here:

- Width measurements do not necessarily need to be taken in the middle of a reach length; ideally about 3 measurements should be taken at characteristic points before a characteristic value is chosen.
- Depth of scour should not just be estimated as depths of visible erosion edges, but an average for the cross-section should be chosen. In v-shaped channels

depth is not the maximum value, but a representative value of the average erosion depth.

- Deposition depth should not be taken from the edges of deposits, without being able to dig or probe.
- There is a tendency of many observers to overestimate average depth of scour and volumes of deposition. Maximum depths (e.g. height of levee, scour depth) are often clearly visible, but it should always be kept in mind that depths are multiplied by the full reach length. If it is difficult to decide on a particular value it may help to choose a shorter reach length.

Aside from measurement errors, differences in the volume budget between net-entrainment and net-deposition may occur for several reasons (e.g. bulk density changes, post-event volume alterations).

New laser range finders significantly enhance the convenience and efficiency of field measurements (distances, angles) compared to the traditional use of hip-chain and inclinometer. This is particularly useful for levelling of channel cross sections and makes field traversing more viable.

The use of the BC field traversing method is encouraged in other regions to advance the understanding of debris flow volume change processes, by comparison of systematically compiled inventories, in order to effectively manage debris flow risks.

2.7 Acknowledgement

The described traversing technique has been refined by many professionals over last three decades. This article is a summary of various efforts made in British Columbia. The authors would like to acknowledge the contributions by numerous professionals that were not referenced in this article.



Figure 2.1 Aerial view on initiation zone in clear-cut of Blueberry Creek debris flow.

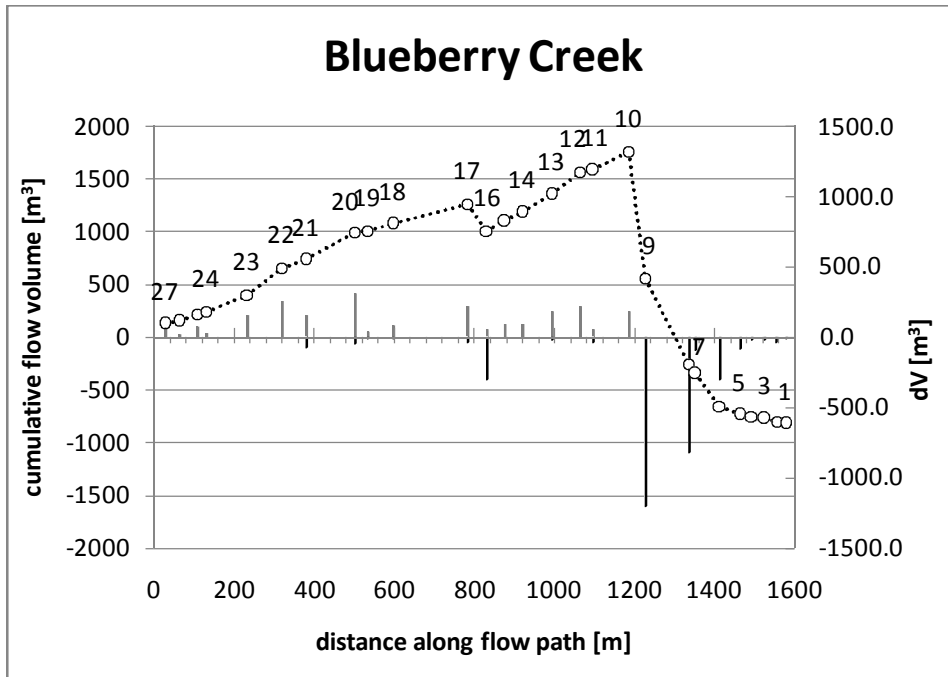


Figure 2.2 Plot of mapped volume changes along the path. Bars; volume change in each reach (dV). Dashed line; cumulative volume. Labels are reach ends; 1 = point of termination.



Figure 2.3 Reach 17-18 of Blueberry Creek; a reach of confined flow.

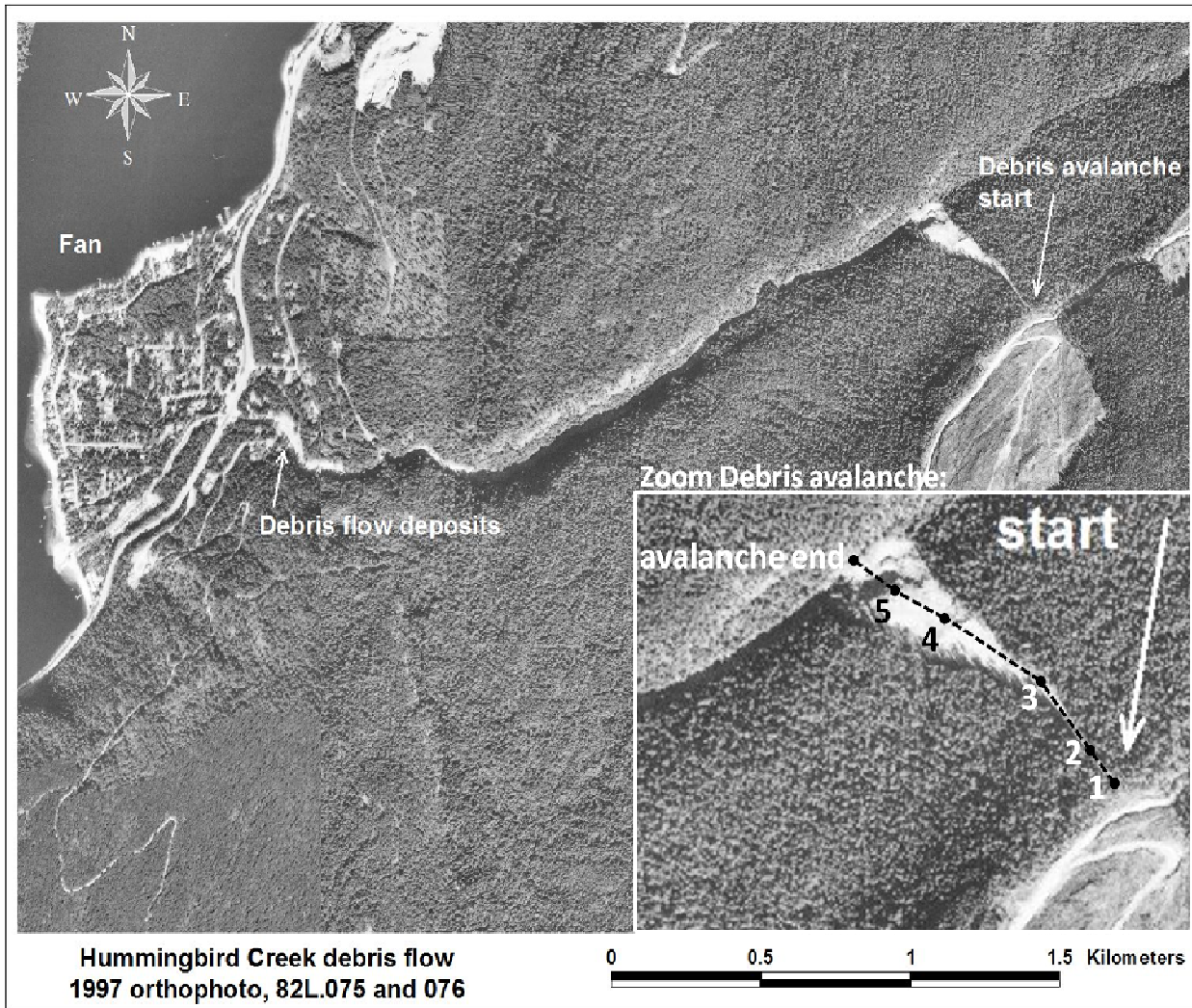


Figure 2.4 Orthophoto of Hummingbird Creek: Dashed line in zoom box indicates approximate centerline, numbers indicate reach ends. (Picture edited from: FORREX Compendium of Forest Hydrology and Geomorphology in British Columbia. In press).



Figure 2.5 Field personnel standing at head scarp of Hummingbird Creek debris avalanche.



Figure 2.6 Looking up from point 4 in the debris avalanche path.

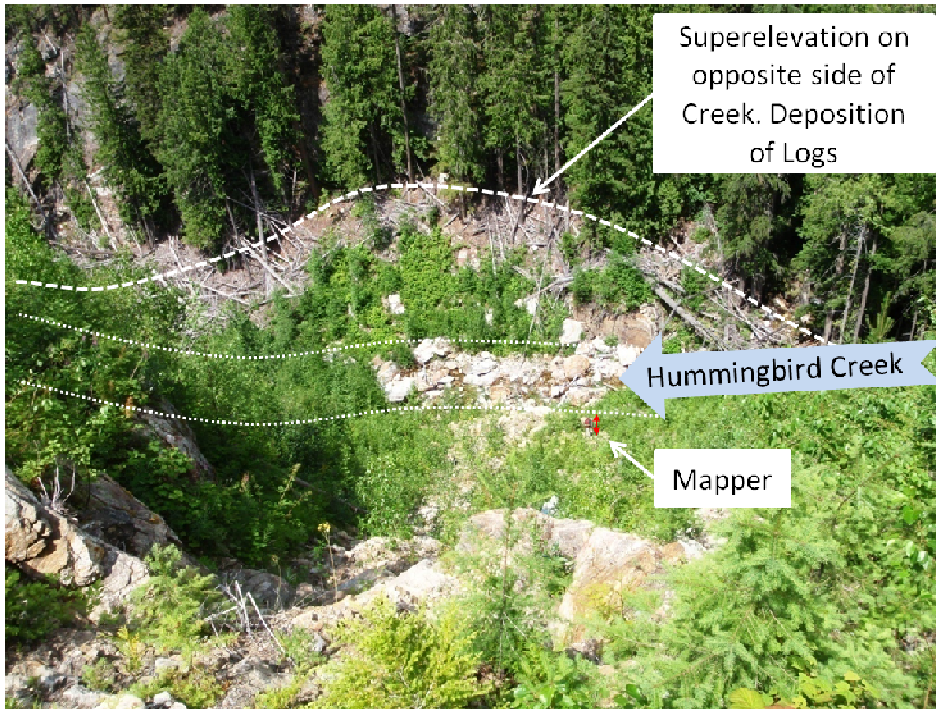


Figure 2.7 Looking down from point 5. Debris avalanche enters confined channel of Hummingbird Creek (flow from right to left).

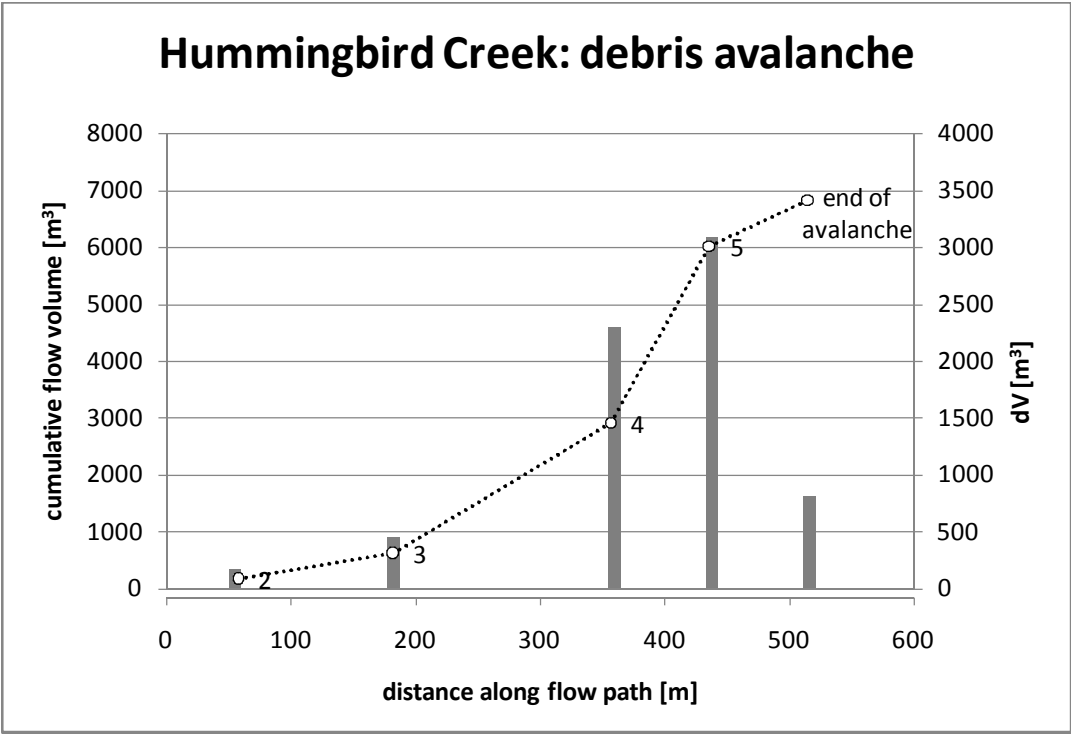


Figure 2.8 Plot of mapped volume changes along the path. Bars; volume change in each reach (dV). Dashed line; cumulative volume. Labels indicate reach ends. Debris enters Hummingbird Creek at end of avalanche.

2.8 References

- Benda, L.E., and Cundy., T.W. 1990. Predicting deposition of debris flows in mountain channels. *Canadian Geotechnical Journal*, **27**(4): 409-417.
- British Columbia Ministry of Forests (BCMOF). 1996.
<http://www.for.gov.bc.ca/isb/forms/lib/fs123-1.pdf>.(last accessed 3. June, 2010).
- British Columbia Ministry of Forests (BCMOF), 1997. Terrain Classification System for British Columbia.
<http://archive.ilmb.gov.bc.ca/risc/pubs/teecolo/terclass/index.html>.
- British Columbia Ministry of Forests (BCMOF), 2004. Forest and Range Practices Act.
<http://www.for.gov.bc.ca/code/>, (last accessed 24. June, 2010).
- Busslinger, M., Fannin, R.J. and Jordan, P. 2010. Field traversing of debris flow volumes. Manuscript prepared for publication (chapter 2).
- Fannin, R.J., Bobicki, E.R., and Jordan, P. 2006. A sensitivity analysis of debris flow travel distance at Blueberry Creek, B.C., Proceedings of 59th Canadian Geotechnical Conference, Vancouver, B.C., Oct. 1-4, pp. 335-341.
- Fannin, R.J., Moore, G.D., Schwab, J.W., and VanDine, D.F. 2005. Landslide risk management in forest practices. *In* Landslide Risk Management, Proceedings International Conference on Landslide Risk Management, Vancouver, Canada, May 1–June 3, 2005. O. Hungr, R. Fell, R. Couture, and E. Eberhardt (editors). A.A. Balkema Publishers. p 299-320.
- Fannin, R.J., and Rollerson, T.P. 1993. Debris flows: Some physical characteristics and behavior. *Canadian Geotechnical Journal*, **30**(1): 71-81.
- Fannin, R.J., and Wise, M.P. 2001. An empirical-statistical model for debris flow travel distance. *Canadian Geotechnical Journal*, **38**(5): 982-994.

- FORREX Compendium of Forest Hydrology and Geomorphology in British Columbia.
<http://www.forrex.org/program/water/compendium.asp>. In press.
- Guthrie, R.H., Hockin, A., Colquhoun, L., Nagy, T., Evans, S.G., and Ayles, C. 2010. An examination of controls on debris flow mobility: Evidence from coastal British Columbia. *Geomorphology*, **114**: 601-613.
- Hungr, O., McDougall, S., and Bovis, M. 2005. Entrainment of material by debris flows. *Edited by M. Jakob and O. Hungr. Debris-flow Hazards and Related Phenomena*, Springer Praxis Publishing Ltd. Chichester, UK, pp. 135–158.
- Hungr, O., Morgan, G.C., and Kellerhals, R. 1984. Quantitative analysis of debris torrent hazards for design of remedial measures. *Canadian Geotechnical Journal*, **21**(4): 663-677.
- Jakob, M., Anderson, D., Fuller, T., Hungr, O., and Ayotte, D. 2000. An unusually large debris flow at Hummingbird Creek, Mara Lake, British Columbia. *Canadian Geotechnical Journal*, **37**(5): 1109-1125.
- Joint Practices Board (JPB) of ABCFP and APEGBC, 2009. Guidelines for Terrain Stability Assessments in the Forest Sector.
www.degifs.com/pdf/ABCPF%20APEGBC%20TSA%20Guidelines%20Oct%202009.doc, (last accessed 24. June, 2010).
- Jordan, P. 2002. Landslide Frequencies and Terrain Attributes in Arrow and Kootenay Lake Forest Districts. *In: Terrain Stability and Forest Management in the Interior of British Columbia: Workshop Proceedings, May 23–25, 2001, Nelson, B.C., Edited by: P. Jordan and J. Orban, British Columbia, Ministry of Forests, Research Branch, Technical Report 3, Victoria, B.C., p. 80-102.*

3 UTILITY OF EMPIRICAL-STATISTICAL RULES FROM THE QUEEN CHARLOTTE ISLANDS FOR DEBRIS FLOW SIMULATION IN THE KOOTENAY REGION⁵

3.1 Outline

Risk assessment of debris flows requires determination of the travel distance. An empirical-statistical tool to simulate travel distance of debris flows on the Queen Charlotte Islands (QCI) has been proposed by Fannin and Wise (2001). The tool is applied to the Kootenay inventory (22 events) with different geo-bio-climatic conditions in order to investigate the portability of the empirical rules from the QCI. The QCI and Kootenay inventories are characterized and contrasted. Simulations of the Kootenay debris flows are compared to field observations.

Despite significant differences between the two study areas in climate, topography, event sizes and travel distances, remarkable similarities were found for dominant volume change processes as a function of slope angles. Average yield rates in the Kootenays are moderate (2 to 3m³/m) and significantly smaller than on the QCI (12 to 23 m³/m).

The empirical rules of the QCI dataset capture the volume change process (entrainment, deposition) correctly for 80% of the lengths in the Kootenay dataset, and therefore appear to be portable from the QCI. However, the QCI regression equations overestimate the magnitude of volume change in the Kootenays, for both entrainment and deposition. In total, 15 out of 22 Kootenay simulations terminate within 89 and 110% of the observed travel distance.

⁵ A version of this chapter will be submitted for publication. Fannin, R.J., Busslinger, M., and Jordan, P. (2010). On the utility of empirical-statistical rules for simulation of debris flow events.

3.2 Introduction

3.2.1 Classification of debris flows

Debris flows are a subtype of landslides comprising soil, rocks and organic material, which typically flow in steep channels (Cruden and Varnes, 1996). Flow-like landslides often begin as debris slides (no internal distortion), with the movement internal distortion of the mass gradually develops into partly saturated debris avalanches or saturated debris flows. In this article the term debris flow is meant to be inclusive of landslides that would otherwise be classified as debris avalanches or debris slides. Hungr et al. (2001) further specify debris flows as very rapid (1.0m/s) to extremely rapid flows (20m/s) of saturated, loose, unsorted material with low plasticity (plasticity index < 5%) that may contain a significant proportion of organic material (logs, tree stumps and organic mulch). Down-slope movement is often accompanied by entrainment and deposition along the path. When entrainment and deposition occur simultaneously the mass changing process is referred to as dual mode of flow. Due to confinement channelized debris flows may travel several kilometres. High velocities causing destructive impact pressures combined with the large spatial impact make this type of landslide important for risk assessment.

Based on morphology Fannin and Rollerson (1993) provided a framework to classify debris flows on the Queen Charlotte Island. They defined three main types of debris flows, briefly summarized below. The reported slope angles apply to debris flow events mapped on the Queen Charlotte Islands.

A type 1 event is a single event which initiates on, and travels down, a relatively uniform, planar slope. Slide movements appear rare, except in the source area. Evidence of flow movements is common, particularly around obstructions and in the form of levees, suggesting a complex progression from sliding to flow. On occasion these events will include a short reach in the path which is a gully. Deposition typically occurs on a relatively uniform, planar slope ($15 \pm 8^\circ$).

A type 2 event is defined as a single event which initiates on an open slope and enters a gully or initiates in a gully. Events travel down relatively steep, confined channels.

Although channel gradients are typically steeper than 15°, occasional short, gentler reaches less than 50 m long may be included in the path. Deposition typically occurs on unconfined fans ($12 \pm 6^\circ$) at the base of the gully. On occasion deposition occurs in the channel of the gully.

A type 3 event is defined as a single event which initiates on an open slope and enters a gully or initiates in a gully. Events travel down relatively steep, confined channels similar to those of type 2 and then continue, often for long distances, along more gentle, confined channels. Channel gradients in the lower reaches of the gully are typically between 5 and 15°: Any event consisting of a reach with gradient less than 15° and longer than 50 m is classified as a type 3. Deposition typically occurs on gentle ($7 \pm 4^\circ$), unconfined fans at the base of the gully. On occasion deposition occurs entirely within the confined channel. Type 3 debris flows are very destructive due to their high velocities and high impact pressures (i.e. damage potential). Due to the long travel distances (spatial impact) they are important in risk assessments. Typical questions in the forest sector ask whether a debris flow initiating on a hill slope will reach a stream and affect water quality, fish habitat or dam a creek.

3.2.2 Concept of risk and spatial impact of debris flows

Effective management and mitigation of landslides require a framework for action, given by the concept of risk. In a very broad sense risk could be explained as any undesirable effect. Wise et al. (2004) describe the concept of risk applied on landslides in typical forest development planning and operation in British Columbia. The specific risk $R(S)$ is the risk of loss or damage to a specific element, resulting from a specific hazardous landslide. Specific risk is mathematically expressed as:

$$[1] \quad R(S) = P(H) \cdot P(S:H) \cdot P(T:S) \cdot V(L:T)$$

$P(H)$ represents the probability of occurrence whereas the remaining terms on the right-hand side of Eq. 1 capture the consequence. More specifically, $P(H)$ is the probability of occurrence of a specific landslide and that landslide being a hazard to an element. $P(S:H)$ is the probability that there will be a spatial effect, given that a specific hazardous landslide occurs. For example in forestry risk analysis this is the probability that an event will reach a fish habitat or a road. $P(T:S)$ is the probability of temporal exposure of the

element, given that a spatial effect occurs. $V(L:T)$ is the vulnerability of an element, conditional on the element being at the site at the time of landslide occurrence.

There is a portfolio of tools available for debris flow risk assessment. Several empirical, mechanics-based or experimental methods are used in practice to assess the spatial impact $P(S:H)$, expressed as either travel distance or inundated area. Travel distance is the length along the path from head scarp to end of deposition, and runout length the distance traveled along the path from onset of terminal deposition to end of deposition.

3.2.3 Empirical rules for debris flow travel distance

This paper focuses on empirical rules and therefore mechanics-based approaches are not discussed herein. A concise overview of empirical methods for debris flow travel distance assessment is presented. Empirical tools can be divided into three main categories; angle of reach models, area inundation models and mass or volume balance models.

3.2.3.1 Angle of reach models

The simplest tools to estimate travel distance are the so called angle of reach models. These models are very simple and easy to use. They are built on quantified field observations. Due to the nature of debris flows these inventories often come with remarkable scatter. Data sets within an area are often small and therefore information of nearby mountain ranges has to be used. While variability within an area may be moderate, combination may increase the overall uncertainty (McClung, 2000). Angle of reach models basically use the total vertical distance h , between point of origin and end of deposition, and the empirically derived angle of reach α , to estimate the maximum horizontal travel distance l , where α is defined as:

$$[2] \quad \alpha = \arctan \left(\frac{h}{l} \right)$$

Heim (1932) introduced the angle of reach model and found that α corresponds with the average friction coefficient in a simple sliding block analysis Scheidegger (1973) related α to the landslide volume and showed that events with larger volumes travel further than smaller events. Corominas (1996) came to the same conclusion when he analyzed a total of 204 events from Spain and from literature. He found that unobstructed landslides

(i.e. without obstacles or restrictions), rockfalls, and rockfall avalanches, irrespective of their dimensions, exhibit higher α (i.e. shorter travel distances) than other kinds of movements. Earthflows, mudflows, and mudslides have low α and translational slides, debris flows, and debris avalanches are in an intermediate position.

Prochaska et al. (2008) proposed another angle of reach method based on 20 debris-flow events in the western United States and British Columbia. Instead of taking the angle from the head scarp, they use a reference point at halfway the vertical distance between top of the drainage basin and apex terminal deposition zone. They tested their model against 6 events, and predicted the horizontal travel distance within 64 to 130% of the observation. While their approach of using a mid-point reference is very interesting, the regression equation would benefit from more data points for model development. Testing the model against events that were not used for model development would further increase the confidence in the mid-point approach.

Angle of reach models are very easy to use but are gross simplifications and come with a large variability. They rely on total volume of an event, however volume magnitudes are a function of the volume change processes along the path of an event. Rickenmann (1999) compared various angle of reach models. He concluded that most of these relationships can only give an order of magnitude estimate of some debris flow parameters, but that they cannot provide an accurate prediction of these values. Nevertheless they are sometimes applied in preliminary risk assessments.

3.2.3.2 Inundation area models

Iverson et al. (1998) introduced semi-empirical equations to predict inundated valley cross-sectional areas (A) and planimetric areas (B) as a functions of lahar volume (V) in the form power laws:

$$[3] \quad A = \beta_A \cdot V^{2/3}$$

$$[4] \quad B = \beta_B \cdot V^{2/3}$$

The concept has been extended by Griswold and Iverson (1998) using 64 non-volcanic debris flows ranging in volume from 10^1 to 10^7 m³ and for 143 rock avalanches ranging from 10^5 to 10^{11} m³. Regression coefficients (β) with a fit of ($r^2 = 0.76 - 0.91$) were found

for the debris-flow and rock-avalanche data with standard errors ranging from 0.45 to 0.32. The resulting regression coefficients for debris flows are $\beta_A = 0.1$ and $\beta_B = 20$, and for rock avalanches $\beta_A = 0.2$ and $\beta_B = 20$. The equations were implemented in the so-called LAHARZ GIS approach using digital elevation models to produce hazard maps. The method allows prediction of events with larger magnitude than available from historical or geologic record. However, the methodology does not respect rheologies, flow dynamics and super-elevation potential that flows may encounter in channel bends or at obstacles. The model cannot determine the onset of terminal deposition. Based on a judgment call the user selects the apex of the fan.

Berti and Simoni (2007) analyzed 27 debris flows in the Italian Alps and reported regression coefficients; $\beta_A = 0.08$ and $\beta_B = 17$. While the LAHARZ model only applies for confined deposition; they proposed a modified version for debris flows called DFLOWZ. This model limits lateral spreading in unconfined terrain using an average deposition depth ($h = 0.06V^{1/3}$). In contrast to LAHARZ it allows input of a user defined flow path and factors to account for uncertainty in regression coefficients. Despite concerns that the cross-sectional area (A) of debris flows might not be constant along the whole deposition zone, good agreement was found between simulated and observed planimetric inundated areas for a constant A . Like LAHARZ, the model is very sensitive to geometry inputs, especially in less confined terrain. Even high-resolution digital elevation models (5m cell-size), derived from detailed topographic maps (1:5000 scale) poorly represented typical channels. More detailed input data gathered from field traverses improved the simulations.

Scheidel and Rickenmann (2010) proposed another GIS based inundation area model called TopRunDF. Based on 75 debris flow events from Austria, Switzerland and Northern Italy they postulated an empirical relation to calculate the mobility coefficient (i.e. β for planimetric area B) as a function of fan slope and channel slope. Model input parameters are event volume, average fan slope, average channel slope and starting point of deposition, number of Monte Carlo iterations as well as a high resolution digital elevation model (2.5m grid; LidAR based). Instead of assuming a constant cross-sectional area (A), a probabilistic algorithm determines depositional flow paths. The areas of all flow pathways are summed and the simulation stops when the sum

approaches the inundated area (B) given by their proposed empirical relation and an input volume. The volume is distributed in proportion to the outflow probability of a cell. Scheidel and Rickenmann (2010) tested TopRunDF for 14 debris flow events in Switzerland, and found reasonable agreement between predicted and observed deposition areas. Simulations are sensitive to the selected starting cell. The main uncertainties related to the flow paths simulation are the number of iterations per Monte Carlo simulation step, which controls the lateral flow spreading. Unfortunately the probabilistic algorithm for determination of flow path may prevent overflow of strongly incised channels and spreading has to be forced manually. An adapted algorithm might help to improve the spreading.

3.2.3.3 Mass or volume balance models

Mass or volume balance approaches form another group of empirical tools. These tools account for volume change along the path of an event. Unlike dynamic models, empirical tools neglect the rheology of debris flows and instead use parameters like geometry or morphology that are easier to obtain. Estimation of volumes in the field is a difficult task. Nevertheless, they give useful insights into debris flow behaviour. Empirical models using the volume update approach rely heavily on the quality of input data used to derive regression equations. A systematic method for data collection of debris flows is described in (Chapter 2).

Hungr et al. (1984) introduced the yield rate concept. Yield rate (Y) is the rate of volume change per unit length. The magnitude (M) of a potential debris flow to be modeled is the volume transported into the terminal deposition zone, comprising the initial landslide volume ($V_{initial}$), any point sources (V_{point}) from any tributary landslides and the sum of a characteristic (i.e. constant) yield rate multiplied by the length along the entire entraining channel (Hungr et al., 2005):

$$[5] \quad M = V_{initial} + \sum V_{point} + \sum_{i=1}^n Y_i \cdot L_i$$

The magnitude divided by a typical deposition thickness gives the size of depositional area.

Benda and Cundy (1990) proposed an empirical model to predict debris flow deposition based on field measurements of 14 debris flows in the Pacific Northwest, USA. The

event path is divided into reaches, and starting from the top, the gradient of each reach is assessed against two criteria: 1) Deposition is assumed for slope angles smaller than 3.5° ; 2) For slope angles between 3.5 and 20° deposition is assumed if the tributary junction angle (i.e. change in azimuth between previous and actual reach) is greater than 70° . A constant empirically derived yield rate (i.e. $8\text{m}^3/\text{m}$) is used to quantify entrainment. Robison et al. (2008) used the Benda and Cundy (1990) model to simulate 361 debris flow events triggered by the February and November storms of 1996, in North West Oregon, USA. Travel distance of 258 simulations matched observations: 73 simulations over-predicted, and 30 simulations under-predicted travel distance. Robison et al. (2008) conclude the Benda and Cundy (1990) model predicted a maximum (i.e. extreme) travel distance (larger or equal observation) for 92% of the simulations. The approach is easy to use, however it does not account for lateral confinement due to path morphology. Onset of deposition (at 3.5°) might be reasonable for the study area in the Pacific Northwest, USA, however it is likely higher in other regions, especially where debris flows contain coarser grained materials.

Based on 26 debris flow events in Hawaii, Cannon (1993) proposed a single regression equation to predict deposition using an initial volume equal to scar volume, segment length, lateral confinement (i.e. radius of flow channel) and slope gradient. The model was built using initial volumes ranging from 25 to 938m^3 , travel distances from 19 to 220m, slope angles from 26 to 47° and confinement defined by channel cross-section radii from 14 to 2000m. Starting with an initial volume, the rate of volume change is calculated reach by reach in the flow direction, and termination is assumed where the flow volume reaches zero. The model is thought to deposit only, and does not account for momentum loss in channel bends. The volume balance approach implicitly assumes constant bulk density.

Fannin and Rollerson (1993) described 449 debris flow events of the original Queen Charlotte Island (QCI) data base. The events were mapped in walk-over field traverses. Fannin and Wise (2001) used this data base and proposed an empirical-statistical tool to simulate travel distance and flow volumes of debris flows. The flow path is divided into reaches with uniform properties. Input parameters are initial volume, morphology (confined, unconfined and transition), slope angle, reach length, width, path azimuth.

Termination is assumed at the end of the reach wherein the flow volume becomes zero. The model by Fannin and Wise (2001) is based on a much larger inventory (i.e. 449 events) than the other volume based approaches discussed above. Three types of morphology are used to characterize lateral confinement. Five regression equations are used to quantify volume change processes. A bend-angle-function accounts for momentum loss in channel bends.

Empirical rules are relatively simple to use and often require only a few input parameters that can be measured in the field or obtained from a desk study. However, simplifying assumptions in the models (e.g. constant bulk density) have to be carefully evaluated. Rheology and mechanics are not considered in the approaches described above. Implicitly unique rheological behaviour is assumed across the model domain and flow behaviour is believed to be determined by terrain characteristics. Therefore they only apply in conditions similar to their origin. But should these empirical rules just be limited to their original study area? In this paper we test the following hypothesis: Within certain limitations, empirical-statistical rules for debris flow travel distance simulation can be applied in conditions different from the original study area. Rickenmann (2005) states that "...experience in applying empirical-statistical methods in different settings is still limited; however, potential exists for applying them in preliminary hazard assessments." This research tests the utility of an empirical-statistical tool in a study area with different climate, topography, event sizes and travel distances than its origin. Based on quantitative measures the success in simulating the correct volume change process, volume magnitude and travel distance is assessed.

3.2.4 Methodology

An empirical-statistical tool to simulate travel distance of debris flows on the Queen Charlotte Islands was proposed by Fannin and Wise (2001). To investigate the portability of these empirical-statistical rules, this tool is applied to a debris flow inventory from the Kootenays with different geo-bio-climatic conditions than the QCI. Both study areas are contrasted and datasets are carefully compared. Similarities in volume change processes are assessed for both inventories, as well as between simulated and observed data. Measures of success for the simulation are introduced and results are

compared to field observations. Applicability and limitations of the tool, and the volume (mass) update approach in general, are addressed.

3.3 Study areas and field investigation

A landslide inventory and terrain attribute study was conducted in the Nelson Forest Region, from 1996 to 2002, with most of the work done in the Kootenay-Columbia area (Jordan, 2002). The methods of field investigation for the Kootenay inventory are briefly summarized. A more detailed description of the field traversing method can be found in Chapter 2 and specific guidelines used for the inventory project are documented in Appendix A.

3.3.1 Field investigation

The Kootenay inventory was assembled by means of ground based survey. Professional geomorphologists traversed event paths along the full length, using methods comparable to those used in the earlier QCI study. Data was collected according to a standard checklist (Appendix A). The path was divided into several reaches with relatively uniform properties. For every reach, length, slope angle, azimuth, width and depth of erosion, width and depth of deposition were measured or estimated; and confinement, soil class, and vegetation were recorded. The width of entrained or deposited material, together with respective depth, was estimated from inspection of scarps, scours, trim-lines and deposits to estimate the according volumes. Photographs, sketches, aerial photographs and comments about further landslide attributes complement the documentation (see Chapter 2).

The size of the sample in the Kootenays is small, compared with the large data set collected in the QCI. Partly this reflects the resources available (two people for one field season). More importantly, in the Kootenays, the typical landslide frequency is much lower than in the QCI, so individual events are located a long distance apart and a large proportion of the available field time is consumed by travel to the sites. Also, since individual debris flow paths in the Kootenays tend to be longer than on the QCI, each field traverse takes relatively longer to traverse and record.

From the 29 events in the Kootenay inventory, 22 events were selected for analysis to include a range of sizes and event types (i.e. open slope, confined gullies). A total of 7 events were rejected; four events had multiple paths and volumes could not be assigned to particular channels; in two events the volumes could not be measured properly; one event ran over a residual snow cover and the analysis is not intended to account for this type of rheology.

The selected debris flows initiated on elevations from 710 to 1760 meters above sea level. For at least 9 events drainage diversion from logging roads played a key role in triggering the event in total 14 events initiation occurred on or below roads or trails. 8 events originated in clear-cut areas that were 6 to 15 years old, 2 events below clear-cut blocks. 4 events were unrelated to forestry activity. At least 3 events were triggered by snowmelt. Several years before one further event occurred, a forest fire caused strength loss in the initiation area and ultimately failure was triggered by seepage. Note that some events may have more than one of the attributes mentioned above.

3.3.2 Characteristic topographies, geologies, climates and vegetation

The Kootenay study area is located in the south east of British Columbia (Figure 3.1) comprising the Columbia Mountains, located west of the Rocky Mountains. The Columbia Mountains are underlain by Proterozoic folded and faulted sedimentary and metamorphic rocks (mainly gneissic), by Palaeozoic and Mesozoic sedimentary and volcanic rocks, and by batholiths and stocks of Jurassic and Cretaceous age. The study area contains mountains which are often quite rugged and plateaus. Elevations range from about 500m in the main valleys to over 3500m at the major peaks. The lower summits were covered by ice at one stage and sculptured by glaciers whereas higher summits form sharp saw tooth ridges. About 12,000 years ago the valleys were intensely glaciated. Glaciers remained on the higher peaks. On the retreat of the ice, glacial drift was deposited; which is typically thicker in valleys bottoms than on steep slopes (Holland, 1964). Steeper slopes may consist of rock outcrops and rubbly colluvium.

The Queen Charlotte Islands (QCI) are located before the Pacific Coast of British Columbia Mainland (Figure 3.1). The QCI have recently been renamed to Haida Gwai,

but for clarity the name Queen Charlotte Islands is used here. The study area is situated on the Skidegate Plateau, which belongs to the Outer Mountain Area of the Western Canadian Cordillera. Elevations range from 50 to 750 meters above sea level, and are characterized by a dissected plateau, with rounded hills and ridges and wide low-gradient valleys. Compared to the Kootenay study area with ragged reliefs of up to 2000m difference in altitude, the topography in the QCI is gentler. Bedrock is primarily Jurassic volcanic (basalt), Cretaceous sediments and metasediments are conglomerates and sandstones, and intrusive rocks are rare. The plateau was fully overridden by ice during the Pleistocene; hence all but the steepest slopes are mantled with glacial materials. Glacial deposits consisting of till, marine drift, stony clays and outwash sands are distributed throughout the area (Sutherland Brown, 1968).

In general the temperate coastal maritime climate of the QCI can be described as much wetter and milder compared to the Kootenay area. The average annual precipitation in Kootenays (Kaslo) is 890mm and a considerable portion falls as snow between November and March (Figure 3.2). The average precipitation on the QCI occurs mainly as rainfall and is significantly higher with 3340mm at Pallant Ck. The west of the QCI faces the open ocean and precipitation is higher (4500mm) than in the east (1200mm) of the islands. Generally the climate on the QCI is milder and less extreme than in the Kootenays.

Runoff of the study areas is illustrated by the discharge of two streams divided by their gross drainage area (Figure 3.2). The Kaslo River watershed is naturally regulated and has a gross drainage area of 453km² flowing into the Kootenay Lake (regulated at 532 masl). The runoff regime in the Kootenays is strongly related to snowmelt and rainfall on snow covers. During the winter months the runoff is moderate and but the discharge increases significantly with snowmelt between April and July. The Pallant Creek watershed (QCI) is naturally regulated and covers an area of 76.7km² including a lake which accounts for approximately 7% of its area. The median elevation of the Pallant Creek watershed is about 300 m. The runoff characteristic is closely related to the precipitation pattern in the area. Snowmelt plays a minor role.

The vegetation in the Kootenays is characterized by Interior Cedar – Hemlock (ICH) and Englemann Spruce – Subalpine Fir (ESSF). Forests typically contain western red cedar,

western hemlock, Douglas fir, lodgepole pine, western white pine, Ponderosa pine, western larch, grand fir, Englemann spruce and subalpine fir. On the Queen Charlotte Islands the vegetation is characterized by Coastal Western Hemlock (CWH); forests typically contain western red cedar, western hemlock, yellow cedar, Sitka spruce (Personal communication Peter Jordan 5th August, 2010).

3.3.3 Logging and road construction methods

Most logging on the QCI has been using cable yarding (high-lead) methods. However in the Kootenays – until the 1980s, most logging was by ground skidding, using skid trails on steeper slopes. Skid trails resulted in much erosion and site loss, and frequent slope instability, especially on slopes greater than 50%. Starting in the 1980s, cable logging has been increasingly used on steep slopes. Before the 1990s, most forest roads in the Kootenays were built with bulldozers, using sidecast (balanced cut-and-fill) construction. Road drainage and maintenance practices were often poor, and roads were often abandoned without deactivation. This resulted in many landslides due to unstable fills and road drainage diversions. Several Ministry of Forests initiatives in the 1980s, including the “Fish-Forestry Interaction Program” on the coast, and development of soil disturbance guidelines in the interior, led to gradual improvements in logging and road construction standards. The Forest Practices Code, which was introduced in 1995, included regulations and guidelines which mandated strict standards for road construction, maintenance, and deactivation, as well as limits on soil disturbance and the size of clear-cuts. The Forest Practices Code was repealed in 2004 and replaced with the Forest and Range Practices Act, which is much less prescriptive and more “results-based” (Fannin et al., 2005). However, most of the improved forest practices which were implemented during the Forest Practices Code period are still widely used, prompted in part by the desire of forest companies for third-party certification.

3.3.4 Landslide densities and frequencies

Average landslide density for the Kootenays, in areas steeper than 20°, ranges between 0.63 to 1.4 Ls/km². It tends to be higher (1 to 6 Ls/km²) in more landslide prone areas which consist mostly of kame and glaciofluvial deposits or deep morainal deposits.

(Jordan, 2002). For the QCI the landslide density is significantly higher. Rollerson et al. (2001) report a landslide density for clear-cut sites on the QCI of 8 to 17 landslides per km².

In terms of forest harvesting related landslide frequencies, Jordan et al (2010) report 0.01 to 0.05 Ls/km²/y for the Kootenays and 1 to 1.7 Ls/km²/y for the QCI. It should be noted that time base for frequency estimates differs between both study areas. The re-growth of vegetation is much faster on the QCI and evidence on airphotos disappears in about 15 years, where it takes 20 to 30 years in the Kootenays (Jordan et al., 2010). In general the landslide frequencies in British Columbia are higher in areas of higher precipitation.

Based on terrain attribute studies, Jordan et al. (2010) report that most significant variables in explaining development-related landslide occurrence in coastal British Columbia (e.g. QCI) are slope angle, presence of gullies, gully depth, presence of natural landslides, and slope configuration. However, these results vary somewhat between study areas. In the south-eastern interior, the most significant variables were terrain category (with glaciofluvial and deep morainal deposits having the highest landslide densities), presence of gullies, and presence of natural landslides.

In the Kootenays, most landslides are caused by roads; either by unstable road fills or road drainage diversions. Jordan (2002) found that the presence of roads in the Kootenays is more significant for landslide occurrence than clear-cuts. In contrast, on the QCI many, or most landslides, are caused by clear-cutting, with root strength loss and local hydrologic changes as contributing factors.

Many landslides in the BC interior have been caused by drainage diversions from forest roads and trails. A common situation results from forest development which occurs on gently sloping plateaus or benchlands above steeper slopes or incised river valleys. Landslides occurring in such topographic situations are commonly referred to as “gentle-over-steep” landslides. Since the gentle upland terrain is perceived by foresters and loggers as being of low hazard with respect to landslides and erosion, development has sometimes been carelessly planned, and drainage control is often poor (Jordan et al., 2010).

3.3.5 Characteristics of debris flow events

Based on slope morphology, the events were grouped into three different types according to the concept of Fannin and Rollerson (1993) summarized in the introduction. Three events of the Kootenay inventory are described for purpose of illustration.

3.3.5.1 Type 1

The event Revelstoke (Bigmouth) 11 is an example of a rather large (1870m^3) type 1 event in the dataset. Snowmelt triggered an initial volume of 780m^3 on a 39° steep slope. The event travelled in forested terrain on an open slope including two confined reaches. Figure 3.3 shows the profile of the event path. In several reaches dual-mode flow occurred (i.e. both entrainment and deposition). Figure 3.4a illustrates a part of the unconfined channel. The apex of the final depositional zone is on a 14° slope. Figure 3.4b is a side view of the main deposit, which exhibits the high log content in the debris. The total travel distance along the path was 660m, with a runout length of 180m.

3.3.5.2 Type 2

Airy Creek 3017 is an example of a type 2 event. Drainage diversion of a deactivated forestry road probably initiated a slide (60m^3) in a 28° steep open slope cut block. The profile in Figure 3.5 illustrates the steep path. Debris traveled through a few steep unconfined reaches (Figure 3.6a) and entered a gully. Figure 3.6b shows one of the steep (30°), confined reaches typical for type 2 events reaching a peak flow volume of 1330m^3 . Dual-mode flow occurred in the lower reaches. After the flow exited confined reaches, final deposition started on a 17° slope. The debris flow reached a creek at the bottom of the slope. The total volume transported into the final depositon zone had a magnitude of 820m^3 . Total travel distance along the path is 800m with 150m runout length.

3.3.5.3 Type 3

Figure 3.8a is a photo of the Blueberry Creek 2037 event taken from the air. A drainage diversion on a forest road during snowmelt triggered a slide of 130m^3 on a 33° slope in a clear-cut and initiated a debris flow that entered forested terrain. Typical for type 3 events; the gradient reduced significantly after entering the confined channel (Figure

3.8b). Lateral confinement allowed the debris flow to be highly mobile and travel 1580m along the profile shown in Figure 3.7. Several reaches show dual-mode flow behaviour. Final deposition of 2580m³ initiated on a 10° slope, due to loss of confinement, over a runout length of 390m.

3.4 Findings from inventory examination

3.4.1 Processes

3.4.1.1 Volume change process in relation to slope angle

Traditionally the onset of deposition is often related to the slope angle. Hungr et al. (2005) pointed out the need to establish two criteria; the slope angle where substantial erosion ends and the slope angle where deposition begins. Neither might be unique values for a given path but they are likely a function of slope angle, width and depth of channel, bed material, as well as the bank-slope angle, height, material, stability and tributary drainage discharge.

It is therefore interesting to see if there is a relation between slope angle and the volume change process (deposition or entrainment). To do so the 367 reaches of the 22 events in the Kootenay inventory were divided by morphology into unconfined (144 reaches), confined (198 reaches) and transition reaches (25 reaches). Transition reaches are defined to occur in the first unconfined reach following a confined reach. The loss of lateral confinement is believed to cause more deposition compared to an unconfined reach. The volume changes of each morphology type were grouped in slope angle bins. Within a bin the percentage of lengths of entrainment, deposition, dual-mode flow was calculated. Dual-mode flow describes reaches wherein both entrainment and deposition happens and the minor process is larger than 20% of the total volume change in the reach.

Figure 3.9 shows the volume behaviour occurrence for the Kootenays. Approximate lines are drawn to conceptually separate deposition, dual-mode flow and entrainment processes. Dashed lines divide deposition-only from dual-mode flow and dotted lines separate dual-mode flow from entrainment-only. The dashed line is used to find the slope angle below which the frequency of occurrence for deposition-only exceeds 50%

(marked with circle). The dotted line is used to find the slope angle where greater than 50% of the process is entrainment-only (marked with triangle).

For unconfined flow in the Kootenays (Figure 3.9a) deposition becomes the main process below 20° and entrainment is the main process above 23°. For confined flow (Figure 3.9b) the limit for deposition is below 6°, however only few data points exist in this range and inspection of the data showed that magnitude of deposition is not important. Entrainment becomes the main process above 10°. However, between 16° (open triangle) and 23° (solid triangle) dual-mode flow and deposition play a subordinate role again. The limited amount of transition flow reaches in the inventory does not allow for detailed interpretation.

Figure 3.10 is a similar plot for the QCI by Fannin and Wise (2001). As previously, approximate lines are drawn to conceptually separate the processes and the reported slope angles are indicated. For unconfined reaches (Figure 3.10a) deposition is the main process below 19° and entrainment above 24°. For confined flow, Fannin and Wise (2001) report deposition not to be important. Although it may actually not be significant, Figure 3.10b suggests that deposition is the main process below 6°. Entrainment is reported to dominate above 10°. For transition flow (Figure 3.10c) entrainment was found to be unusual and deposition governed on slopes gentler than 22°.

For confined and unconfined flow in the Kootenay, as well as in the QCI inventory, deposition governs on gentler gradients whereas entrainment dominates at steeper slope angles. An intermediate range of slope angles exists wherein entrainment, deposition and dual-mode flow processes occur. This has some important implications for deterministic models and is commented later in the discussion. Interestingly dual-mode flow is more frequent in the Kootenays.

3.4.1.2 Onset of terminal deposition

Slope angles at onset of terminal deposition were sampled from each event in the Kootenay inventory, by taking the slope angle in uppermost reach of terminal deposition. Whereas deposition might occasionally occur along the path, onset of terminal deposition was assumed where the debris flow begins to significantly deposit material. For all events in the inventory, onset of terminal deposition ranges between 0° and 30°.

The 0° refers to an event depositing on a road and the 30° to an event that crossed a road and started to deposit on the short steep embankment of the road. Exempting these two events from analysis, the following values were observed for the remaining 20 events: For onset of terminal deposition occurring in unconfined reaches (9 events) slope angles varied between 5° and 24° with a mean of 14° and median of 11°. In confined reaches (5 events) onset terminal deposition occurs between 8° to 10° with a mean and median of 9°. For transition reaches (6 events) the gradients vary between 3° and 17° with a mean and median of 10.0°.

For the Queen Charlotte Islands Fannin et al. (1997) report the following: Events on open slopes (type 1) are seen to deposit on greater slope angles ($15 \pm 8^\circ$) than type 2 events ($12 \pm 6^\circ$) which, in turn deposit at greater angles than type 3 events in relatively gentle gullies ($7 \pm 4^\circ$). Fannin and Rollerson (1993) further report that average gradients of events terminating in confined channels do not exceed 20°, with significant variation below this value. They conclude that gradient is not the only factor controlling the onset of deposition and observed that confinement of the channel, which is a function of channel width, also exerts an influence on deposition in channels with similar gradients.

3.4.2 Debris flow magnitudes and yield rates

Using volume as a criterion for event magnitude, defined as the total volume transported beyond the point of onset terminal deposition (V_d), the total range of magnitudes in the Kootenay inventory is between $97 < V_d < 4840 \text{ m}^3$. 1 event has a magnitude $V_d \leq 10^2 \text{ m}^3$, 10 events are between $10^2 < V_d < 10^3 \text{ m}^3$, and 11 events between $10^3 < V_d < 10^4 \text{ m}^3$.

Hungr et al. (1984) introduced the concept of yield rate. They suggested that an average channel yield rate Y (m^3/m) can be defined as:

$$[6] \quad Y = \frac{V_d}{(L-l)}$$

Where V_d (m^3) is the volume transported into the terminal deposition zone, L (m) is the total travel distance along the path and l (m) is the length of the terminal deposition zone (i.e. runout length). For the Kootenay inventory the yield rates are listed in (Table 3.1a). Average and mean yield rate of the Kootenay inventory are approximately between 2 and $3 \text{ m}^3/\text{m}$. Fannin and Rollerson (1993) reported yield rates for the QCI (Table 3.1b)

with averages between 12.4 and 22.7m³/m and medians between 8.6 and 12.4m³/m depending on event type.

3.4.3 Travel distances

For the 22 events in the Kootenay inventory the following observations were made regarding travel distance (Table 3.1a): 7 events initiated and terminated on an open slope (i.e. type 1) with an average travel distance of 416m. 10 events initiated either on an open slope or in a gully and entered mostly steep, confined reaches before depositing on fans or occasionally in low gradient confined channels (i.e. type 2). Average travel distance for type 2 events is 674m. Another 5 events initiated either on an open slope or in a gully and entered a confined channel as well, but in addition they traveled further due to low gradient confined reaches (i.e. type 3) with an average travel distance of 1862m. Like the total travel distance, the length of the terminal deposition zone is similar for type 1 and 2 but significantly longer for type 3 (Table 3.1a).

In the QCI inventory (Table 3.1b) type 1 events on open slopes were the most prevalent with 158 events, followed by 71 type 2 events in relatively short, gullied paths and 18 type 3 events in confined, long paths. Regardless of event type, the average travel distances as well as lengths of terminal deposition are considerably shorter compared to the Kootenay data.

3.5 Simulation of the Kootenay inventory

UBCDFLOW is an empirical-statistical tool for debris flow simulation, built from a data base of 449 events on the Queen Charlotte Islands. The simulation tool is applied to an inventory of 22 events from the Kootenay area. This section highlights key elements of the UBCDFLOW model and how simulated travel distances were derived. Measures of simulation success are introduced to assess the performance of the tool in comparison to field observations in the Kootenay area.

3.5.1 The UBCDFLOW model

The UBCDFLOW model proposed by Fannin and Wise (2001) uses a volume balance approach to simulate travel distance and volume change along the path of a debris flow.

The path is divided into reaches with uniform properties (Figure 3.11). Predictor variables are initial volume, slope angle, morphology (i.e. confinement), length, width and azimuth. A sensitivity analysis by Fannin et al. (2006) found width to be the most sensitive parameter for volume and travel distance simulation. Starting with an initial volume, the change in volume for each reach is calculated and the cumulative volume is updated in the flow direction. Based on slope angle and morphology an empirical algorithm determines whether deposition or entrainment occurs (Figure 3.12). The magnitude of volume change is calculated from the regression equations. Constant bulk density for all volume changes is implicitly assumed. Termination occurs where the cumulative volume becomes zero.

The original algorithm of UBCDFLOW in Fannin and Wise (2001) assumes the point of termination at the end of the reach wherein the cumulative flow volume becomes zero. Termination can happen anywhere in this reach but is assumed to happen at the end. While this approach is conservative, it only allows termination at arbitrarily chosen ends of reaches. To overcome this limitation we linearly interpolate the point of termination using the rate of volume change in the terminating reach. The rate of volume change is obtained by dividing the volume change in the reach by the reach length.

The Kootenay inventory contains no information about the path beyond the observed point of deposition. However 17 simulations do not terminate within the length of the traversed path, which prevents a calculation of travel distance. This issue is addressed by means of linear extrapolation. More specifically, the simulated rate of deposition in the last observed reach is used to establish the distance for which the volume diminishes to zero. 15 simulations are depositing in the last reach. Path profiles in the inventory generally flatten out towards the lower end, indicating that an additional reach would be governed by deposition as well. It is assumed that linear extrapolation yields in reasonable approximations for a maximum of 110% of the mapped travel distance. For two events where the simulation entrains in the last observed reach it is assumed that the simulation would exceed 110% of the observed travel distance.

For convenience in analysis of outputs for the whole inventory the model was programmed in a spread-sheet program. Alternatively a free online version is available under <http://www.civil.ubc.ca/UBCDFLOW>.

3.5.2 Quantitative simulation success indicators

Three indicators are introduced to assess the success of the simulation in the Kootenay study area. Appendix E illustrates the success indicators schematically.

The process indicator (PI) quantifies the percentage of observed travel distance along which volume change process was correctly simulated. The lengths ($L_{i,p}$) of every reach in which the simulated process was found in agreement with field observation of entrainment or deposition are summed up and divided by the total observed travel distance, given by the sum of all reaches (L_i) within an event.

$$[7] \quad PI = \frac{\sum_{i=1}^n L_{i,p}}{\sum_{i=1}^n L_i} \cdot 100\%$$

The process indicator shows how well the empirical core of UBCDFLOW captures the volume change process, regardless of the magnitude of volume change.

Cumulative volume is defined as the sum of initial volume plus all volume changes upslope of the point of interest. The highest cumulative volume often occurs immediately before onset of terminal deposition and may be interpreted as a measure of magnitude. The simulated cumulative volumes $V_{i,s}$ are plotted along the path indicating the volume balance. The maximum value of the volume balance is the peak cumulative volume of a simulation. Similarly the peak cumulative volume for the field observations is found by summing up the observed volume changes in flow direction and selecting the maximum value. The magnitude indicator MI is the ratio of simulated peak volume ($V_{s,peak}$) to the observed ($V_{o,peak}$):

$$[8] \quad MI = \frac{V_{s,peak}}{V_{o,peak}} \cdot 100\%$$

The MI quantifies how well the simulated magnitude agrees with field observations. In the ideal case, where the peak simulated volume of simulation and observation are the same, the indicator is 100%.

The relative success for the spatial impact of the simulation is quantified by the travel distance indicator (DI). The DI is simply the ratio of simulated to observed total travel distance:

$$[9] \quad DI = \frac{L_{s,t}}{L_{o,t}} \cdot 100\%$$

If total travel distance is under-predicted the indicator is smaller than 100%, if the simulated travel distance exceeds the observation it is higher than 100%.

3.6 Results of simulation

Following a description of the simulation routine, examples of three simulations are illustrated to provide an understanding of how the results were derived. Thereafter, key results of the entire analysis are summarized. A guideline for interpretation of field data as UBCDFLOW input is given in Appendix F.

3.6.1 Simulation algorithm

The simulation routine starts with the initial volume (V_{init}) and moves on to the next reach (see flow chart in Figure 3.12). The mode of flow and the slope angle determine what regression equation has to be used and the corresponding volume change (dV_i) in the reach is calculated. Subsequently the volume change is added to the cumulative volume of the previous reach in to obtain a new cumulative volume. If the updated cumulative volume is larger than zero, the same procedure is carried out for the next reach. Otherwise termination occurs within the reach.

3.6.2 Example volume balances

In Figure 3.13, examples of simulated and observed cumulative flow volumes along the path are plotted for the previously introduced examples of type 1, 2 and 3 events in section 3.3.5. The observed cumulative flow volumes, indicated with a dashed line, are a simple summation of observed volume changes starting from top. These volumes were not corrected for errors in estimation, change in density etc. and therefore the observed cumulative volume is not necessarily zero at the point of termination. However, the last point in the curve indicates the observed end of the event, regardless of the volume balance. The simulated cumulative flow volumes, indicated with a black solid line, were calculated using UBCDFLOW. The point of termination was inter- or extrapolated as described above.

The type 1 event, Revelstoke (Bigmouth) 11 (Figure 3.13a), started with an initial volume of 780m^3 . Observation shows that entrainment was moderate in the upper path yielding in a peak cumulative flow volume of 1500m^3 . In the middle reaches comparatively small volume changes (ranging from -40 to 140m^3) were observed. This is typical for open slope events where the path is mostly unconfined. However, in the middle reaches, the simulation entrained up to a very large peak cumulative flow volume of 2690m^3 , yielding a magnitude indicator $MI=179\%$. Thereafter, the slope angle dropped from approximately 23° to 14° and both simulation and field observation show a clear trend of deposition. The simulation did not reach zero volume at the end of the traversed path, and therefore the travel distance is extrapolated to 690m or a travel distance indicator $DI=104\%$. For 480m of the total 660m of observed travel distance the simulated volume change agreed with observation, yielding in a process indicator $PI=72\%$.

The type 2 event Airy Creek 3017 (Figure 3.13b) started with a very small initial volume of 60m^3 and entrained significantly more along the path. The observed peak cumulative flow volume of 1330m^3 was matched by the simulation. Immediately after the flow crossed a road (reach 7-6) it entered an unconfined reach. The simulation captures the observed deposition. The following reaches were again confined and the simulation agrees with the observation that no significant volume change occurred despite the low slope gradients (6 to 10°). The main part of deposition happened after confinement was lost on an open slope with a gradient of approximately 3° . The point of termination for the simulation was extrapolated to 820m or a $DI=102\%$. The simulated volume change process was identical to the observed yielding $PI=100\%$.

The type 3 event Blueberry Creek 2037 (Figure 3.13c) started with a relatively small initial volume of 130m^3 . After passing a few unconfined reaches, the debris flow entered a confined channel and observed cumulative volume peaked at 1760m^3 . The simulation captured this behaviour, but overestimated entrainment in the confined channel resulting in 2630m^3 peak cumulative volume or a magnitude indicator $MI=149\%$. Except for one, all other reaches after the peak were unconfined and deposition was observed. However, for the one confined reach the model simulated no volume change. The point of termination was extrapolated to 1650m or a $DI=104\%$. For 1470m of 1580m total

mapped travel distance the simulated volume change had the same trend as observed resulting in a PI=93%.

In general the example simulations in Figure 3.13 captured the observed trend in volume change reasonably well (PI of 72%, 100% and 93%). However, where the magnitudes agreed for Airy Creek 3017, the simulation overestimated peak cumulative volumes for the other two events; MI=179% for Revelstoke (Bigmouth) 11, and MI=149% for Blueberry Creek 2037. Regardless, simulated travel distances were remarkably close to field observations (DI 104%, 102% and 104%).

3.6.3 Key results of the Kootenay inventory simulation

In Table 3.2 the results of all 22 events in the Kootenay inventory are summarized. The mean value of process indicator for the dataset is 80%, with a median of 81%, and a range from 58 % to 100%. Hence the predicted volume change process (entrainment, deposition or zero volume change) agreed with field observations in 80% of the traversed lengths in the inventory. A similar rate of success can be found with respect to number of reaches. The inventory contains a total of 367 reaches, and the volume change was correctly simulated for 281 reaches (77%).

The average magnitude indicator MI is 180%, with considerable scatter from 51% to 552%. The geometric mean (159%) indicates that a few extreme values are quite large. Only for two events is the MI less than 100%, which indicates the simulation consistently overestimated entrainment-volume.

The travel distance indicator DI was between 89% and 110% for 15 of 22 events. Extrapolation of travel distance for the remaining 7 simulations exceeded the maximum limit for extrapolation (i.e. 110% of observed travel distance).

3.7 Discussion

3.7.1 Patterns and attributes of inventories

3.7.1.1 Processes

Despite these differences, similarities in volume change behaviour were found for both study areas. In Figure 3.9 and Figure 3.10 volume change processes vs. slope angle

are given for the different morphology types. The interpretation of slope angle domains for governing processes is somewhat subjective, but it allows for some important comparisons. For unconfined flow in the Kootenays, deposition is the main process below 20° and entrainment above 23° . This range is approximately the same for the QCI, with 19° and 24° . For confined flow, deposition is the main process below 6° , but it is not an important factor in both study areas. Above 10° entrainment is the governing process in the QCI. Interestingly the same limit is found for the Kootenays as well, but between 16° and 23° dual-mode flow and deposition again play a role. More data may help to explain the increased frequency of deposition in that range. Individual mapping preferences of terrain professionals may be related to the high frequency of dual-mode of flow. The similarity in process occurrence is critical for the simulation success because the UBCDFLOW algorithm uses slope angle and morphology type to decide on the algebraic sign and magnitude of volume change.

In general dual-mode flow is more frequent in the Kootenays, and it is not clear why this is the case. Where the volume change behaviour between the study areas differs, it might be due to different individual interpretation of by the individual field mappers plays another important role in each study area.

Various studies on the onset of deposition are discussed in Hungr et al. (2005) and summarized in Table 3.3. Hungr et al. (1984) and Fannin and Wise (2001) (for Queen Charlotte Islands) make a distinction between confined and unconfined flow and in both studies deposition starts on steeper slopes for unconfined flow. The observed mean (14°) and median (11°) for onset in unconfined reaches, and mean and median (9°) in confined reaches agree with these findings. From a mechanical point of view, it could be argued that confined events are likely to have higher pore-pressures and experience higher flow velocities than unconfined events, causing them to flow further into gentler terrain. However, the data points in the Kootenays vary in a large range (0° to 30°). Similarly Fannin et al. (1997) found large scatter for the QCI.

There are several reasons for the low gradients observed in some unconfined reaches of the Kootenay dataset. For a few events the channel above the onset of terminal deposition was confined and therefore allows debris flow to travel far into relatively flat terrain. As soon as confinement is lost deposition occurs in unconfined low gradient

reaches. Abrupt changes in terrain from relatively steep to flatter slopes are further reasons for onset of deposition on low, unconfined slope angles. The idea of terrain breaks or sharp changes in flow direction is also reflected in the research of Benda and Cundy (1990). Overall the mean and median for onset of terminal deposition in the Kootenays agrees with the work of others listed in Table 3.3, except for Wong et al. (1997) who report deposition on fairly steep terrain (>30-40°) for small debris flows in Hong Kong. Inspection of the Kootenay data showed that road-crossings (low gradients) may also be critical for onset of deposition.

3.7.1.2 Yield rates

The yield rates in the Kootenay data base (Table 3.1a) range between 2 and 3m³/m on average. For the QCI the average ranges between 12 and 23 m³/m depending on type of event. Average yield rates for the Kootenay inventory were approximately a factor of 5 lower compared to the QCI (depending on event type). There might be several factors controlling the yield rate, e.g. erodibility of the channel bed itself, material available from adjacent bank slopes, rates of weathering in different climate regions, competence of bedrock, thickness of humus layers, frequency of occurrence (time in-between events), and magnitude of events and discharge of water. Most of the events in the QCI occurred in clear-cuts, compared to only a third of the Kootenay events. The paths had various degrees of vegetation, likely contributing to the low yield rates. Unfortunately, no information is available regarding typical grain size distributions of the debris in both study areas that would allow further speculation on typical material characteristics.

Hungr et al. (2005) summarized debris flow yield rates from the literature. The reported values suggest that yield rates in the Kootenays are rather moderate. No significant correlations were found between observed yield rate and event magnitude. It should be noted that yield rates are a gross simplification of the volume change behaviour and actual yield rates along the path may vary considerably from the average value.

3.7.1.3 Travel distances

In general debris flow paths were shorter on the QCI (Table 3.1). Average travel distances in the Kootenays were longer compared to the QCI (roughly by a factor 2.8 to 3.8, depending on event type). This is likely related to differences in the topographic

settings. In the Kootenays the reliefs are ragged and differences in altitude between summits and valley bottoms can be as large as 2000m. This allows events to travel over larger distances, compared to the gentler topography in the QCI, where the relief is more rounded and vertical differences are smaller.

3.7.2 Simulation vs. observation

This section discusses the simulation success of the empirical-statistical UBCDFLOW rules established from field data of the QCI and applied on Kootenay inventory.

3.7.2.1 Process

The performance of the empirical rules (Figure 3.12) is addressed by the process indicator PI (Eq. 7). Regardless of the magnitude, the PI informs if the correct process (i.e. entrainment, deposition or no volume change) is simulated. An average PI of 80% (Table 3.2) for the entire inventory shows that UBCDFLOW is capable to correctly capture the processes for the majority of reaches. The largest part of the error in process simulation happens in low gradient ($<10.5^\circ$) confined reaches, where the empirical rules predict zero volume change instead of deposition or entrainment as observed.

To a certain extent the success process simulation implies that empirical rules describing the volume change process in the QCI, also apply in the Kootenay area. This encouraging finding is likely due to the similar ranges for dominant processes in both inventories (Figure 3.9 and Figure 3.10).

3.7.2.2 Magnitude

The magnitude indicator MI (Eq. 8) illustrates the success of quantitative volume change estimations. For almost all events it is well above 100%. This means that simulated peak cumulative volumes are significantly higher than observed. This over-prediction suggests that the model is not capable to match the volumetric magnitude of debris flow events in the Kootenays.

A partial explanation for the high peak cumulative volumes of the simulation can be found in the yield rates. Table 3.1 suggests that average yield rate for QCI is approximately 5 times (or more) the yield rate in the Kootenay area. A correlation test

between MI and yield rates for each event showed no strong trend that would suggest the use of yield rates for scaling rules. Errors in estimating the volumes in the field are another reason, for simulation and observation to disagree.

3.7.2.3 Travel distance

Travel distances in the Kootenays were roughly a factor 2.8 to 3.8 longer than on the QCI, reflecting the typically greater local relief and longer channels. Consequently the tool had to simulate longer travel distances. Overall 15 out of 22 events (or 68% of all simulations) terminated within 89 and 110% of the observed travel distance (Table 3.2). The remaining 7 events overestimated travel distance beyond 110%. This fair agreement and the overall good agreement in process simulation (i.e. high PI) imply that the tool partially compensates for the over-prediction in entrainment. However, the amount of volume compensated depends not only on the simulated rate of deposition but also the length available to deposit and the length wherein no volume change is simulated (i.e. low gradient confined reaches).

However it should be noted that for a total of 7 events travel distances were slightly underestimated (i.e. travel distance indicators smaller than 100%) with the most unconservative simulation (i.e. East Kootenay 5001) of 89% of the observed travel distance.

3.7.2.4 Overall simulation success

With an average process indicator of 80% for the whole Kootenay inventory UBCDFLOW seems to capture the volume change processes fairly well. However it overestimates volume changes. Nevertheless 68% of the simulated events terminated between 89% and 110% of the observed travel distance. These results emphasize the utility of the tool for preliminary risk assessment.

3.8 Summary and conclusions

A dataset of 22 debris flow events from the Kootenay region was selected to investigate the utility of empirical-statistical rules originally proposed by Fannin and Wise (2001) to simulate events on the Queen Charlotte Islands (QCI). Both study areas have significantly different geo-bio-climatic attributes. The Kootenay mountains have greater

relief and generally steeper slopes, with bedrock outcrops and shallow colluviums, compared with deeper glacial deposits in the QCI. The climate in the QCI is considerably wetter and milder in contrast to the Kootenays where a part of the annual precipitation occurs as snowfall. Average travel distances in the Kootenays were longer compared to the QCI (roughly by a factor 2.8 to 3.8, depending on event type), reflecting the greater relief and longer channels. Average yield rates for the Kootenay inventory (i.e. 2 to 3m³/m) were approximately a factor of 5 lower compared to the QCI (12 and 23 m³/m, depending on event type).

Despite these differences, remarkable similarities were found regarding the volume change processes as a function of the slope angle. Especially the upper limit for deposition is of particular interest in engineering practice:

- For unconfined reaches of the Kootenay inventory deposition is the main process below a slope angle of 20° and entrainment above 23°. This is very similar to the corresponding values of 19° and 24° observed in the QCI data.
- In confined reaches of the Kootenay inventory deposition is the main process below 6°, but deposition rates are not significant. Entrainment is the main process above 10°, with dual-mode flow (i.e. simultaneous occurrence of entrainment and deposition) playing a lesser role. These observations agree with the corresponding values of 6° and 10° in the QCI.
- Between the limits listed above, there is an intermediate range of slope gradient where both entrainment and deposition occur frequently. In addition, dual-mode flow was observed in both data sets, for unconfined as well as confined flow in various ranges of slope angle. This implies that the volume change process cannot be inferred from slope angle and confinement alone. The existence of an intermediate range of slope angles, where the process is not clearly defined by slope angle, may also have important implications for the use of other decision support tools that consider mass or volume changes.

The simulation of the Kootenay inventory using the empirical-statistical rules from the QCI was assessed based on three quantitative measures of success for process, magnitude and travel distance:

- For 80% of the lengths in the Kootenay dataset the empirical rules from the QCI captured the observed volume change process correctly (entrainment, deposition or zero volume change). The UBCDFLOW algorithm determines the process based on the slope angle. Similar patterns in observed process as a function of slope angle for both study areas explain this simulation success. Therefore, the rules deciding on the process seem to be portable from QCI to Kootenay.
- For the whole dataset the average magnitude indicator was 180%, pointing out that the empirical-statistical rules over-predict the magnitude of volume change in the Kootenays. The higher yield rates in the QCI explaining over-prediction of volumes in the Kootenays. Consequently, magnitude simulations are not applicable in the Kootenays.
- For 15 out of 22 events the simulation terminated within 89 and 110% of the observed travel distance. For 7 events the simulation went beyond 110%. This fair, generally conservative agreement on travel distance is probably due to an overall reasonable simulation of the process and to a certain degree the over-prediction in entrainment is compensated with an over-prediction of deposition.

Table 3.1 a) Kootenay inventory overview by event type. Total travel distance along path L, length of terminal deposition zone I and yield rate Y. b) QCI inventory overview by event type (data from Fannin and Rollerson 1993).

a) Kootenays

Event type	# of events	L (m)						I (m)						Y (m ³ /m)					
		Avg	Med	GM	SD	Min	Max	Avg	Med	GM	SD	Min	Max	Avg	Med	GM	SD	Min	Max
1	7	416	327	363	n.a.	154	667	111	107	92	n.a.	31	215	3.1	2.3	1.6	n.a.	1.6	7.5
2	10	674	588	629	n.a.	377	1431	134	104	112	n.a.	51	352	2.6	2.3	2.3	n.a.	0.8	4.5
3	5	1862	1653	1798	n.a.	1442	2933	290	225	261	n.a.	128	482	2.0	1.7	1.0	n.a.	0.0	5.0

b) Queen Charlotte Islands

Event type	# of events	L (m)						I (m)						Y (m ³ /m)					
		Avg	Med	GM	SD	Min	Max	Avg	Med	GM	SD	Min	Max	Avg	Med	GM	SD	Min	Max
1	158	122	84	97	99	-	-	40	31	32	31	-	-	22.7	12.4	11.3	29.0	-	-
2	71	177	155	142	125	-	-	46	36	35	35	-	-	12.9	6.3	6.5	20.1	-	-
3	18	668	485	523	509	-	-	181	93	114	181	-	-	12.4	8.6	6.7	13.2	-	-

Notes: L= total event length; I= length terminal deposition zone; Y= yield rate (after Hungr et al.1984); Avg= arithmetic mean; Med= Median; SD= standard deviation; Min= Minimum; Max= Maximum; n.a.= not applicable; -=unknown

Table 3.2 Simulation results.

	Area	Slide	Process PI ^a (%)	Magnitude MI ^a (%)	Distance DI ^a (%)
Type 1	Airy Creek	1620	71	394	> 110 ^b
	East Kootenay (Dewan)	5000	58	217	> 110 ^b
	East Kootenay (Hellroaring)	5001	94	187	89
	East Kootenay (Hellroaring)	5002	74	239	104
	Nelson Area (SandyCk)	2018	94	197	96
	Revelstoke (Bigmouth)	11	72	179	104
	Giveout Creek	5006	62	108	> 110 ^b
Type 2	Airy Creek	1621	97	51	89
	Airy Creek	3017	88	100	102
	Burton Creek	1660	84	164	> 110 ^b
	Koch	507	85	136	101
	Koch (Little Slocan)	1637	58	200	> 110 ^b
	Nelson Area (Cottonwood)	2017	80	162	99
	Nelson Area (Duhanel)	1740	82	183	95
	Revelstoke (Bigmouth)	5	100	112	105
	Sitkom Area (Bourke)	3000	63	88	> 110 ^b
	Summit-Shanron	5004	94	145	97
Type 3	Blueberry Creek	2037	93	149	104
	Burton Creek	106	93	173	105
	Fitzstobbs	1689	78	134	97
	Koch	1738	71	552	> 110 ^b
	Fortynine Creek	2026	70	103	102
All Types	Arithmetic Mean		80	181	n.a.
	Median		81	163	n.a.
	Geometric Mean		79	159	n.a.
	Minimum		58	51	89
	Maximum		100	552	n.a.

^a see Eq. [7];[8];[9] for definition of indicators.

^b extrapolated point of termination exceeds 110% of observed travel distance.

Table 3.3 Characteristic slope angles from literature.

Authors	Description	Confinement	Onset Deposition
Ikeya (1981), Okubo and Mizuyama (1981)			10°
Hungre et al. (1984)	coarse-grained non-volcanic debris flows, south British Columbia, CA	Confined	8-12°
		Unconfined	10-14°
Wong et al. (1997)	small debris flows and debris avalanches, Hong Kong		>30-40°
Benda and Cundy (1990)	Debris flows in the Pacific Northwest, USA		3.5 ^o
Fannin and Wise (2001)	Debris flows QCI and coastal British Columbia, CA	Confined	10-22°
		Unconfined	19-24°
Jordan (1994)	Coarse-grained debris flows derived from igneous rocks of Coast Plutonic Complex, south British Columbia, CA		7-15°

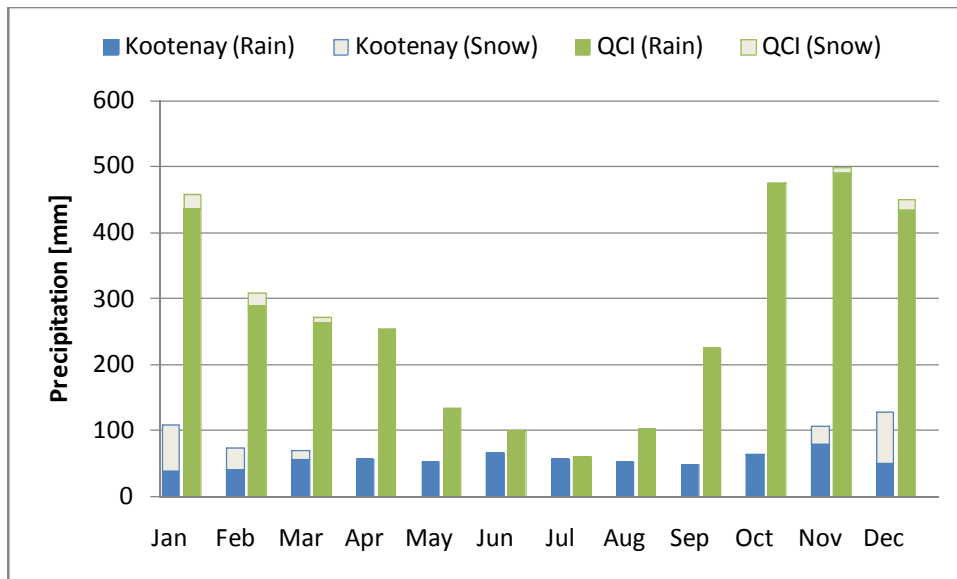
Note: Reported values for Lahars excluded from table, Vargas State disaster excluded because onset of deposition not reported

^o or earlier if a sharp change in flow direction



Figure 3.1 Location map: Queen Charlotte Islands on the coast of British Columbia and Kootenay study area in the interior. Points indicate location of weather/ hydrometric stations.

Precipitation



Runoff

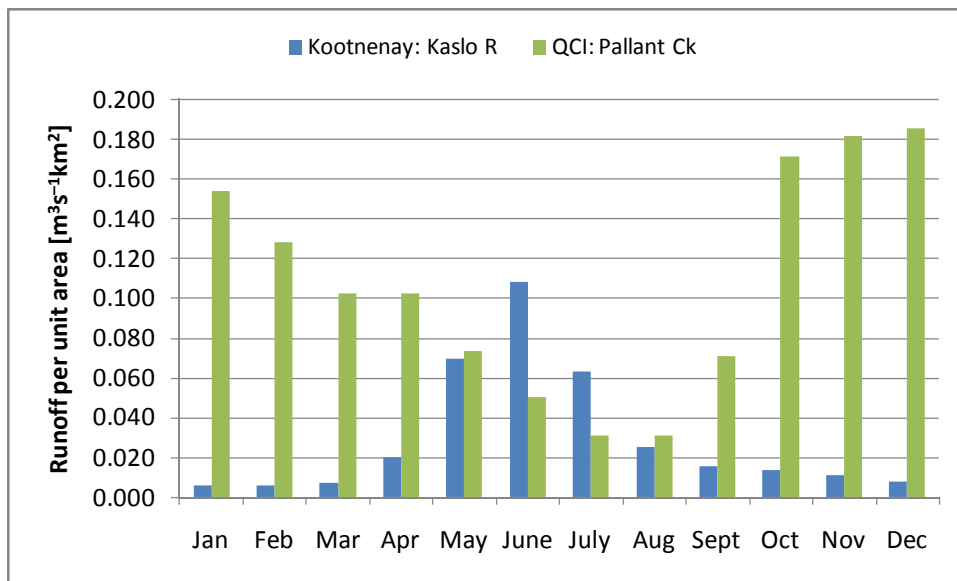


Figure 3.2 Precipitation in Kootenays (Kaslo R.) is significantly smaller, with a considerable portion of snow, compared to QCI (Pallant Ck.). Runoff regime in Kootenays (Kaslo R.) is strongly related to snowmelt, whereas it is controlled by precipitation on QCI.

Data: <http://www.climate.weatheroffice.ec.gc.ca>; <http://www.ec.gc.ca/rhc-wsc/>

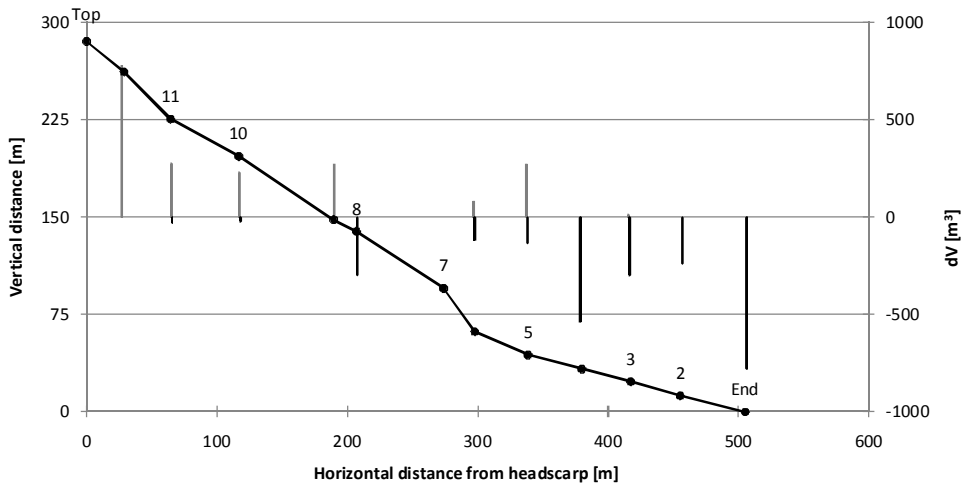


Figure 3.3 Example of event type 1: Revelstoke (Bigmouth) 11. Solid line indicates path profile, bars are volume changes in each reach.

a)



b)



Figure 3.4 Example of Type 1 event Revelstoke Bigmouth 11. a) from point 10, looking down the path of the open slope event. b) main deposit in reach 2-end (geomorphologist for scale).

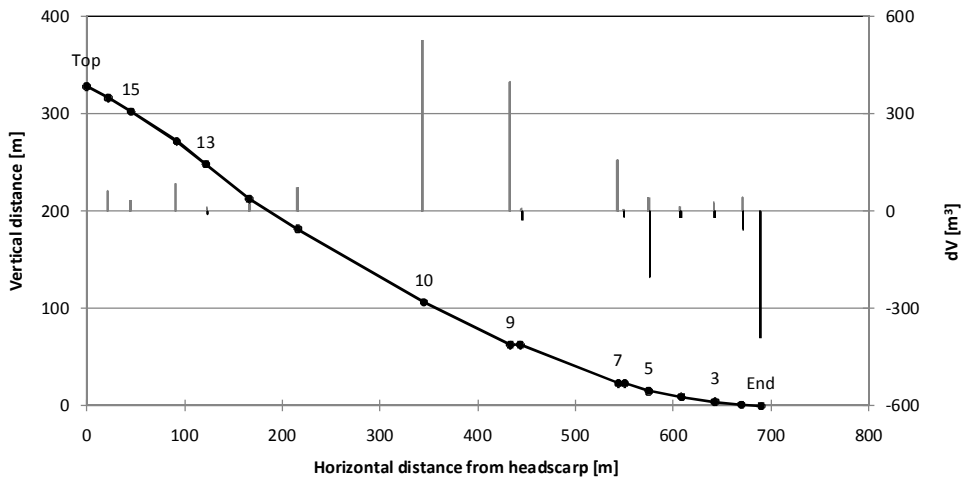


Figure 3.5 Example of event type 2: Airy Creek 3017. Solid line indicates path profile, bars are volume changes in each reach.

a)



b)



Figure 3.6 Example of Type 2 event Airy Creek 3017. a) looking up into unconfined path (reach 14-15) before the flow becomes confined (mapper for scale). b) Looking down the path of the confined channel (reach 10-11), average width 15m.

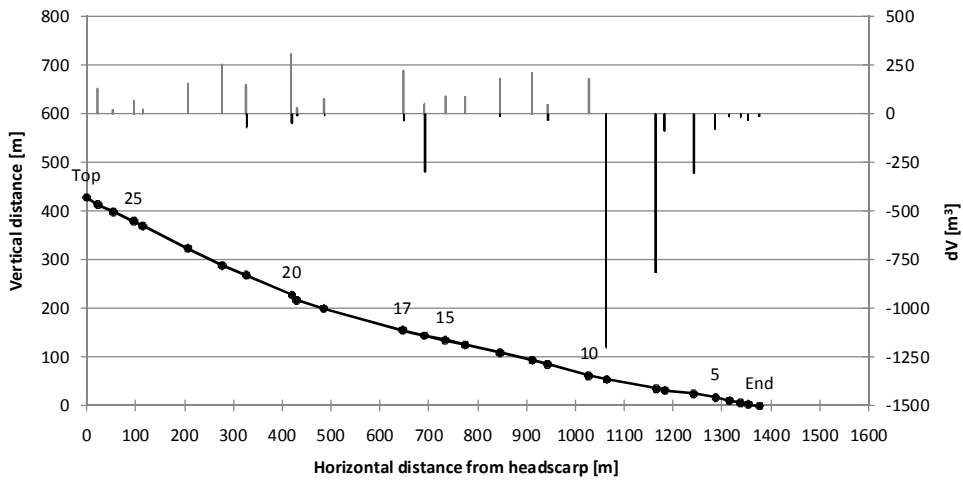


Figure 3.7 Example of event type 3: Blueberry Creek 2037. Solid line indicates path profile, bars are volume changes in each reach.

a)



b)



Figure 3.8 Example of Type 3 event Blueberry Creek 2037. a) Photo taken from air. b) looking down the confined channel (from point 17).

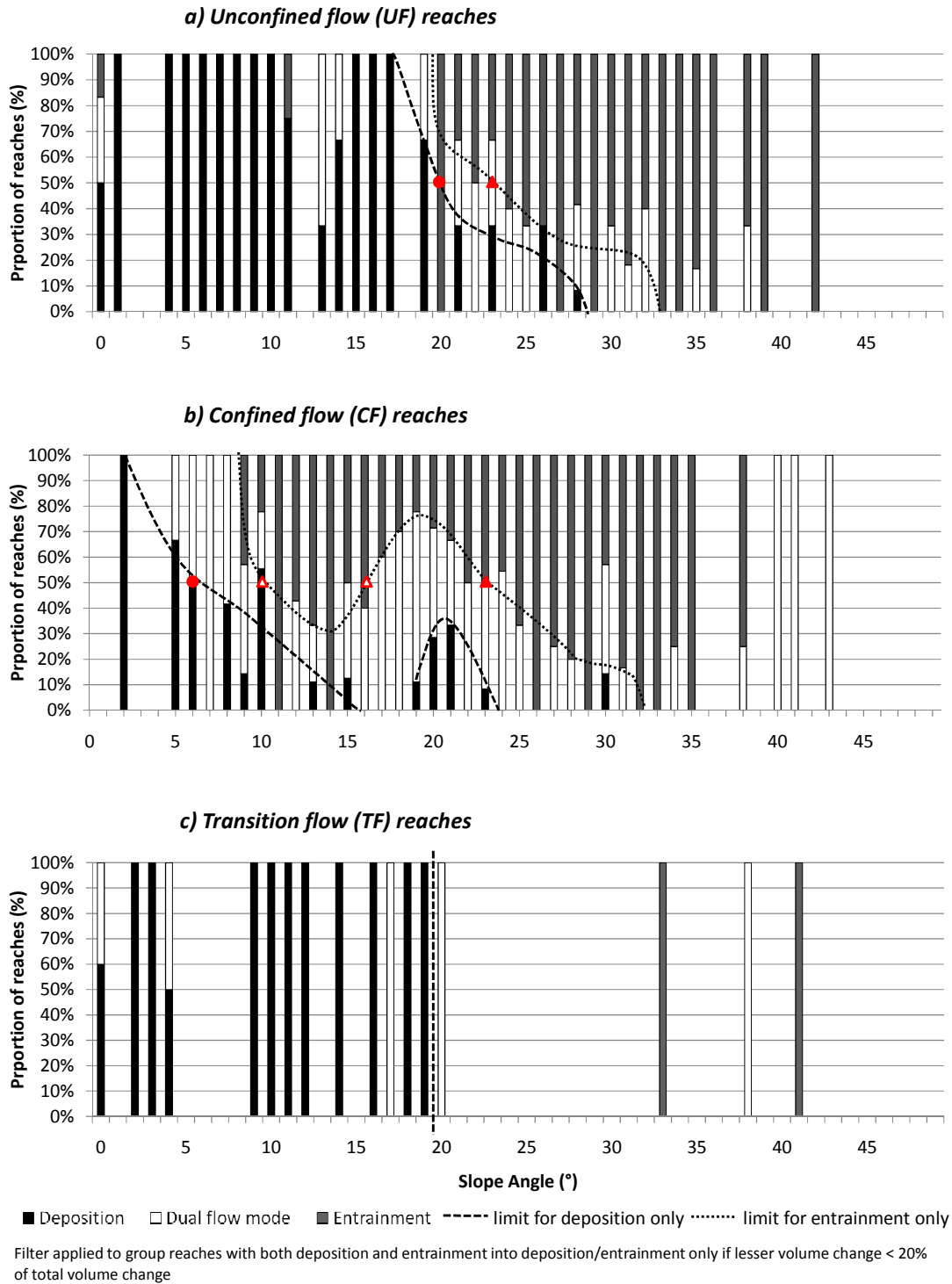


Figure 3.9 Volume behaviour occurrence Kootenay.

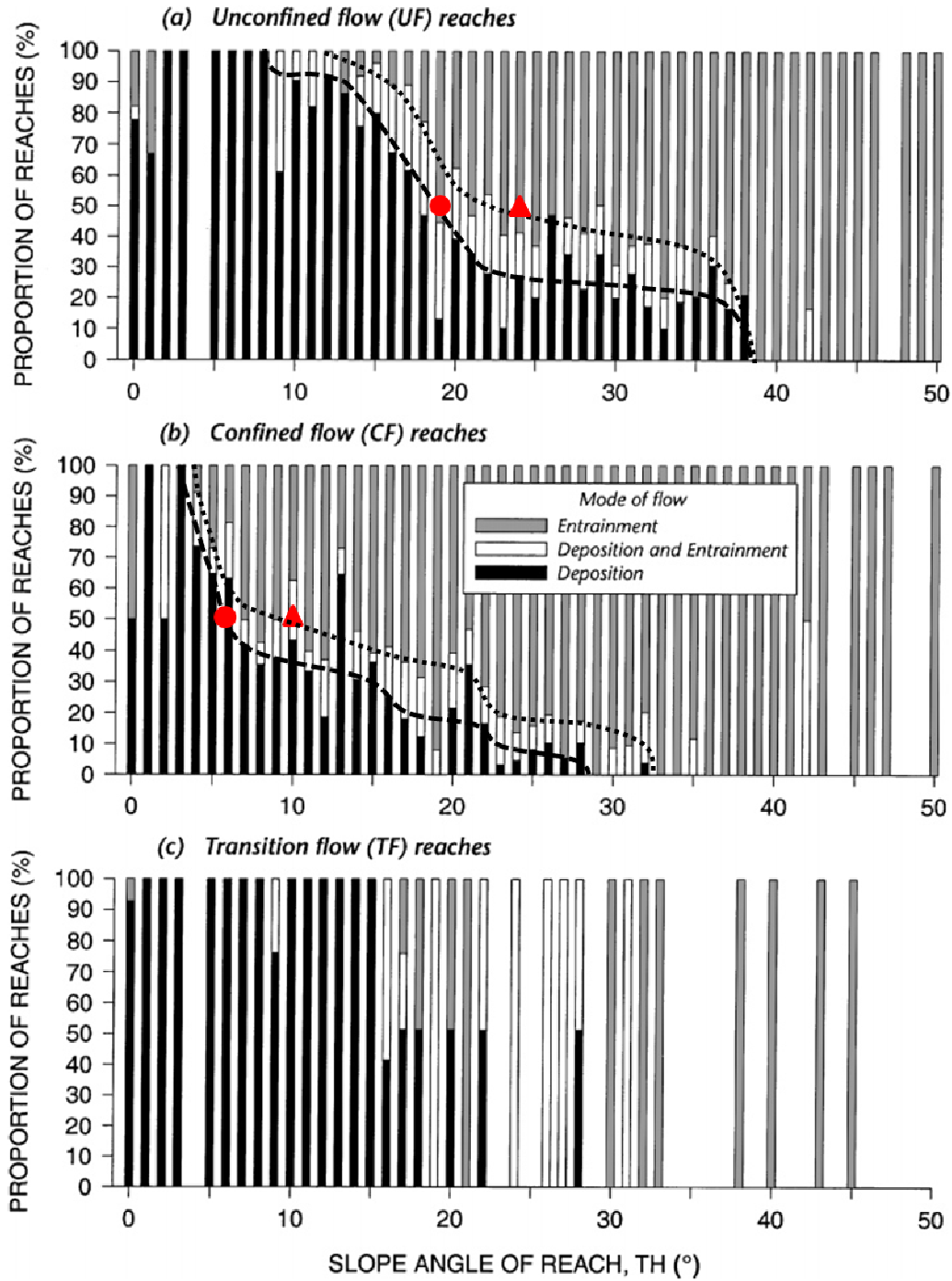


Figure 3.10 Volume behaviour occurrence QCI.

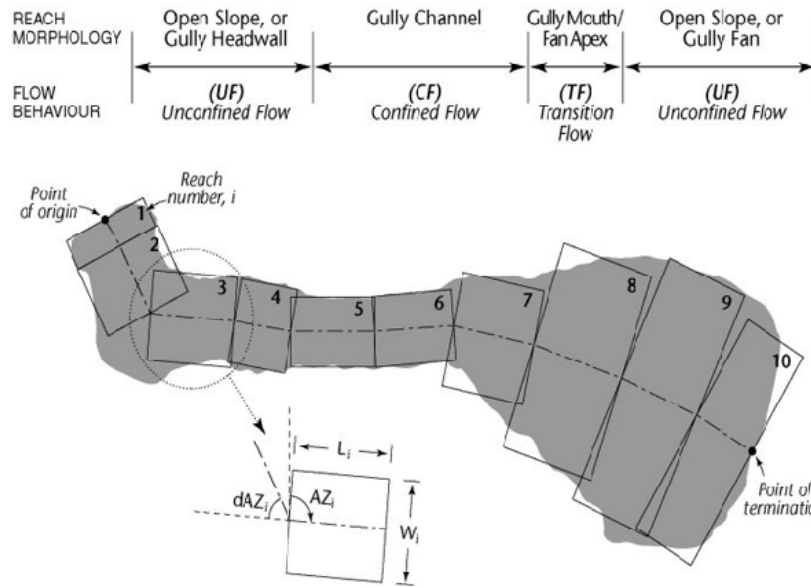
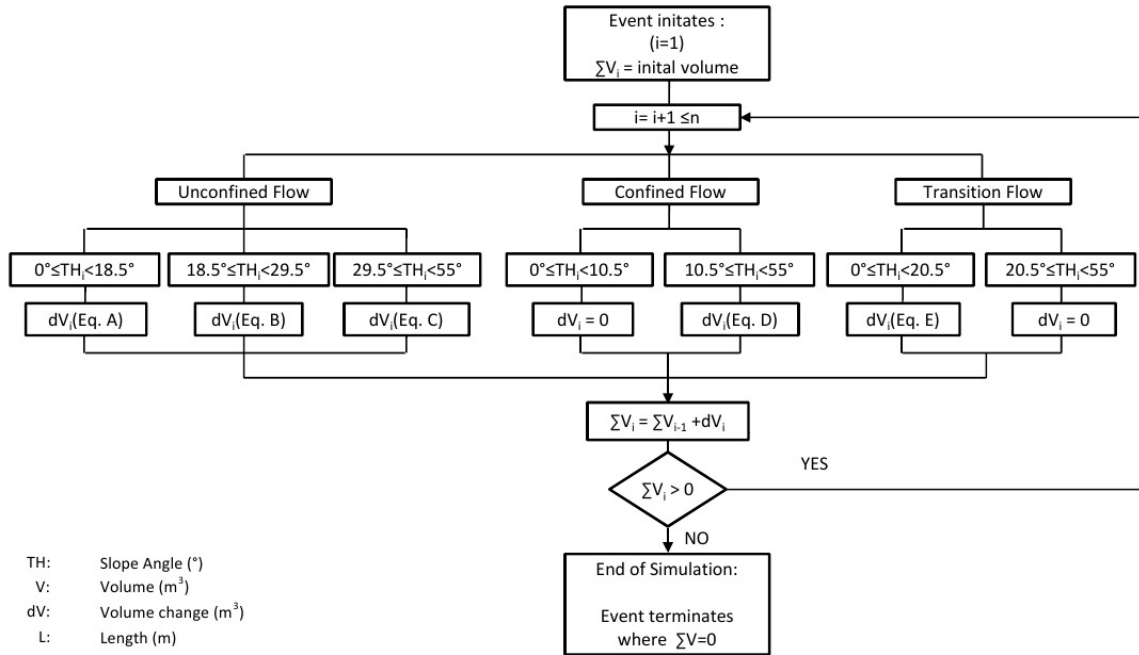


Figure 3.11 Schematic plan view of a debris flow path.



Eq.	Morphology	Mode of flow	Regression equation	Range of slope angles
A	Unconfined flow	Deposition	$\ln(-dV_i) = -0.514 - 0.988 \ln(W_{d,i}) - 0.101(BAF_i) - 0.731 \ln(L_i) + 0.0155(TH_i)$	$0 \leq TH_i < 18.5^\circ$
B	Unconfined flow	Entrainment	$\ln(+dV_i) = 1.13 \ln(W_{e,i}) + 0.787 \ln(L_i) - 0.0636 \ln(\Sigma V_{i-1})$	$18.5 \leq TH_i < 29.5^\circ$
C	Unconfined flow	Entrainment	$\ln(+dV_i) = 0.728 + 1.31 \ln(W_{e,i}) + 0.742 \ln(L_i) - 0.0464(TH_i)$	$29.5 \leq TH_i < 55^\circ$
D	Confined flow	Entrainment	$\ln(+dV_i) = 0.344 + 0.851 \ln(W_{e,i}) + 0.898 \ln(L_i) - 0.0162(TH_i)$	$10.5 \leq TH_i < 55^\circ$
E	Transition flow	Deposition	$\ln(-dV_i) = -1.54 \ln(W_{d,i}) - 0.90 \ln(L_i) + 0.123(BAF_i)$	$0 \leq TH_i < 20.5^\circ$

$BAF_i = \cos(dTH_i) \cos(dAZ_i) \ln(\Sigma V_{i-1})$

Figure 3.12 Conceptual framework used in UBCDFLOW. Starting with an initial volume, flow behaviour and slope angle determine how the simulation changes volume along the path. The event terminates in the reach where the volume becomes zero.

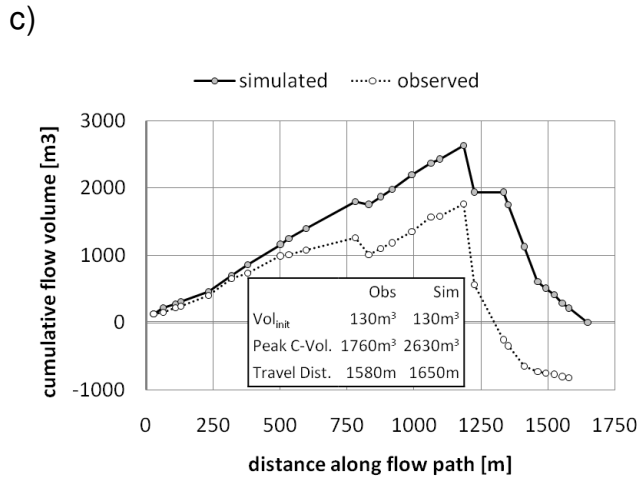
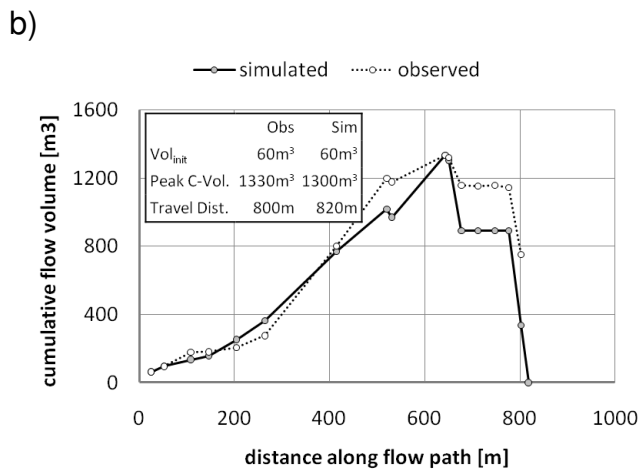
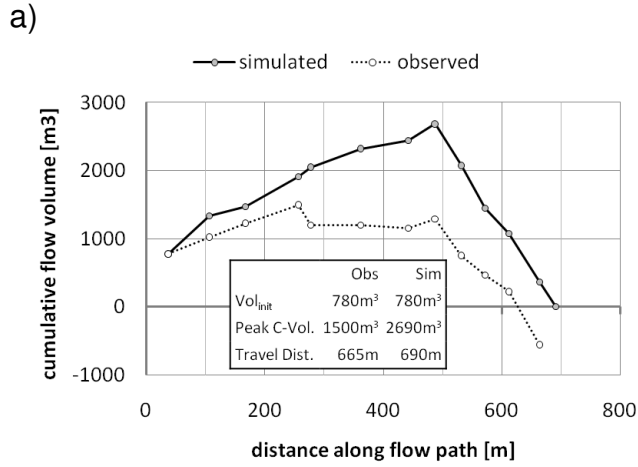


Figure 3.13 Comparison of volume balance along the path for a) Type 1: Revelstoke (Bigmouth) 11, b) Type 2: Airy Creek 3017 and c) Type 3: Blueberry Creek 2037.

3.9 References

- Benda, L.E., and Cundy., T.W. 1990. Predicting deposition of debris flows in mountain channels. *Canadian Geotechnical Journal*, **27**(4): 409-417.
- Berti, M., and Simoni, A. 2007. Prediction of debris flow inundation areas using empirical mobility relationships. *Geomorphology*, **90** (1) 144–161.
- Cannon, S.H. 1993. Empirical model for the volume-change behavior of debris flows. *In Proceedings of the National Conference on Hydraulic Engineering*, July 25, 1993 - July 30, pp. 1768-1773.
- Corominas, J. 1996. The angle of reach as a mobility index for small and large landslides. *Canadian Geotechnical Journal*, **33**(2): 260-271.
- Cruden, D.M., and Varnes., D.J. 1996. Landslide types and processes. *In Landslides: investigation and mitigation. Edited by A.K. Turner and R.L. Schuster.* Transportation Research Board, Special Report 247, pp. 36–75.
- Fannin, R.J., Bobicki, E.R., and Jordan, P. 2006. A sensitivity analysis of debris flow travel distance at Blueberry Creek. B.C., *Proceedings of 59th Canadian Geotechnical Conference*, Vancouver, B.C., Oct. 1-4, pp. 335-341.
- Fannin, R.J., Busslinger, M., and Jordan, P. 2010. On the utility of empirical-statistical rules for simulation of debris flow events. Manuscript prepared for publication (chapter 3).
- Fannin, R.J., Moore, G.D., Schwab, J.W., and VanDine, D.F. 2005. Landslide risk management in forest practices. *In Landslide Risk Management, Proceedings International Conference on Landslide Risk Management*, Vancouver, Canada, May 1–June 3, 2005. O. Hungr, R. Fell, R. Couture, and E. Eberhardt (editors). A.A. Balkema Publishers. p 299-320.

- Fannin, R.J., and Rollerson, T.P. 1993. Debris flows: Some physical characteristics and behavior. *Canadian Geotechnical Journal*, **30**(1): 71-81.
- Fannin, R.J., and Wise, M.P. 2001. An empirical-statistical model for debris flow travel distance. *Canadian Geotechnical Journal*, **38**(5): 982-994.
- Fannin, R.J., Wise, M.P., Wilkinson, J.M.T., Thomson, B., and Hetherington, E.D. 1997. Debris flow hazard assessment in British Columbia. Proceedings of First International Conference on Debris-Flow Hazards Mitigation, San Francisco, California, August 7-9, 1997, pp. 197-206.
- Griswold, J.P., and Iverson, R.M. 2008. Mobility statistics and automated hazard mapping for debris flows and rock avalanches. USGS Scientific Investigations Report 2007-5276, 59 p.
- Heim, A. 1932. *Bergsturz und Menschenleben*. Vierteljahreszeitschrift der Naturforschenden Gesellschaft, Fretz & Wasmuth, Zürich, *Translated by* Skermer, N.A., 1989. *Landslides and Human Lives*. BiTech Publishers, Vancouver British Columbia.
- Holland, S. 1964. *Landforms of British Columbia: A Physiographic Outline*, by S. Holland 1964 (revised 1976), British Columbia Ministry of Energy, Mines and Petroleum Resources. <http://www.em.gov.bc.ca/DL/GSBPubs/Bulletin/Bull48/Bull48-txt.pdf>. (last accessed July 16, 2010).
- Hungr, O., Evans, S.G., Bovis, M.J., and Hutchinson, J.N. 2001. A Review of the Classification of landslides of the flow type. *Environmental and Engineering Geoscience* **7**: 221–238.
- Hungr, O., McDougall, S., and Bovis, M. 2005. Entrainment of material by debris flows. *Edited by* M. Jakob and O. Hungr. *Debris-flow Hazards and Related Phenomena*, Springer Praxis Publishing Ltd. Chichester, UK, pp. 135–158.

- Hungr, O., Morgan, G.C., and Kellerhals, R. 1984. Quantitative analysis of debris torrent hazards for design of remedial measures. *Canadian Geotechnical Journal*, **21**(4): 663-677.
- Iverson, R.M., Schilling, S.P., Vallance, J.W., 1998. Objective delineation of lahar-hazard zones downstream from volcanoes. *Geological Society of America Bulletin*, **110**: 972–984.
- McClung, D.M. 2000. Extreme avalanche runout in space and time. *Canadian Geotechnical Journal*, **37**: 161-170.
- Jordan, P. 2002. Landslide Frequencies and Terrain Attributes in Arrow and Kootenay Lake Forest Districts. *In: Terrain Stability and Forest Management in the Interior of British Columbia: Workshop Proceedings, May 23–25, 2001, Nelson, B.C., Edited by: P. Jordan and J. Orban, British Columbia, Ministry of Forests, Research Branch, Technical Report 3, Victoria, B.C., p. 80-102.*
- Jordan, P., Millard, T., Campbell, D., Schwab, J., Wilford, D., Nicol, D., and Collins, D., 2010 (in press). Forest Management Effects on Hillslope Processes. Chapter 9 *In: Pike, R.G., T.E. Redding, R.D. Moore, R.D. Winker and K.D. Bladon (editors). Compendium of Forest Hydrology and Geomorphology in British Columbia. B.C. Ministry of Forests and Range, Victoria, B.C. and FORREX Forum for Research and Extension in Natural Resources, Kamloops, B.C. Land Management Handbook 66.*
- Prochaska, A.B., Santi, P.M., Higgins, J.D., and Cannon, S.H. 2008. Debris-flow runout predictions based on the average channel slope (ACS). *Engineering Geology*, **98**: 29–40.
- Rickenmann, D. 1999. Empirical Relationships for Debris Flows. *Natural Hazards*, **19**: 47–77.

- Rickenmann, D. 2005. Runout prediction methods. *Edited by M. Jakob and O. Hungr. Debris-flow Hazards and Related Phenomena*, Springer Praxis Publishing Ltd. Chichester, UK, pp. 305–324.
- Rollerson, T., Millard, T., Jones, C., Trainor, K., and Thomson. B., 2001. Predicting post-logging landslide activity using terrain attributes: Coast Mountains, BC. B.C. Ministry of Forests, Vancouver Forest Region, Technical Report TR-011. 20 p.
- Scheidegger, A.E. 1973. On the prediction of the reach and velocity of catastrophic landslides, *Rock Mechanics*, **5**(4): 231-236.
- Scheidel, C. and Rickenmann, D. 2010. Empirical prediction of debris-flow mobility and deposition on fans. *Earth Surface Processes and Landforms*, **35**: 157–173.
- Sutherland Brown, A. 1968. Geology of the Queen Charlotte Islands, British Columbia. Bulletin No 54, British Columbia Department of Mines and Petroleum Resources, Available from <http://www.llbc.leg.bc.ca/public/pubdocs/bcdocs/360978/bull54toc.pdf>.
- Wise, M. P. 1997. Probabilistic modelling of debris flow travel distance using empirical volumetric relationships. M.A.Sc. Thesis. Department of Civil Engineering, University of British Columbia, Vancouver B.C. Canada.
- Wise, M.P., Moore, G.D., and VanDine, D.F. (eds.) 2004. *Landslide Risk Case Studies in Forest Development Planning and Operations*. B.C. Ministry of Forests, Land Management Handbook 56, 119 p.

4 A SENSITIVITY ANALYSIS TO SLOPE ANGLE OF DEBRIS FLOW VOLUME CHANGE PROCESSES⁶

4.1 *Outline*

Concerns were raised that the deterministic version of an empirical-statistical model for debris flow simulation is sensitive to slope angle. The deterministic model is extended, by means of a Monte Carlo type analysis, to quantify the sensitivity to randomly sampled slope angle input between $\pm 2^\circ$ of the observed slope gradient. The model is applied to 22 events in the Kootenay study area. A total of 13 simulations of volume change process are found sensitive to variations in slope angle. For a total of 11 events the simulations show significant variability in volume estimates. As the point of termination is assumed where the volume becomes zero, variability in volume estimates has implications for travel distance. Therefore it is recommended that variable slope angles be considered in analysis.

⁶ A version of this chapter will be submitted for publication. Busslinger, M. and Fannin, R.J. (2010). A sensitivity analysis to slope angle of debris flow volume change processes.

4.2 Introduction

Findings on the utility of the empirical-statistical UBCDFLOW model (Fannin and Wise, 2001), from the Queen Charlotte Islands, for simulation of the Kootenay debris flow inventory of 22 events in south-eastern British Columbia are reported in Chapter 3. UBCDFLOW is capable of simulating the correct volume change process for 80% of the lengths in the Kootenay study area. Although event magnitudes were not matched, fair agreement was found for simulation of travel distance. While it is encouraging that empirical rules developed for the Queen Charlotte Islands appear to capture volume change processes in the Kootenay area, it is of concern that the simulations may be sensitive to small variations in slope angle inputs. The UBCDFLOW algorithm (see Figure 3.12) uses a) morphology (unconfined, confined or transition) and b) slope angle (TH) to determine the governing regression equation (A to E) to calculate volume change (dV). Accordingly small variations in slope angle of a reach may cause the algorithm to select the adjacent regression equation. Consequently volume estimates may vary significantly.

This article discusses sources of uncertainties in slope angle input. Effects of variable slope angle inputs on simulation results are investigated. In addition the original field observations of the Kootenay inventory are re-examined in order to identify other attributes that had an influence on volume change behaviour of the debris flows.

4.2.1 Sources of uncertainties in debris flow analysis

Nadim et al. (2005) discuss the uncertainties involved in probabilistic slope stability analysis. For engineering practice it is useful to distinguish between aleatory and epistemic uncertainties. Aleatory uncertainty is inherent and cannot be reduced. In a strict sense it represents the natural randomness of a variable. Epistemic uncertainties are due to ignorance or the lack of knowledge on a variable, and can be reduced by taking more accurate measurements, collecting more data, and using more representative models.

Kiureghian and Ditlevsen (2009) suggest the distinction between aleatory or epistemic uncertainty should be made from a modeling point of view. For example it may have

been desirable to have information about attributes like shear strength, water content, bulk density, antecedent rainfall records and so forth to build a sophisticated model. However, resources and budget did not allow collection of such information and it is unlikely that this will happen in the near future. Therefore these variables are not respected in the model, and are allocated to the aleatory category.

Consequently the variables available for model building are reduced to a few geometrical attributes (i.e. initial volume, slope angle, reach length and width, and path azimuth) and also reach morphology (confined, unconfined and transition). The type of morphology is defined by judgment and it is difficult to quantify the consequent uncertainty. The other variables come with epistemic uncertainties like measuring errors, statistical uncertainties (due to limited information) and model uncertainties. Model uncertainties may have several sources. The volume balance approach and the implicit assumption of constant bulk density in UBCDFLOW are simplifications of a more complex phenomenon. Goodness-of-fit between regression equations and the original inventory is a further source of model uncertainty.

Dividing the path into reaches with constant attributes allows for solving the analysis in convenient steps, but the discretization introduces further uncertainty. Reach ends are usually defined at distinct changes in morphology (e.g. from confined to unconfined flow), terrain breaks (slope angle), turns (azimuth), junction of streams or simply at a point of convenience. However, the choice of reach end location is largely subjective and all reach attributes measurements depend on this choice. Unfortunately, the data at hand does not allow describing how the measured reach attributes depend on the choice of reach ends. For most input parameters this may not have a significant influence, except for the slope angle. The slope angle of a reach may vary, if for example the reach length is arbitrarily chosen to be shorter. In other words; the choice of reach end points may influence the slope angle measured in the field.

Fannin and Wise (2001) proposed a probabilistic version of the UBCDFLOW model (UBCDFLOW-P) addressing the potential for a dual mode of flow (i.e. occurrence of both entrainment and deposition within a reach); as well as uncertainties in initial volume and path width and initial volume. While UBCDFLOW-P allows entraining and depositing processes to occur simultaneously, it does not address effects of uncertainties in slope

angle input. Fannin et al. (2006) carried out a sensitivity analysis of the Blueberry Creek debris flow event and found that the model was more sensitive to variations in path width than initial volume. However, they did not account for variations in slope angle either. Appreciating the existing uncertainties in slope angle discussed above it is interesting to investigate the sensitivity of UBCDFLOW to variable slope angles.

4.2.2 Study objectives

Slope angle is an important parameter in debris flow analysis (Benda and Cundy, 1990; Cannon, 1993; Guthrie et al., 2010; Hungr et al., 1984). Analysis of 22 debris flows in the Kootenay area (Chapter 3) found good agreement on volume change process using the deterministic version of UBCDFLOW. While it is encouraging that these empirical rules developed for the Queen Charlotte Islands appear to capture volume change processes in the Kootenay area, it is of concern that simulation outputs may be sensitive to small variations in slope angle inputs. As discussed above, variations in slope angle inputs will have aleatory and epistemic sources (e.g. measuring errors, discretizing of path). Regardless of the source of error, small differences in slope angle may result in significantly different volume estimates. This article tests the hypothesis that accounting for variable slope angles yields a better-informed estimate of travel distance. Analysis address matters of volume change process, event magnitude and travel distance exceedance.

4.3 Methodology

A sensitivity analysis is carried out in order to investigate the effect of varying reach slope angles on simulations of 22 debris flow events in the Kootenay study area (characterized in Chapter 3). The deterministic version of UBCDFLOW is extended to a Monte Carlo type analysis, using slope angle as a random predictor variable, with all remaining variables held constant at the observed value in the field. Effects of variable slope angle inputs on simulation of correct volume change process, magnitude and travel distance are quantified and assessed based on indicators of success. Results are compared with original field observations, and also with the prior deterministic simulation. Findings of the sensitivity analysis are used in a re-examination of field

observations in the Kootenay inventory, yielding an improved understanding of the debris flow behaviour.

4.3.1 Monte Carlo simulation

A Monte Carlo model (Figure 4.1) is built from the deterministic version of UBCDFLOW described in Fannin and Wise (2001). A specified number of trials (i.e. $N_t = 10,000$) is performed for simulation of each event. In each trial, random slope angles (TH_i) are sampled for all reaches in the path. The remaining input parameters (initial volume V_1 ; morphology; length L_i ; width W_i ; azimuth AZ_i) are held constant at the value observed in the field for each reach from $i = 1$ to n . The deterministic UBCDFLOW algorithm is used to calculate volume change along the path of a trial. After the trial is finished, the results are saved and the simulation generates new random slope angles. The procedure continues until the specified number of trials N_t is reached.

In selection of the probability density function (pdf) for input parameters, the following aspects are considered: The reported slope angle for each reach is believed to be representative, although the actual gradient within a reach is not entirely constant over its length. Typical measuring resolutions for inclinometers are approximately 0.5° . Errors exist due to discretizing (i.e. subjective selection of reach ends). Upper and lower limits of the pdf should be sufficiently wide to overlap slope domain boundaries of the UBCDFLOW regression equations, yet sufficiently narrow to maintain clarity in simulation results. Based on field traversing experience, a range of $\pm 2^\circ$ is believed reasonable to account for the epistemic (measuring errors, discretizing) and aleatory (inherent variability of micro-topography) uncertainties mentioned above. Hammond et al. (1992) suggest that a uniform distribution is appropriate when limited information is available, allowing an estimate of minimum and maximum, but not an estimate of distribution shape. No quantitative information is available that would suggest the preference of a particular shape for the slope angle input pdf. It is assumed that values between lower and upper limit are equally likely to occur. Therefore a uniform pdf, between the limits of $\pm 2^\circ$ of the slope angle measured in the field, is used in analysis. As the logarithmic equations in UBCDFLOW do not apply for negative input values, 0° is the lowest limit used.

4.3.2 Simulation output

The effects of variable slope angle on debris flow simulations are analyzed for simulation of volume change process, volume magnitude and travel distance. This is only done for the observed travel distance only. No information about the observed point of termination was available and the results are not extrapolated in order to maintain clarity about the effects about variable slope angle and avoid elements of speculation. Success indicators (i.e. PI, MI and DI) used in the deterministic analysis (Chapter 3.5.2; Appendix E), are slightly adjusted in this paragraph, to accommodate the large amount of output data (i.e. 10,000 trials).

4.3.2.1 Volume change process

The process indicator (PI_{MC}) quantifies the percentage of observed travel distance along which volume change process was correctly simulated. The lengths ($L_{i,p}$) of every reach in which the simulated process was found in agreement with field observation of entrainment or deposition are summed up and divided by the total observed travel distance, given by the sum of all reaches (L_i) within an event.

$$[1] \quad PI_{MC} = \frac{\sum_{i=1}^n L_{i,p}}{\sum_{i=1}^n L_i} \cdot 100\%$$

The process indicator is sampled for every trial (i.e. 10,000 times) within the Monte Carlo type simulation of an event and subsequently analyzed in a histogram. The minimum and maximum values are reported together with the mode. The mode of the PI_{MC} represents the most likely success of simulating the correct volume change process. The difference between max and min PI_{MC} informs on the sensitivity of process to a variable slope angle.

4.3.2.2 Event volume magnitude

Cumulative volume is defined as the sum of initial volume plus all volume changes upslope of the point of interest. For every trial in the Monte Carlo simulation the cumulative volumes of each reach are logged in a file. After the simulation of an event is completed these cumulative volumes are analyzed for each reach using a histogram: The most frequently simulated cumulative volume is selected from the histogram and plotted for every reach along the path indicating the most likely volume balance. This

simulated volume balance is only plotted for the observed length of the path. No information about the path beyond the observed point of termination is available and no speculation is made to extrapolate the point where the simulated volume becomes zero.

The maximum value of this volume balance represents the most likely peak cumulative volume of a simulation ($V_{s,peak}$). Similarly the peak cumulative volume for the field observations ($V_{o,peak}$) is found by summing up the observed volume changes in flow direction and selecting the maximum value. The magnitude indicator MI_{MC} is given by:

$$[2] \quad MI_{MC} = \frac{V_{s,peak}}{V_{o,peak}} \cdot 100\%$$

Some cumulative volume histograms have bimodal distributions. However, only the mode (i.e. most frequent bin in the histogram) is used for interpretation of simulation output. Histograms of cumulative volumes are useful for decision making because they illustrate how outputs cluster around a mode, and hence inform about its significance. Therefore the histogram of the last observed reach is inspected and a note about modality is made.

Besides the most likely cumulative volumes, lower and upper confidence limits (i.e. 5 and 95% percentiles of histograms) of each reach are plotted along the path to indicate the range wherein 90% of the simulated volumes lay. Again, no speculation is made to extrapolate the point where the confidence limits would become zero.

The range between upper and lower confidence interval ($V_{s,95}-V_{s,5}$) is a measure for the variability in simulation output. Interpretation of the absolute magnitude of the range alone would not account for the different sizes of the simulated events. Consequently the range is normalized by the peak cumulative volume of the simulation ($V_{s,peak}$). Inspection of confidence intervals showed that the variability generally increases with travel distance and therefore a variability indicator VI_{MC} is used to quantify the variability in volume estimates at the observed end of deposition:

$$[3] \quad VI_{MC} = \frac{(V_{s,95}-V_{s,5})}{V_{s,peak}} \cdot 100\%$$

4.3.2.3 Travel distance exceedance probability

In a Monte Carlo type analysis probability of travel distance exceedance can be conveniently derived using the assumption of termination where the volume becomes zero. The number of trials that continue beyond a point of interest ($N_{i,Ex}$) have cumulative volumes larger than zero. Knowing the total number of trials (N_t), the probability of travel distance exceedance ($P_{Ex,i}$) is given as:

$$[4] \quad P_{Ex,i} = \frac{N_{i,Ex}}{N_t}$$

Plots of $P_{Ex,i}$ along the path inform on the likelihood that a simulation will travel beyond the point of interest. For comparison within the inventory $P_{Ex,n}$ at the observed point of termination of each event is used.

4.4 Results

For illustrative purposes, results of three events are reported below. The events are selected to highlight different aspects of the probabilistic simulation. Subsequently the key results for the whole dataset are presented.

4.4.1 Example events

This section describes simulations of an unconfined open slope event (type 1), a relatively short, steep gullied event (type 2) and a longer confined event that travelled in relatively flatter reaches (type 3). Field observations and Monte Carlo simulation results are contrasted, to highlight important aspects of slope angle variation.

Type 1 event East Kootenay (Dewan) 5000 initiated in the embankment of a logging trail. An initial volume of 200m^3 was likely triggered by drainage diversion. Figure 4.2 is a photograph looking up from the main deposit into the open slope with the unconfined path of the event. The volumes mapped in the field are summed along the path (dotted line) in Figure 4.3a. Traveling over an open slope (29° to 38°) the flow reached a peak cumulative volume of 450m^3 before depositing in the last two reaches with slope angles of 19.3° (reach 7-8) and 15.1° (reach 8-9), respectively. Note that observed volumes at the observed end of an event are not necessarily zero, as they are simply field observations summed up in flow direction without correction. Results of the simulation

are indicated with solid lines, for both the mode and the confidence intervals. The confidence intervals illustrate the importance of reach 7-8 on an unconfined slope with a gradient of 19.3°. This gradient is close the limit of 18.5° in the UBCDFLOW algorithm, separating the domains of regression equation A and B (Figure 4.1), where A simulates deposition and B simulates entrainment.

The PI_{MC} (Eq. 1) expresses the percentage of travel distance where the volume change process was correctly simulated. For every trial in the Monte Carlo analysis the process indicator was sampled and found to vary between of 57% to 80%, with a mode of 58%. The relatively low mode indicates that the processes are poorly simulated for this event. The considerable range between maximum and minimum implies that simulation of the processes is quite sensitive to slope angle. To capture the success in simulating the volume magnitude, the ratio (Eq. 2) between simulated ($V_{s,peak} = 950m^3$) and observed ($V_{o,peak} = 450m^3$) is used, for which the resulting $MI_{MC} = 213\%$. The MI_{MC} shows that the simulation significantly overestimates the volume magnitude. The low success of the simulation in capturing the process (i.e. $57 < PI_{MC} < 80\%$) introduced a large variability of the volume estimates as described by the $VI_{MC} = 94\%$. The histogram of simulated volumes at the observed point of termination (Figure 4.3b) exhibits two distinct clusters: 71% of the calculations cluster around Mode 1 ($707m^3$) and 29% around Mode 2 ($102m^3$). The finding implies approximately 7 in 10 simulations travel beyond the observed point of termination, and 3 in 10 would not. Probability of travel distance exceedance ($P_{Ex,i}$) is plotted along the path in Figure 4.3c. Beyond point 7 the $P_{Ex,i}$ becomes less than 1.0 and at the events end $P_{Ex,n}$ is 0.71.

Type 2 event Revelstoke (Bigmouth) 5 was caused by a poorly placed culvert of a logging road and the according drainage diversion. The dotted line in Figure 4.5a indicates the observed volumes summed in the flow direction. The event started as a shallow slide on a 35° slope in mature forest with an initial volume of $280m^3$. Subsequently it entered a steep (33° to 35°), confined channel and entrained up to a $V_{o,peak}$ of $840m^3$ in a confined channel of a clear-cut block. Figure 4.4 is a photograph looking up into the steep, confined channel of the clear-cut block. Subsequent reaches were considerably flatter (i.e. 4° and 8°) and no longer confined, allowing the flow to deposit and come to a halt after 380m of total travel distance.

The simulation (solid line in Figure 4.5a) captured the volume change processes correctly along the entire travel distance. The process indicator PI_{MC} is therefore 100%. The mode of the simulation slightly overestimated the peak cumulative flow volume ($V_{s,peak}=940m^3$), quantified by the $MI_{MC}=112\%$. In Figure 4.5a the 95% and 5% confidence limits are very close together for the entire simulation, indicating that the 90% of the outputs occurred in this narrow band. The resulting small variation in volume estimates, and companion 100% success in simulating process, yield in a VI_{MC} of 4%. The histogram of simulated volumes at the observed point of termination (Figure 4.5b) has a unimodal shape, for which the mode and the mean are essentially the same. Figure 4.5c shows that the simulated exceedance probability $P_{Ex,i}$ for the entire path is 1.0.

Type 3 event Blueberry Creek 2037 was initiated by snowmelt. Figure 4.6 is an aerial view on the upper part of the event showing the clear-cut where the event initiated on a 33° slope in a clear-cut with a relatively small initial volume of $130m^3$. Subsequently the event passed through three unconfined reaches before the debris flow entered a confined channel and observed cumulative volume peaked at $V_{o,peak}=1760m^3$ (dotted line Figure 4.7.a). The simulation (solid line) captured this behaviour, but overestimated entrainment in the confined channel, resulting in $V_{s,peak}= 2630m^3$, or a magnitude indicator of MI_{MC} 149%. Except for one, all reaches after the peak were unconfined and deposition was observed.

For 93% of the observed travel distance the simulated volume change processes were correct. The difference between the 95% and 5% confidence intervals (Figure 4.7.a) is small from initiation until point 14 and from there moderate until point 9. Moderate variability is due to two confined reaches with slope angles of 12.4° , close to the value of 10.5° where the UBCDFLOW algorithm simulates either entrainment (Eq. D in Figure 4.1) or no volume change (i.e. $dV=0$). The variability increases significantly in reach 8-9; a further confined reach with a gradient of 10.2° . At the observed point of termination the range is as large as 22% of the peak simulated volume. The histogram of simulated volumes in the last reach (Figure 4.7.b) has a bimodal distribution with 54% of the answers clustered around Mode 1 ($228m^3$). The probability of travel distance exceedance in Figure 4.7.c is 1.0 all along the path and just about 0.99 at the observed

point of termination, meaning that chances are very high for the simulation to flow beyond the observed point of termination.

Figures Figure 4.3d, Figure 4.5d and Figure 4.7d are plots of the deterministic result (dotted line with cross) together with the mode of the Monte Carlo simulation (black solid line). Comparison shows that the Monte Carlo result is essentially the same as the deterministic answer. Further, comparing the PI from deterministic analysis (i.e. 58%, 100% and 93%) with the mode of PI_{MC} for the three events (i.e. 58%, 100% and 93%), illustrates that the Monte Carlo type analysis is capable of reproducing the deterministic answer. Similarly the MI from deterministic analysis (i.e. 217%, 112% and 149%) and the MI_{MC} (i.e. 213%, 112%, 149%) agree. These encouraging agreements exist for all events in the dataset and build confidence in the Monte Carlo type analysis.

4.4.2 Analysis of the Kootenay dataset

The key results for the Monte Carlo simulations are summarized in Table 4.1. In addition the variability in simulated volumes is described at the observed point of termination. These volumes were also analyzed in the form of histograms, and the shape of the resulting distribution is tabulated.

Within the entire inventory the arithmetic mean of the most likely PI_{MC} is 80% and varies between 58% and 100%. For comparison the arithmetic mean of the PI in the deterministic analysis was 80% as well (c.f. Table 3.2). This encouraging agreement builds confidence that the Monte Carlo type analysis is capable of reproducing the deterministic answer, but in addition quantifies effects of variations of slope angle. Where the PI_{MC} is insensitive (i.e. min and max PI_{MC} are equal) for 9 of 22 simulations, the remaining 13 events are sensitive, and the difference between minimum and maximum PI_{MC} ranges from 3% (i.e. Koch 507) to 44% (i.e. Fortynine Ck. 2026).

For simulation of magnitude the arithmetic mean of MI_{MC} is 183%, compared to 181% of the arithmetic mean of the deterministic MI. This confirms again that the Monte Carlo analysis is capable of reproducing the deterministic result. However, the Monte Carlo analysis does not improve the over-prediction of magnitude by UBCDFLOW and the considerable scatter of MI_{MC} (between 51 to 590%). These issues were discussed for the deterministic analysis in Chapter 3.7.2.2.

For the entire inventory the VI_{MC} ranges between 3% and 175% with an average of 30%. The geometric mean of 18% indicates that for a few simulations the variation is quite large. For 11 out of 22 simulations the VI_{MC} is actually 10% or higher. Analysis of sensitive reaches found that unconfined reaches with slope angles around 17 to 20° induced larger variability than other reaches. This may be related to the fact that unconfined reaches tend to be wider than confined reaches, and consequently widths in unconfined reaches amplify volume estimates by a larger factor.

Regarding the distribution of simulated cumulative volumes at the observed point of termination following observations are made: 12 out of 22 events have bimodal distributions (with two distinct modes) and the rest are unimodal. For most unimodal distributions the variability (i.e. VI_{MC}) is low, whereas for bimodal distributions the variability is generally higher.

On the matter of exceedance probability ($P_{Ex,n}$) at the observed point of termination: 12 of 22 events have a $P_{Ex,n}=1.0$, meaning that the likelihood of traveling further than the observed point of termination is 100%. In addition, 5 events have a $P_{Ex,n}=0.0$, meaning that those simulations have no chance to reach the observed point of termination. While the $P_{Ex,i}$ does not inform about the size of simulated volume flowing past a point of interest (e.g. $1m^3$ vs. $1000m^3$), it is a useful indicator of whether a spatial impact may be expected.

4.5 Discussion

A variable process indicator PI_{MC} for 13 of 22 events, and a volume variability index $VI_{MC} \geq 10\%$ for 11 of 22 events, confirm that the simulations are sensitive to variable slope angles (i.e. $\pm 2^\circ$ of observed value in the field). The determination of slope angle in the field is slightly subjective and comes with epistemic uncertainties. A Monte Carlo type analysis is very useful because it quantifies the effects of simulations where the slope angle is variable. More specifically plots of confidence limits (c.f. Figure 4.3) along the path immediately identify sensitive reaches. A deterministic result of travel distance represents only one single output, whereas plots of $P_{Ex,i}$ along the path describe the answer under consideration of variable input. Therefore a Monte Carlo type analysis yields better-informed estimates of debris flow travel distance. However, the biggest

challenge remains the characterization of input parameters. Only good quality input will result in meaningful results.

As an alternative to a Monte Carlo analysis, a rough check of sensitivity to slope angle (TH_i) can be performed by running two deterministic simulations with extreme scenarios (e.g. all observed $TH_i +2^\circ$; all observed $TH_i -2^\circ$) and plotting the results in one graph. Generally, the model is most sensitive when the slope angle input is close to domain boundaries of the regression equations and sensitive reaches can be “spotted”. However, the user should be aware that such extreme scenarios yield in extreme estimates of volume change in each reach (dV_i). Volumes are cumulative in flow direction: As incoming volume (ΣV_{i-1}) is used as predictor variable in three regression equations (c.f. Fig 4.1. Eq. B; and substituted in BAF for Eq. A and Eq. E), extreme results may be amplified in the flow direction. In contrast, using a Monte Carlo analysis and realistic confidence limits (e.g. 5 or 10%) to identify sensitive reaches allows to exclude the most extreme values.

While the Monte Carlo type analysis brings better informed answers, there are other types of uncertainties for which the model does not account for. The Kootenay events are documented in a comprehensive, detailed manner, and the inventory was re-evaluated to identify additional attributes that influence debris flow travel distance: For instance, some sensitive reaches were closely located to crossings of roads or skid trails. Such terrain features may be sufficiently critical to cause the event to deposit. Roads and skid trails are often related to drainage diversion of surface water and seepage, influencing the water content and erodibility of material. Appreciation of material supply limits (e.g. shallow bedrock) is important to understand debris flow behaviour and magnitude. High contents of organic debris, such as logs and tree stumps, were found to have implications for the termination of some events. For example the event Sitkum Area 3000 deposited on rather steep terrain (around 18 to 19°) because logs jammed and piled up, causing a dam that terminated the event. Further, snow-cover or denser tree stands had an influence on debris flow behaviour. These examples highlight that accounting for rheology in debris flow simulation does not necessarily guarantee a correct simulation.

4.6 Summary and conclusions

Concerns have been raised that step-wise regression equations of an empirical debris flow simulation model (UBCDFLOW) might lead to a sensitivity to slope angle inputs. The model is extended into a Monte Carlo type simulation to quantify the uncertainties involved where the input slope angle is randomly sampled between $\pm 2^\circ$ of the observed slope gradient. 22 events from the Kootenay area were analyzed.

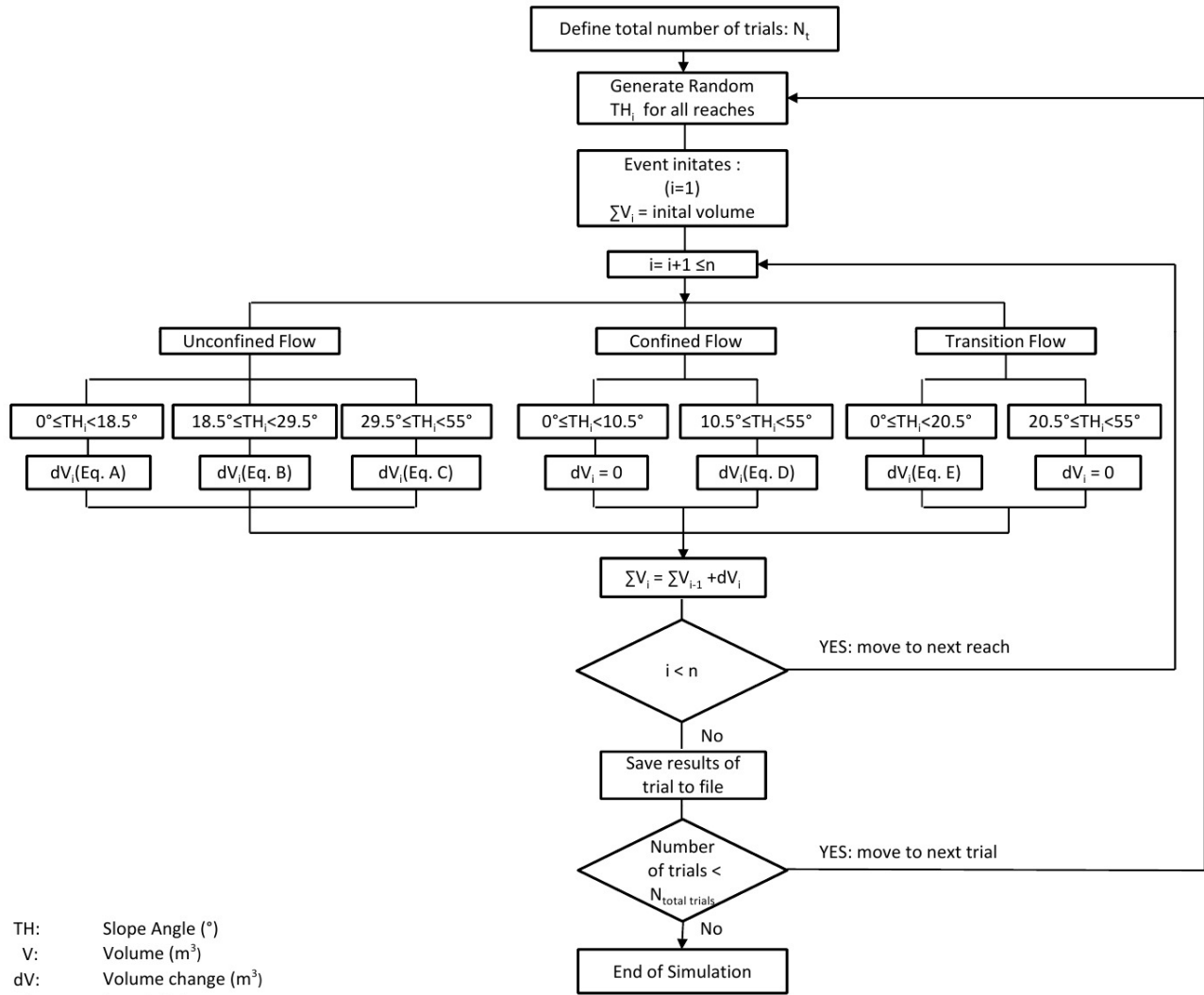
The average result for process and magnitude in the Monte Carlo type analysis is essentially the same as the deterministic result. This encouraging agreement builds confidence that the Monte Carlo type analysis is capable of reproducing the deterministic answer, but in addition quantifies effects of variations of slope angle. However, in 13 simulations, prediction of the volume change process is sensitive to random slope angle input (i.e. $PI_{MC,min} \neq PI_{MC,max}$ in Table 4.1) In 11 simulations, volume estimates experience considerable variability (i.e. $VI_{MC} \geq 10\%$ in Table 4.1). As the point of termination is assumed where the volume becomes zero, variability in volume estimates has implications on travel distance. Similar to the deterministic analysis, the volume magnitudes of the Monte Carlo type analysis are too high when compared to field observations. Simulated travel distance exceedance probability in a Monte Carlo type analysis accounts for input variability, and consequently yields in better-informed estimates, compared to computation of a single deterministic travel distance.

Both deterministic and Monte Carlo type analysis of the Kootenay inventory found that UBCDFLOW overestimates volume changes, but still yields a fair estimate of travel distance. Among other factors, this is likely due to a combination of simulating the correct process and compensation between entrainment and deposition. It is therefore crucial to simulate the correct process. This research shows that the process is sensitive to random slope angle inputs. Therefore a variable slope angle should be considered in the analysis.

Table 4.1 Simulation results.

	Area	Slide	Process			Magnitude	Variability		Travel Dist.
			PI _{MC,mode} [%]	PI _{MC,min} [%]	PI _{MC,max} [%]	MI _{MC} [%]	VI _{MC} [%]	Distribution	P _{ex,n} [-]
Type 1	Airy Creek	1620	71	71	71	404	12	unimodal	1.00
	East Kootenay (Dewan)	5000	58	57	80	213	94	bimodal	0.71
	East Kootenay (Hellroaring)	5001	94	94	94	183	8	unimodal	0.00
	East Kootenay (Hellroaring)	5002	74	74	74	239	7	bimodal	1.00
	Nelson Area (Sandy Ck)	2018	94	94	94	200	6	unimodal	0.00
	Revelstoke (Bigmouth)	11	72	72	72	179	5	unimodal	1.00
	Giveout Creek	5006	62	62	62	108	4	unimodal	1.00
Type 2	Airy Creek	1621	97	97	97	51	8	unimodal	0.00
	Airy Creek	3017	88	84	88	100	51	bimodal	1.00
	Burton Creek	1660	84	79	84	163	5	bimodal	1.00
	Koch	507	85	82	85	135	5	unimodal	1.00
	Koch (Little Slocan)	1637	58	43	58	200	18	bimodal	1.00
	Nelson Area (Cottonwood)	2017	79	66	87	163	48	bimodal	0.00
	Nelson Area (Duhamel)	1740	82	71	82	183	8	bimodal	0.00
	Revelstoke (Bigmouth)	5	100	100	100	112	4	unimodal	1.00
	Sitkum Area (Bourke)	3000	63	57	66	89	69	bimodal	1.00
Summit-Shannon	5004	94	81	94	145	175	bimodal	0.05	
Type 3	Blueberry Creek	2037	93	88	93	149	22	bimodal	0.99
	Burton Creek	106	93	93	93	173	3	unimodal	1.00
	Fitzstubs	1689	77	63	78	133	55	bimodal	0.45
	Koch	1738	71	71	73	590	10	bimodal	1.00
	Fortynine Creek	2026	69	56	100	114	46	unimodal	0.92
All types	Arithmetic mean		80			183	30		n.a.
	Median		80			163	9		n.a.
	Geometric mean		79			160	14		n.a.
	Minimum		58			51	3		0.00
	Maximum		100			590	175		1.00

Note: Output parameter defined in Eq. 1 to 5.



Eq.	Morphology	Mode of flow	Regression equation	Range of slope angles
A	Unconfined	Deposition	$\ln(-dV_i) = -0.514 - 0.988 \ln(W_{d_i}) - 0.101(BAF_i) - 0.731 \ln(L_i) + 0.0155(TH_i)$	$0 \leq TH_i < 18.5^\circ$
B	Unconfined	Entrainment	$\ln(+dV_i) = 1.13 \ln(W_{e_i}) + 0.787 \ln(L_i) - 0.0636 \ln(\Sigma V_{i-1})$	$18.5 \leq TH_i < 29.5^\circ$
C	Unconfined	Entrainment	$\ln(+dV_i) = 0.728 + 1.31 \ln(W_{e_i}) + 0.742 \ln(L_i) - 0.0464(TH_i)$	$29.5 \leq TH_i < 55^\circ$
D	Confined	Entrainment	$\ln(+dV_i) = 0.344 + 0.851 \ln(W_{e_i}) + 0.898 \ln(L_i) - 0.0162(TH_i)$	$10.5 \leq TH_i < 55^\circ$
E	Transition	Deposition	$\ln(-dV_i) = -1.54 \ln(W_{d_i}) - 0.90 \ln(L_i) + 0.123(BAF_i)$	$0 \leq TH_i < 20.5^\circ$

$BAF_i = \cos(dTH_i) \cos(dAZ_i) \ln(\Sigma V_{i-1})$

Figure 4.1 Flow chart for Monte Carlo simulation.



Figure 4.2 Looking up into the path of East Kootenay (Dewan) 5000 event. The event occurred on an open slope and traveled down on an unconfined path.

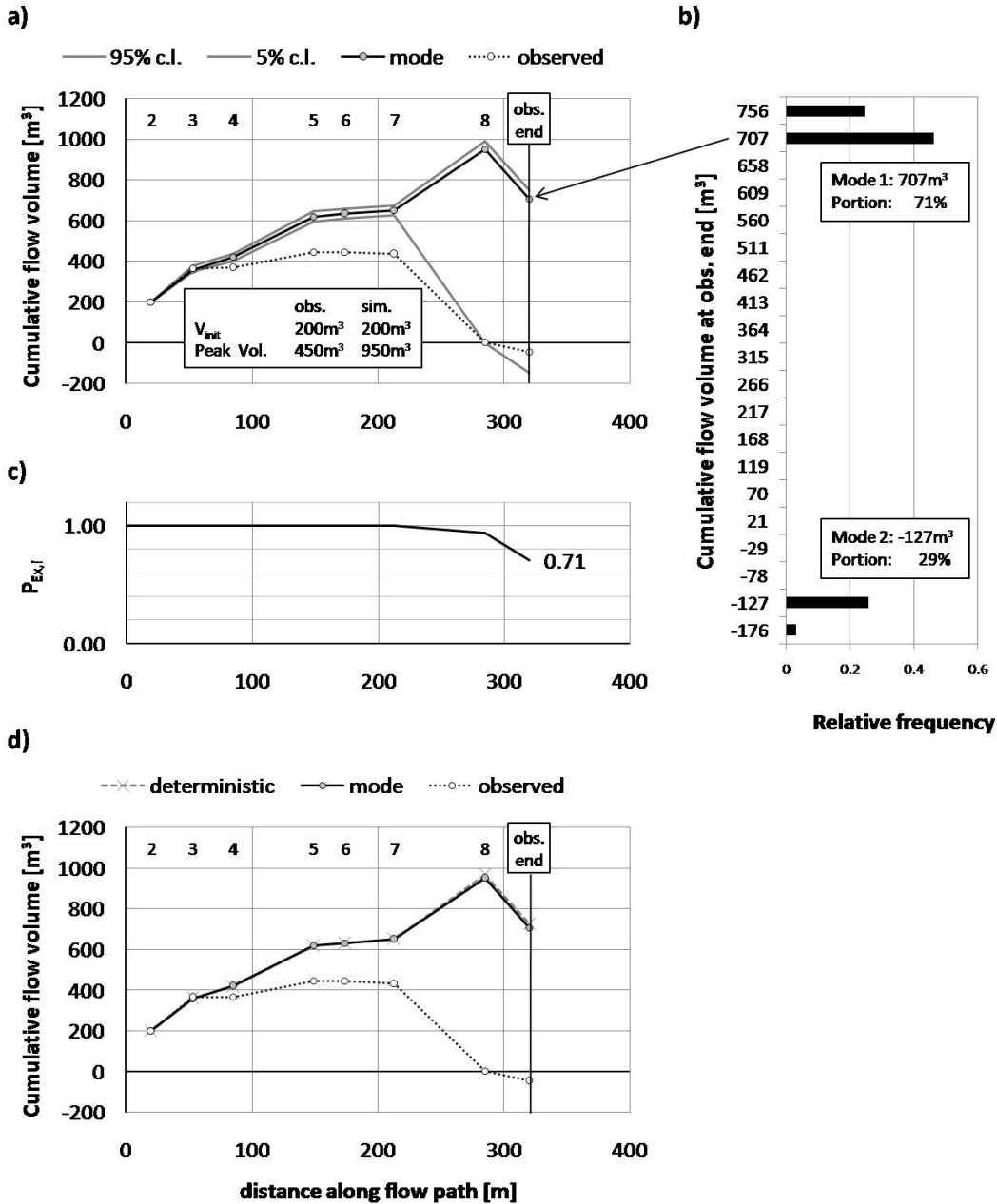


Figure 4.3 Simulation results East Kootenay (Dewan) 5000: a) dotted line = observed volume balance; grey solid lines = confidence limits; black solid line = mode of simulations; reach endpoints are indicated on top. b) histogram of simulated volumes at the observed point of termination. c) Probability of travel distance exceedance ($P_{Ex,i}$) along the path. d) Comparison of deterministic result and mode of Monte Carlo simulation.



Figure 4.4 Looking up into the lower part of the confined path of event Revelstoke Bigmouth 5 before terminal deposition started. Further above the event travelled through a gully in mature forest.

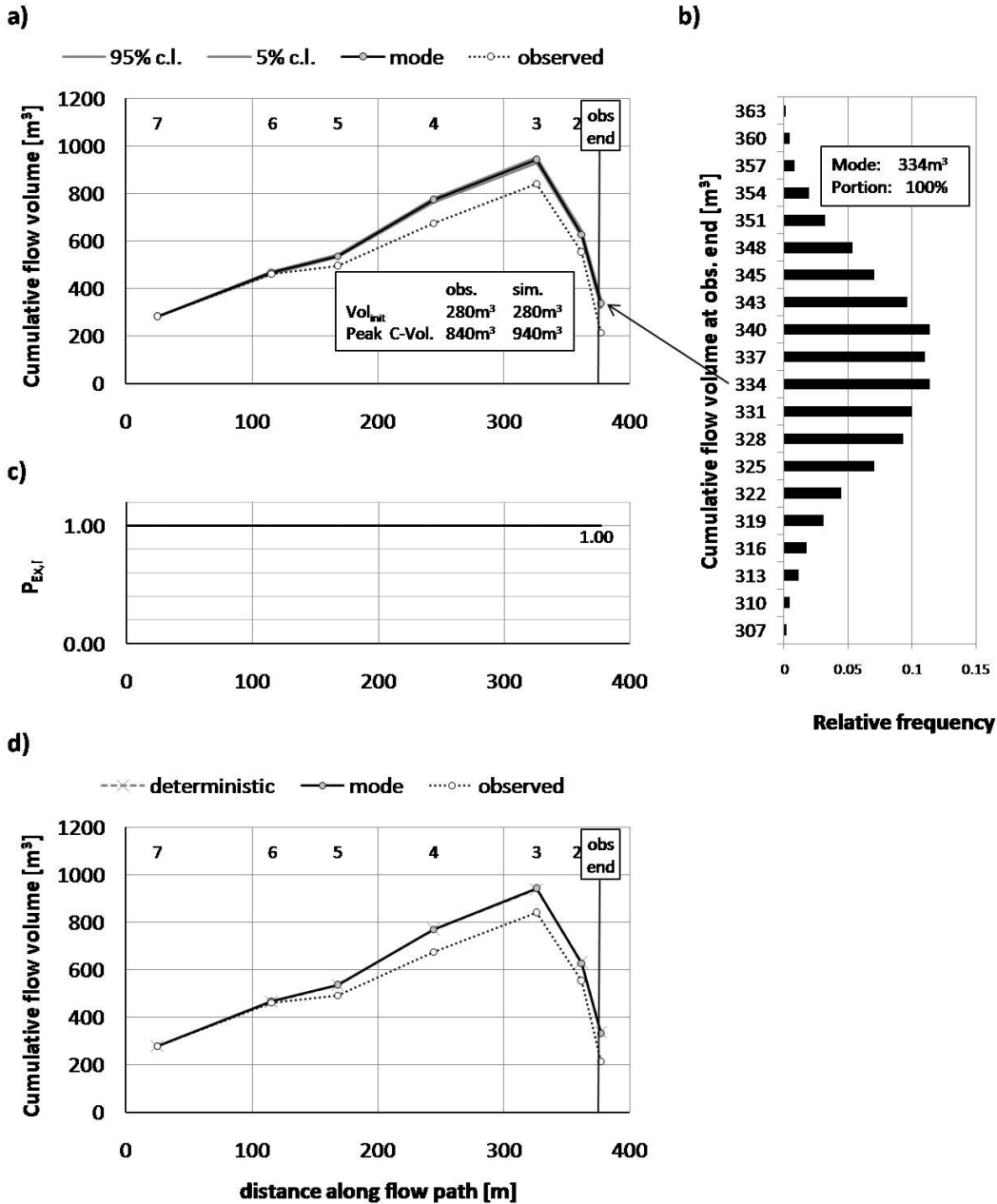


Figure 4.5 Simulation results Revelstoke Bigmouth 5: a) dotted line = observed volume balance; grey solid lines = confidence limits; black solid line = mode of simulations; reach endpoints are indicated on top. b) histogram of simulated volumes at the observed point of termination. c) Probability of travel distance exceedance ($P_{Ex,i}$) along the path. d) Comparison of deterministic result and mode of Monte Carlo simulation.



Figure 4.6 Photo taken from air on upper part of event Blueberry Creek 2037.
The event initiated in a cut-block and entered a confined gully.

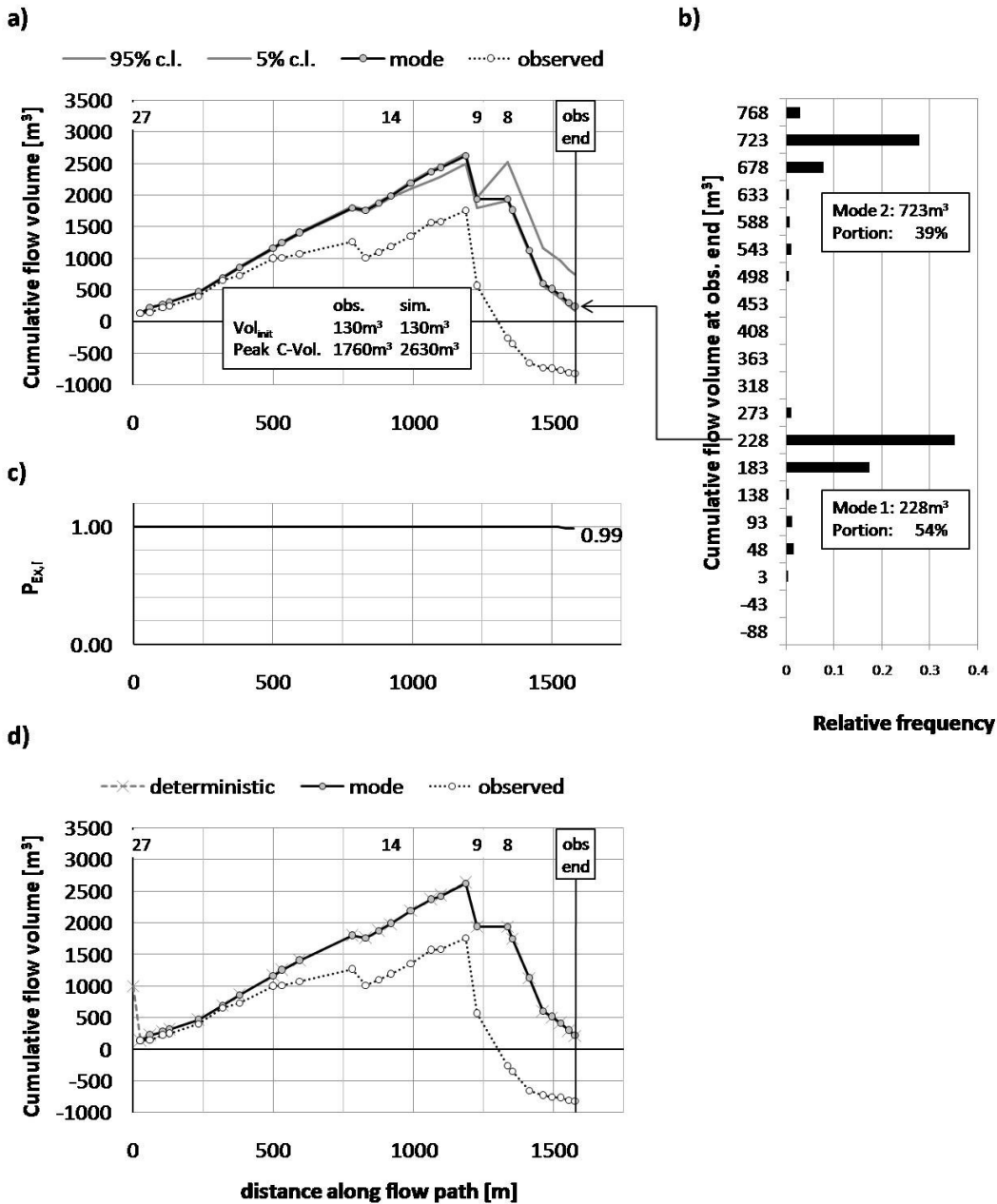


Figure 4.7 Simulation results Blueberry Creek 2037: a) dotted line = observed volume balance; grey solid lines = confidence limits; black solid line = mode of simulations; reach endpoints are indicated on top. b) histogram of simulated volumes at the observed point of termination. c) Probability of travel distance exceedance ($P_{Ex,i}$) along the path. d) Comparison of deterministic result and mode of Monte Carlo simulation.

4.7 References

- Benda, L.E., and Cundy., T.W. 1990. Predicting deposition of debris flows in mountain channels, *Canadian Geotechnical Journal*, **27**(4): 409-417.
- Busslinger, M., and Fannin, R.J., 2010. A sensitivity analysis to slope angle of debris flow volume change processes. Manuscript prepared for publication (chapter 4).
- Cannon, S.H. 1993. Empirical model for the volume-change behavior of debris flows. *In* Proceedings of the National Conference on Hydraulic Engineering, July 25, 1993 - July 30, pp. 1768-1773.
- Fannin, R.J., Bobicki, E.R., and Jordan, P. 2006. A sensitivity analysis of debris flow travel distance at Blueberry Creek, B.C., Proceedings of 59th Canadian Geotechnical Conference, Vancouver, B.C., Oct. 1-4, pp. 335-341.
- Fannin, R.J., and Wise, M.P. 2001. An empirical-statistical model for debris flow travel distance, *Canadian Geotechnical Journal*, **38**(5): 982-994.
- Guthrie, R.H., Hockin, A., Colquhuon, L., Nagy, T., Evans, S.G., and Ayles, C. 2010. An examination of controls on debris flow mobility: Evidence from coastal British Columbia. *Geomorphology*, **114**: 601-613.
- Hammond, C., Hall, D., Miller, S., and Swetik, P. 1992. Level I Stability Analysis (LISA) Documentation for Version 2.0. U.S. Dept. of Agriculture, Forest Service, Intermountain Research Station, General Technical Report INT-285.
- Hungr, O., Morgan, G.C., and Kellerhals, R. 1984. Quantitative analysis of debris torrent hazards for design of remedial measures, *Canadian geotechnical journal*, **21**(4): 663-677.
- Nadim, F., Einstein, H., and Roberds, W. 2005. Probabilistic stability analysis for individual slopes in soil and rock. *In* Landslide Risk Management. Edited by O.

Hungr, R. Fell, R. Couture and E. Eberhardt. Taylor & Francis Group, London.
ISBN 04 1538 043 X. pp. 66-70.

Kiureghian, A.D., and Ditlevsen, O. 2009. Aleatory or epistemic? Does it matter?
Structural Safety **31**: 105–112.

5 CONCLUSIONS AND RECOMMENDATIONS

5.1 Research objectives

The application of empirical tools for simulation of debris flow travel distance is generally limited to biogeoclimatic conditions similar to those of the original study area. There is little experience, and hence limited confidence, in applying empirical decision support tools to areas where the conditions differ significantly (Rickenmann, 2005). UBCDFLOW (Fannin and Wise, 2001) is an empirical-statistical model developed for simulation of travel distance that was developed from field data on the Queen Charlotte Islands, B.C. (Fannin and Rollerson, 1993). Its utility is assessed from examination of field events in the Kootenay area, where the biogeoclimatic conditions differ significantly from those of the QCI. Accordingly, the main objectives of the research are as follows:

- To describe and evaluate the benefits arising from a systematic methodology for traversing debris flow events in the field, in order to characterize the event path from point of origin to point of terminal deposition;
- to report a quantitative assessment of the empirical-statistical rules of the UBCDFLOW model, and thus evaluate the general utility of its application, in conditions that differ from those of its original development; and
- to address the sensitivity of the model rules, and hence simulation of travel distance, to variations in slope angle as a predictor variable.

5.2 Conclusions

Findings of the research are presented, below, in the order in which they are reported in the manuscript chapters.

5.2.1 Field traverse methodology

Traversing a debris flow event in order to record attributes of the path is a complex task that requires training and experience. In this study, use of the “Landslide Profile Data Card”, developed over the last 35 years for support of forest resources management in British Columbia, was evaluated for its utility. The evaluation was based on use of the card to acquire data at the Hummingbird Creek event, and a companion forensic

interpretation of data acquired using it at an additional 22 events in the Kootenay area. The following conclusions are drawn:

- Ground-based inventories are important to any improved understanding of debris flow travel distance and bring more refined estimates of debris flow volumes compared to desk studies. Traversing the path in reasonably short reaches with uniform attributes is the key to the systematic approach. The methodology is particularly attractive for high-frequency, low-magnitude events, where the initial failure volume is small in comparison to the peak cumulative volume.
- The quantitative data can be used to characterize volume change processes, magnitude, and travel distance of events. They greatly facilitate comparison between debris flow inventories as illustrated for the Kootenay and Queen Charlotte Island study areas in Chapters 3.3 and 3.4.
- Estimates of debris volume may be complicated when evidence of pre-event topography is gone. It should be appreciated that above-ground woody debris may add a substantial proportion to the total debris flow volume.
- Careful measurement of slope angle is particularly important where depositional processes become significant, and especially around the point of onset terminal deposition (Hungry et al., 2005; Guthrie et al., 2010). Measured slope angles are often used to establish or apply rules for spatial impacts of debris flows, and exert an important influence in empirical tools for debris flow simulation (Benda and Cundy, 1990; Cannon, 1993; Fannin and Wise, 2001).
- The path of an event should be mapped for an additional distance beyond the end of deposition. This greatly enhances the utility of the gathered data for calibration of numerical models, where simulations may exceed the observed point of termination.

5.2.2 Utility assessment of empirical rules

To assess the utility of an empirical tool in a different area, the original study area and the area of interest have to be described, and debris flow inventories must be characterized. A systematic, quantitative characterization of both study areas facilitates

that comparison. The Kootenay inventory has been characterized, in comparison to the Queen Charlotte Islands (QCI), yielding the following insights:

- Average travel distance in the Kootenays was longer compared to the QCI (roughly by a factor 2.8 to 3.8, depending on event type).
- Average yield rates for the Kootenay inventory (i.e. 2 to 3m³/m) were approximately a factor of 5 lower compared to the QCI (12 and 23 m³/m, depending on event type).

Both study areas have significantly different biogeoclimatic attributes, with considerably wetter and milder climate on the QCI, in contrast to the Kootenays where part of the annual precipitation occurs as snowfall. Nevertheless, remarkable similarities were found regarding the volume change processes as a function of the slope angle (c.f. Figure 3.9 and Figure 3.10).

- For unconfined reaches of the Kootenay inventory deposition is the main process below a slope angle of 20° and entrainment above 23°. This is very similar to the corresponding values of 19° and 24° observed in the QCI data.
- In confined reaches of the Kootenay inventory deposition is the main process below 6°, but the actual deposition rates are not significant. Entrainment is the main process above 10°, with dual-mode flow (i.e. simultaneous occurrence of entrainment and deposition) playing a lesser role. These observations agree with the corresponding values of 6° and 10° observed in the QCI data.
- Between the limits listed above, there is an intermediate range of slope angle where both entrainment and deposition occur frequently. In addition, dual-mode flow was observed in both data sets, for unconfined as well as confined flow in various ranges of slope angle. This implies that the volume change process cannot be inferred from slope angle and confinement alone. The existence of an intermediate range of slope angles, where the process is not clearly defined by slope angle, may also have important implications for the use of other decision support tools that consider mass or volume changes.

The success of UBCDFLOW in simulating events of the Kootenay study area is evaluated based on indicators for process (PI), magnitude (MI), and travel distance (DI).

The overall simulation success is schematically illustrated in Figure 5.1. Evidence suggests that the tool is capable of simulating the correct volume change process for 80% of the lengths, but overestimates the magnitude (i.e. peak cumulative volume) by 180%. Regardless, agreement on travel distance is fair; 15 out of 22 simulations terminate within 89 to 110% of observed travel distance and the remaining 7 exceed 110%. Following conclusions are made:

- UBCDFLOW uses slope angle and morphology (i.e. confinement) to simulate process (Figure 3.12). Similar patterns in volume change process as a function of slope angle for both study areas (Figure 3.9 and Figure 3.10) explain the success for process simulation. Therefore, the rules deciding on process seem to be portable from QCI to Kootenay.
- The higher yield rates in the QCI explain over-prediction of volumes in the Kootenays. Consequently, magnitude simulations are not applicable in the Kootenays and the rules on volume change (Eq. A to E in Figure 3.12) are not portable.
- The fair, yet generally conservative agreement on travel distance is tentatively attributed to an overall reasonable simulation of process and to a certain degree over-prediction in entrainment is compensated with an over-prediction of deposition.

5.2.3 Sensitivity analysis to slope angle

In the UBCDFLOW algorithm different regression equations apply for given slope angle ranges (Eq. A to E in Figure 3.12). A small variation in slope angle input may cause the algorithm to choose a different regression equation, resulting in “step-like” volume estimates. It is therefore important to understand how small variations in slope angle input influence simulation of volume magnitude and ultimately travel distance. The model is extended into a Monte Carlo analysis to quantify the uncertainties involved in simulating debris flows when the input slope angle is randomly sampled between $\pm 2^\circ$ of the observed gradient. The following conclusions are drawn:

- Success in simulating the observed volume change processes varied for 13 of 22 Monte Carlo simulations, the remaining did not vary. Consequently, about half of the simulations are considered sensitive to the random slope angle input.
- For 11 of 22 events considerable variability was found for simulation of peak flow volume and therefore half of the events are considered sensitive to slope angle input.

The fair agreement on travel distance in the deterministic analysis (Chapter 3) is likely due to a combination of simulating the correct process and compensation between entrained and deposited volumes. Termination of an event is defined at the point where the flow volume becomes zero, hence variability in volume estimates causes uncertainty in determination of travel distance. For about half of the events, simulation of both process and volume was sensitive to small variations in slope angle input. It is therefore recommended to consider variable slope angle when carrying out an analysis.

A Plot of confidence limits for flow volumes in a Monte Carlo type analysis is useful to identify sensitive reaches. A Plot of simulated travel distance exceedance probability accounts for input variability, and hence represents a better informed estimate of travel distance than a single deterministic computation.

5.3 Recommendations

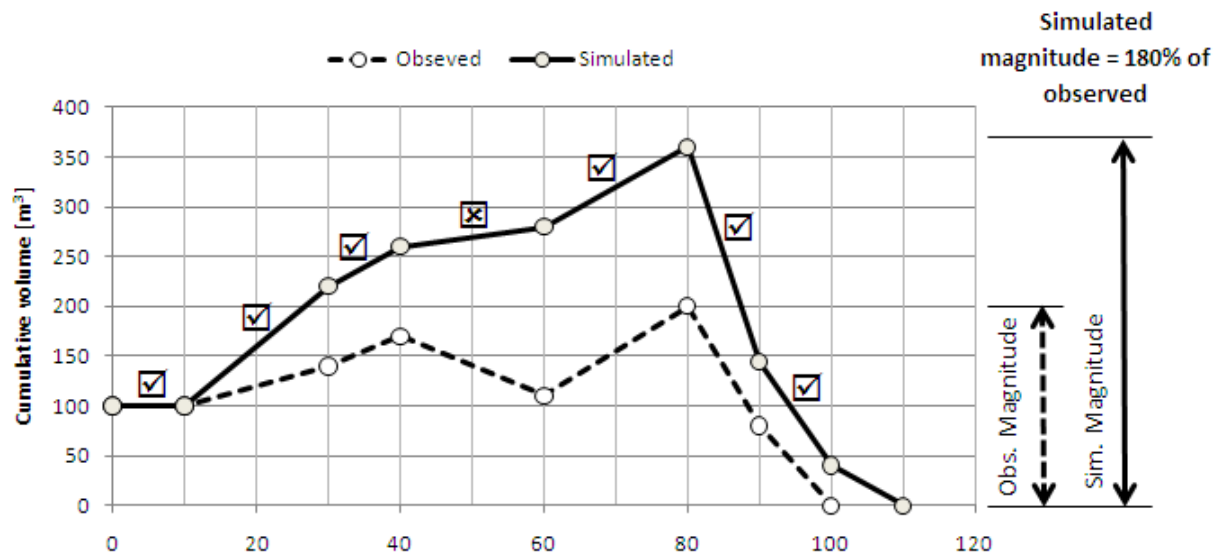
Based on the experience in this research the following recommendations are made for future research:

- The systematic, quantitative approach taken in this research to assess the utility of UBCDFLOW in different settings from its origin can be applied to additional study areas. A study area with higher yield rates than the Kootenay area, and maybe shorter travel distances may bring additional insights. While no simple scaling rules were found to calibrate the volume estimates to the Kootenay area, a combined interpretation with information of an additional study area may help to find ways to calibrate the tool to different areas.

- More research is needed to better characterize the variability of input parameters in a quantitative manner. This would greatly enhance the applicability and confidence in probabilistic simulations.
- Interpretation of the Kootenay data confirms the findings of Fannin and Wise (2001) for the Queen Charlotte Islands that an intermediate range of slope angles exists wherein it is not clear whether erosion or deposition occurs. In the Kootenay inventory both processes occur frequently between 20° and 23° for unconfined flow, and between 6° and 10° for confined flow. Dual-mode flow was observed in both data sets for unconfined and confined flow with various ranges of slope angle. More work is needed to understand dual-mode flow.
- Slope angles at onset terminal deposition in the Kootenays scattered widely between 0° to 30°. More research is needed to better understand factors controlling the onset of terminal deposition like slope angle, confinement, event size magnitude. Flow velocity may play a further role as high flow velocity would imply that the event would deposit further down-slope compared to a slow moving event.

Specific Risk $R(S) = P(H) \cdot P(S:H) \cdot P(T:S) \cdot V(L:T)$

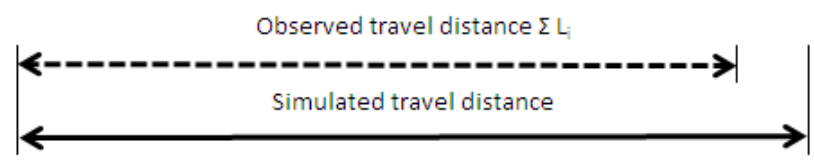
\downarrow \downarrow
 Travel distance Magnitude



Sim.	V_{init}	+dV	+dV	+dV	+dV	-dV	-dV
Obs.	V_{init}	+dV	+dV	-dV	+dV	-dV	-dV
	$L_{i,p}$	$L_{i,p}$	$L_{i,p}$	0	$L_{i,p}$	$L_{i,p}$	$L_{i,p}$
							$\Sigma L_{i,p}$

$$PI = \frac{\sum_{i=1}^n L_{i,p}}{\sum_{i=1}^n L_i} \cdot 100\%$$

Simulated process correct over 80% of length



15 simulations stop between 89 to 110% obs. travel distance, 7 exceed 110%



Figure 5.1 Conceptual overview of overall success in simulation of Kootenay events using UBCDFLOW.

5.4 References

- Benda, L.E., and Cundy., T.W. 1990. Predicting deposition of debris flows in mountain channels, *Canadian Geotechnical Journal*, **27**(4): 409-417.
- Cannon, S.H. 1993. Empirical model for the volume-change behavior of debris flows. *In* Proceedings of the National Conference on Hydraulic Engineering, July 25, 1993 - July 30, pp. 1768-1773.
- Fannin, R.J., and Wise, M.P. 2001. An empirical-statistical model for debris flow travel distance, *Canadian Geotechnical Journal*, **38**(5): 982-994.
- Fannin, R.J., and Rollerson, T.P. 1993. Debris flows: Some physical characteristics and behaviour, *Canadian Geotechnical Journal*, **30**(1): 71-81.
- Guthrie, R.H., Hockin, A., Colquhoun, L., Nagy, T., Evans, S.G., and Ayles, C. 2010. An examination of controls on debris flow mobility: Evidence from coastal British Columbia. *Geomorphology*, **114**: 601-613.
- Hungr, O., McDougall, S., and Bovis, M. 2005. Entrainment of material by debris flows. Edited by M. Jakob and O. Hungr. *Debris-flow Hazards and Related Phenomena*, Springer Praxis Publishing Ltd. Chichester, UK, pp. 135–158.
- Rickenmann, D. 2005. Runout prediction methods. *Edited by* M. Jakob and O. Hungr. *Debris-flow Hazards and Related Phenomena*, Springer Praxis Publishing Ltd. Chichester, UK, pp. 305–324.

APPENDIX A: NOTES LANDSLIDE INVENTORY PROJECT

This appendix documents the notes on the landslide inventory project, carried out in the Nelson Forest Region under by Peter Jordan, Research Geomorphologist. These guidelines where used to compile the Kootenay inventory (Jordan, 2002).

Jordan, P. 2002. Landslide Frequencies and Terrain Attributes in Arrow and Kootenay Lake Forest Districts. *In: Terrain Stability and Forest Management in the Interior of British Columbia: Workshop Proceedings, May 23–25, 2001, Nelson, B.C., Edited by: P. Jordan and J. Orban, British Columbia, Ministry of Forests, Research Branch, Technical Report 3, Victoria, B.C., p. 80-102.*

LANDSLIDE INVENTORY PROJECT - NELSON FOREST REGION, FOREST SCIENCES

Air photo reconnaissance form: 1999, version 3.1

LSFORMS3.DOC

P.Jordan 1999-07-19

Project	Date of inventory	Data base ID
Forest District	Mapper	

LOCATION INFORMATION

Map sheet	Air photo & yr.	Landslide number	
Drainage name:	Elevation (m)	Bedrock formation/group (from map)	Category:
Terrain mapping? recce ___ detailed ___ none ___	If yes: poly.no. ___ stability class: terrain class.: Terrain Category:	If no, or if recce mapping only: apparent terrain class. (from air photo)	
Landslide previously reported? (reference & remarks ...)			

LANDSLIDE INFORMATION

Landslide type	sketch or remarks
Size class	
Slope at initiation (from map, %)	
Aspect (compass octant)	
Slope position (macro): apex ___ upper ___ middle ___ lower ___ escarp. ___ head. ___	
Terminus: stream ___ valley flat ___ lower slope ___ mid slope ___ gully ___ road ___ lake ___ other:	
Damage to: timber ___ plantation ___ road ___ hwy ___ stream ___ none ___ other ...	
Age: date of event if known _____ or: apparent age in years from photo _____	
(check one) first-time event ___ repeated event ___ chronic failure ___ re-activated old failure ___	
Previous natural failures in polygon? yes ___ no ___ uncertain ___ Type: same ___ deep-seated ___ gullying/raveling ___	
Initiation point - slope configuration on contour: gully ___ concave/bowl ___ planar/straight ___ convex/ridge ___ irregular/complex ___	
• slope configuration on fall-line: concave ___ planar ___ convex ___ irregular ___ break/escarpment ___	
Most likely natural (no disturb.) ___ clearcut ___ apparent cause: road fill failure ___ blowdown ___ (up to 3) road cut failure ___ burn ___ drainage diversion by road ___ other: drainage diversion by skid trails ___ (incl. highway, mine waste, etc. - specify)	

DEVELOPMENT INFORMATION

Landslide initiation point is: (up to 2) > on road ___ below road ___ below switchback ___ in cutblock ___ below cutblock ___ on landing ___ below landing ___ unrelated to development ___ other:
If road involved, road is apparently (as of age of air photo): (? if unsure) > active/presently used ___ inactive/light use ___ abandoned/unusable ___ permanently deactivated ___ > mainline ___ operation/major spur ___ minor spur ___ mine road ___ other ...
If cutblock involved, cutblock is apparently: > clearcut ___ selection >50% (heavy) ___ selection <50% (light) ___ > cable ___ skyline ___ helicopter ___ skid trails ___ random skid ___

Notes on landslide inventory project - (revised 1999-07-16)

General procedure for air photo inventory:

1. On TRIM map, outline area to be mapped. This area should include all forested areas, below an upper-elevation limit that corresponds roughly to timberline or to where open alpine forest starts. (This is like a very generous upper-elevation operability line. Basically the same as is often used for reconnaissance terrain stability mapping.)

It is important to map this area, as it defines the forested area in km² for which landslide frequencies will be calculated.

Also, if relevant, outline major areas of non-forest land types in the valley bottom, such as grassland, urban, agricultural, open-pit mines, etc.

On the map, label these areas “A” (alpine) and “U” (other unforested).

2. Locate all landslides, development-related and natural, on air photos. (see note below)
3. Interpret the terrain class at the landslide headscarp/starting point, as if you were preparing a detailed terrain map. However, the terrain polygon does not have to be delineated (unless of course it is part of an area you are terrain mapping).
4. Transfer the landslide location to the map.
5. Assign a number, and classify using the inventory form.
6. Transfer information from completed form to spreadsheet/database.

Landslides to include:

- Only those landslides of types typically caused (or reactivated) by roads or logging.
 - debris slides/avalanches
 - debris flows (starting from discrete sources)
 - rockslides (first-time only)
 - slumps (first-time or reactivated)

- Do not include:
 - chronic failures, e.g. multiple rockfall, talus slopes, or gully headwall failures
 - chronic sediment sources, e.g. cutbanks on outside of river bends
 - repeated natural debris flow gullies or debris flows from multiple or diffuse sources, e.g. in snow avalanche gullies or from extensive rockfall areas
 - large deep-seated slump-earthflow or sackung features
(however, these should be marked on the map with an on-site symbol, as they are important evidence of natural failures in the area)
 - landslides/rockfall/ravelling in obviously inoperable class V areas
 - very old landslide features (> 100 years, especially old rock avalanches which don't reforest and therefore may look fresh for many centuries)
 - snow avalanche or seepage features (sometimes these look like old landslide scars, e.g. small avalanches which come off of rock bluffs and create a linear streak below which stays unforested).

Type of landslide:

- ds debris slide/avalanche
 - df debris flow (entirely or partly confined in gully)
 - ds-df debris slide → debris flow (started as slide on open slope, progressed to debris flow)
 - ss slump - confined to surficial material (usually but not necessarily small)
 - sr slump - bedrock involved
 - ses slump-earthflow in deep surficial material
 - ser slump-earthflow in bedrock
 - sk sackung (slow slump-type movement in bedrock, without defined edges)
 - rf rockfall (include only if obvious discrete event; talus slopes fed by infrequent dispersed rockfall should not be identified as a landslide)
 - rf-ds rockfall → debris slide
 - rf-df rockfall → debris flow
 - rs rock slide (fairly rare - planar slide only)
 - ra rock avalanche
 - av-ds snow avalanche → debris slide
 - av-df snow avalanche →debris flow
 - ge-df gully erosion →debris flow (debris flow which originates by undercutting or piping in gully headwall in deep surficial material, not apparently a debris slide)
 - ch-s chronic failure/sediment source in surficial material (e.g. bank undercutting, retrogressing gully, not obviously a slide or slump)
 - ch-r chronic failure/sediment source in bedrock (e.g. unstable gullied rock, constantly active)
 - w debris flood or washout (not a true debris flow, but enough sediment to consider it a "failure")
 - x complex of several failures (use as suffix) (if several failures of same type and age close together, count as one event and use combined total size)
- other: describe

Size classes:

		landslides (ha)	debris flows (km)	
0	tiny (below our limit)	< 0.02	< 0.1	(Don't include class 0 or 1)
1	small	0.02-0.05	0.1-0.2	
2	medium	0.05-0.2	0.2- 0.5	
3	large	0.2- 1	0.5 - 1	
4	very large	1 - 5	1 - 2.5	
5	humongus	> 5	> 2.5	

Age/rate categories

- first-time event - no obvious indication of repeated events - usual for debris slides
- repeated event - if there appear to be earlier failures at same site - common for debris flows and rockfall
- chronic failure - natural rapid (non-slump) failures only, frequent enough to be kept unvegetated
- re-activated old failure - use for apparently old (revegetated), chronic, or slow-moving failures that have been re-activated or accelerated by a road or logging etc.
- active rapid retrogressing slump - fast enough to have disturbed or seral vegetation, or fresh cracks/scarps

- active slow slump - evidence of ongoing or recent movement, but slow enough to have mature forest cover (e.g. Downie Slide)
- inactive/ancient failure - refers to large slumps, rock avalanches, etc. with no evidence of ongoing or recent movement.

General instructions/other

Location information:

- Map sheet - 1:20,000 TRIM/forest cover
- Air photo - give year if not obvious from roll number
- Landslide number - give a unique number for each map sheet. Data base ID will be assigned later.
- Bedrock: use 1:250,000 GSC map or MoEMPR compilation - e.g. Toby formation, Lardeau group

Apparent cause:

- Check up to three choices. If "other", specify. If unknown, put "unknown" at "other".
- If enhanced snowmelt from cutblocks above, snow avalanches, or other unusual factors are suspected as a cause, indicate under "other" and provide detail in "remarks".

Development information:

- For "landslide initiation point", check up to 2 choices.
- For "If road" and "If cutblock", check one item on each line.
- If unsure, use ? instead of a check.
- If unknown (for example, if you don't know whether or not an old landslide predates development), leave check boxes blank and write "unknown".

TERRAIN DATA CARD

Nelson Forest Region, Landslide inventory, 1999 3.1

Map sheet		Polygon		Air photo		Landslide Y N	
Elev		Aspect		Slope %: av		min	max
Slope config. u ir sg mg be sb			Vert.Curv.: cv cx str		Horiz.Curv.: cv cx und str		
TERRAIN CLASS.						Category	
Terrain components: (av. depth = surficial deposit; soil depth = A+B. Depths in m.)							
/10	Material	Texture	% c.f.	av. depth	compact./hard./structure		soil depth
/10	Soil Drainage Class		soil description or remarks				
	r w m i p vp						
	r w m i p vp						
BEDROCK: Form.			Lithol.		Structure		Category
dip		dip direct.		hardness		av. joint space.	
Natural landslides? large Y N				small Y N		type	
Gullies?		shallow(<5m)		sidewalls: gentle(<65%)		activity:	
single infreq. freq.		deep(>5m)		steep(>65%)		inactive slight very	
Other indicators:							
DEVELOPMENT AND LAND USE INFORMATION:							
Forest cover:		mature	immat.	clearcut	sel. logged	burned	other disturbance:
Logging:		approx. age	Yarding:		cable sky heli skid	Trails:	deact? Y N
						none few many	
Roads:		type	constr.	condition	drainage control	deact?	
		1					
		2					
Remarks:						Stability class:	
Recorded by:				Date:			

LANDSLIDE DATA CARD

Nelson Forest Region, Landslide inventory, 1999 3.1

Landslide number:	Polygon no:	single multiple no.of init.points:		
Type	headscarp elev.		aspect	
Position/ slope type	approx. age		Old failures? Y N (at/adjacent)	
Failure origin. (circle 1 or 2)	road cut below road natural (no road/block)	road fill below switchback	on trail below trail other:	in cutblock below cutblock
Slope at headscarp	Slope above		Slope below	
Headscarp height:		width:		
Primary slide:	length:	av. width:	av. depth:	
Secondary slide?	length:	av. width:	av. depth:	
Slope config: u ir sg mg be sb		Horiz.Curv.: cv cx str	Vert.Curv.: cv cx str	
Drainage class: r w m i p vp		Seepage? major minor absent		
Terrain class. (at failure scarp)		Failure plane (circle 1 or 2)	R C road fill	M D other:
Terrain category:		Texture at failure plane:		% c.f.
Indicators of instability at site:				
Bedrock at slide scarp:		none	typical of polygon	other:
Fate of debris:		approx. % in water course:		
Contributing factors:		primary	secondary	
State of preservation:		good mod. poor	Regen: bare eroding	weeds/grass brush conifers retrogressing/enlarging
Evidence of causes: obvious suspected not evident				

Sketch/remarks:

Nelson Forest Region, Landslide inventory, 1999 - Abbreviation codes

Terrain Card:

Slope configuration:	u	- uniform	mg	- multiple gullies (or dissected)
	ir	- irregular	be	- benchy
	sg	- single gully	sb	- slope break

Vertical/Horizontal Curvature:	cv	- concave	und	- undulating (repeated cv/cx)
	cx	- convex	str	- straight

Compactness (coarse grained soil)	very loose	Easily penetrated with shovel handle.
	loose	Easily excavated with shovel.
	compact	Difficult to excavate with shovel.
	dense	Must be loosened with pick to excavate.
	very dense	Very difficult to excavate with pick.

Hardness (clayey soil)	soft	Wet: Sensitive - flows if remolded.	Dry: Easily absorbs water and softens, crumbly when dry.
	n.c. (normally consolidated)	Easy to roll ribbon with a little added water.	Hard; moderately difficult to work water in with fingers.
	hard	Hard or blocky, difficult to remold by hand.	Brick-hard; very difficult to soften with water.

Drainage Class:	r	- rapid	i	- imperfect (gleyed horizons)
	w	- well	p	- poor (gleysols)
	m	- mod. well (some moisture indicators)	vp	- very poor (organic soils)

Bedrock structure:	m	massive	bd	bedded
	gp	glacially polished	fr	fractured
	jt	jointed	lb	loose blocks
	fl	foliated	rt	rotten (or saprolitic)
	other:			

Bedrock hardness:	R0	extremely weak	Indented by thumbnail
	R1	very weak	Crumbles under hammer blow
	R2	weak	Shallow indentations with hammer point
	R3	medium strong	Fractured by single hammer blow
	R4	strong	Fractured by more than one hammer blow
	R5	very strong	Requires many blows of hammer to fracture
R6	extremely strong	Can only be chipped by hammer	

Joint spacing:	J0	extremely close	< 2 cm
	J1	very close	2 - 6 cm
	J2	close	6 - 20 cm
	J3	moderately close	20 - 60 cm
	J4	wide	60 cm - 2 m
	J5	very wide	2 - 6 m
J6	extremely wide	> 6 m	

Indicators of slope instability: abbreviations for most common ones
(see also list from guidebook supplement)

1. ls-rec Recent landslide scar
2. ls-old Old landslide scar
3. ten-crk Tension cracks on hillside
4. debris Debris at base of slope
5. scarp Small scarps, hollows, or linear depressions
6. step Stepped slope profile
7. piping Piping erosion
8. regosol Regosol or immature soil profile
9. strat Stratified deposits with silt/clay layers (kame or glaciolacustrine)
10. buried Buried soil profiles
11. g-head Gully headwalls or extensive gullying
12. g-scour Recently scoured gully (by debris flows)
13. levee Debris flow levees on gully sides or fan
14. lean-tree Leaning or jack-strawed trees
15. curv-tree Curved (sweeping) trees
16. mois-veg Moisture-indicating vegetation
17. tufa Tufa (CaCO₃ spring deposits)
18. seepage Extensive seepage or springs
19. bedding Bedrock bedding or joints parallel to slope
20. rotten Rotten or highly weathered rock
21. road-cutf Road cut-slope failures
22. road-tc Road tension cracks
- other (describe)

Roads:	<u>Type</u>	<u>Construction</u> (dominant method)
	ml mainline (heavy use, ≥6m)	cf cut/fill
	ml-n mainline new (1993 or later)	fb full bench
	op operation (mod. use, typically 5m)	fb/eh full bench - endhaul
	op-n operation new	pb part bench
	sp spur (minor use, typically 4m)	
	sp-n spur new	<u>Drainage control</u>
	mine mine road	good meets standards
	other	fair OK, somewhat lacking in design or maintenance
	<u>Condition</u>	poor generally substandard but somewhat functional
	good well-maintained	v.poor dysfunctional or none
	fair infrequently maintained, some deterioration	
	poor unmaintained except for patchup, passable to light vehicles, much erosion or deterioration	<u>Deactivation</u>
	v.poor abandoned or unmaintained, undriveable or difficult 4x4, severely eroded	none
	(use abbreviations g, f, p, vp)	wb water bars (minor/seasonal)
		xd cross-ditches (temporary deact., culverts backed up or removed)
		fp fill pulled (rotational deact.)
		rec recontoured (permanent deact.)

Landslide Card:

Landslide type:	ds	debris slide/avalanche	sr	slump - bedrock involved
	df	debris flow (in gully)	rf	rockfall
	ds-df	debris slide ⇒ debris flow	rf-ds	rockfall ⇒ debris slide
	ss	slump - in surficial material	rf-df	rockfall ⇒ debris flow
	others - use air photo inventory categories			

Position/ slope type	os	open slope	esc	escarpment
	os→g	os into gully	gh	gully headwall
	osd	os depression (incipient gully <2m)	gc	gully channel
			gs	gully sidewall

Contributing factors: (Note: Use these only when the cause is readily apparent or there is strong evidence. If road drainage or cut/fill instability has been repaired following the event, but one of these causes is suspected, “dd” or “r” can be used.)

- road:

- r-cut - cut removed toe support
- r-seep - cut intercepted seepage at failure
- r-uf - unstable fill (too steep, poorly placed, poor quality material)
- r-wf - wood in fill
- r-tsfc - tree-supported fill
- r - cut or fill, undifferentiated

- drainage diversion/concentration: (failure is caused by accidental diversion of water down road or trail, or concentration of subsurface flow by cut/ditch)

- dd-rc - road, creek/gully flow diverted
- dd-rd - road, ditch/cutbank seepage
- dd-sc - skid trails, creek/gully
- dd-sd - skid trails, cut seepage
- dd-y - yarding disturbance
- dd - undifferentiated (use if exact drainage cause not obvious)

- road drainage: (failure is directly below or caused by a drainage structure, without major accidental diversion from up road)

- rd-ic - inadequate number of culverts
- rd-im - inadequate maintenance of culverts
- rd-pc - poorly located culverts
- rd-co - culvert outlet poorly protected
- rd-id - inadequate ditch
- rd-db - ditch blocked
- rd-wb - water bar/X-ditch poorly located

- skid trails (or other trails):

- st-uf - unstable fill
- st-cut - unstable cut

- landing:

- L-uf - unstable fill
- L-cut - unstable cut
- L-dd - drainage diversion

- clearcut (and partial cut, burns):

- cc-sm - clearcut - enhanced snowmelt
- cc-rs - clearcut - root strength loss
- cc-wt - clearcut - windthrow at edge
- cc-y - clearcut - yarding disturbance
- cc - clearcut, undifferentiated
- pc-wt - partial cut - windthrow
- pc-y - partial cut - yarding disturbance
- b-sm - burn - enhanced snowmelt
- b-rs - burn - root strength loss

- deactivation of roads or trails (failures after):

- deact-f - failure of fill material
- deact-dd - drainage diversion/concentration
- deact-wb - water bar/X-ditch poorly located

- gullies:

- g-rf - road fill material in gully
- g-cb - culvert blocked
- g-logd - logging debris in gully
- g-land - landing debris in gully
- g-yd - yarding disturbance
- g-av - snow avalanche debris in gully

- other categories:

- mine-w - mine waste pile failure
- mine-d - mine, drainage diversion/interception/discharge
- nat - natural - no probable development-related cause

other: - other (describe)

unknown - enter this if no cause is evident

General instructions:

1. If there is more than one landslide in a terrain polygon, fill out the terrain card for the first one only.
2. If there are several nearly identical landslides in a polygon, fill out one landslide card only, and under remarks, indicate others are similar. (e.g. for # 23, "24 and 25 are similar")
3. All slopes are in percent. Azimuths are in degrees from true north. Indicate units for length measurements, normally m or cm.
4. For terrain card, min. and max. slopes, estimate slopes over a distance of several 10's of m. Ignore small anomalies. (min and max should be equivalent to about 10th and 90th percentiles)
5. Terrain card: vert. & horiz. curvature are over scale of whole polygon; configuration is shorter slopes within the polygon.
Landslide card: vert. & horiz. curvature and configuration are on a scale comparable to the landslide headscarp, typically in the order of 10 m.
6. For terrain classification labels, use terrain textural terms. For all other textures, use standard soil classification terms for < 2 mm. Terrain textures are unaltered parent material. If surface soil is different, indicate in remarks.
7. Terrain component, structure: If relevant, describe surficial deposit structure, e.g. stratified, laminated, dipping, etc. Also include notes on minor components, e.g. "rare L^G beds". Use stratigraphic indicator sparingly, only where it's consistent across the terrain unit.
8. Terrain components and soil drainage class: Indicate decile (proportion out of 10).
9. Kame deposits (stratified ice-contact deposits): Describe according to most abundant material (F^G or M); indicate "kame" in structure column, and describe more fully under Remarks.
10. Indicators of instability: Enter the number or use abbreviations provided.
11. Terrain card, development information: This describes present conditions. If a landslide occurred before the logging or road construction, indicate this as a remark on the landslide card. If there are two land uses in the polygon, circle two and mark them with "1" and "2" in order of abundance. (Ignore if < 10% of area.)
12. Roads: Use "1" and "2" if there are two different types of road in a polygon.
"Mainline" is major valley-bottom road accessing several operating areas; "operation" is a road accessing one operating area such as a mid-sized watershed; "spur" accesses only one or several blocks.
Use "other" for highways, private-land access roads, etc.
13. Landslide card, Primary/secondary slide: Use secondary if there are two obviously different types of landslide in the event; e.g. a debris slide/avalanche progressing into a debris flow.
14. Landslide card, Fate of debris: Indicate where most of the debris went, e.g. into creek, onto road, lower slope, etc. Provide rough estimate of percent entering creek.
15. Landslide card, Contributing factors: Enter one or more in approximate order of importance. If causes are not evident, do not guess.
16. If additional data are collected for a landslide, use a blank page, or use other forms if available. Refer to this under Remarks.
17. For all data fields - if the information is unknown, not collected, or not applicable, enter ? or - .

< = less than, > = greater than

P. Jordan, revised 1999-07-16

More notes on landslide and terrain cards

Each landslide is to have a consecutive number starting at 1, in addition to the original number from the air photo inventory (typically something like K042-9a). The consecutive number is what's shown on the air photo.

For multiple similar landslides in a polygon: If you judge the landslides to be different events, then each must have a different number (e.g. 5,6,7, not 5a,5b,5c), and each should have one line in the data base (maybe all with the same data). If you figure it's really one landslide with two or more starting points, then it should have just one number and only a single dot should be shown on the air photo. In this case, on the landslide form, circle "multiple" and enter the number of starting points .

Air photos to show: Terrain polygon number in each polygon (black); Landslide number beside each landslide symbol (red); field check numbers in the form of C5 (black). Field check symbols have a black dot inside a red circle.

Landslides - use "crescent" symbol with a dot (red) at the exact starting point. Arrow for runout is to be shown only where it's a debris flow.

If a landslide is on the exact border of two polygons (which isn't unusual), then the data should be entered with the downslope polygon (e.g. in the FGs polygon, not the FGp.)

Polygons gentler than 40% - If it's only sporadic polygons, just map them. But if there are extensive areas < 40%, those polygons can be labelled "0" which means unmapped, if you want.

Each mapped polygon to have a terrain stability symbol (I II III IV V) according to your standard practice. (This won't be used in the analysis, it's just for the benefit of the licensee and the forest district, who will get a copy of the mapping when it's finished.)

The map area name (Ferguson, Crawford etc) is to appear in each data base (it's the only way we can distinguish the different polygon and landslide numbers).

Polygon number must be written on every landslide card (important!)

Terrain card: Enter "terrain class" in the database as a single text string. If there are stratigraphic symbols, they are shown using a vertical bar, and parentheses if necessary. e.g. (sEvlsgFGt)/gzMb or sEvl(sgFGb/zsMb).

Under "terrain components", avoid using stratigraphic symbols. Instead give the approximate tenth's of surface exposure of each material in the polygon. e.g. szMblsgFGs might be

8 FG s 70 ...
2 M \$L 40 ...

In the "...structure" column you can describe stratigraphy.

Texture for "terrain components" should be using soils terminology e.g. \$L or SiL for silt loam. In the single-field terrain class, use the usual terrain mapping textural symbols, e.g. gsz. (OK to use z or \$, whichever you're used to.)

Each polygon is to have a "terrain assemblage" entered, followed by any modifying geomorphic modifiers. These are the fields T_ASSEMB, T_MOD1, T_MOD2, T_MOD3 in the database. This are the fields that will be used for statistical analysis.

e.g. xCbk/sMv-VAR would be

C+
V
A
R

Same goes for the landslide card.

Drainage class is an important parameter for analysis. So each polygon must have a drainage class shown, even if it's a "best guess" for unvisited polygons. (Just like in operational terrain mapping!) If you want to show a range, put the secondary drainage class on the second line.

For unvisited polygons, the terrain components columns should still be filled in. Fill in the /10, Material, Texture, and %cf, even if they are guesses. Other fields beyond this are optional, depending on how confidently you can extrapolate information from nearby checked polygons.

"Forest cover" and "Logging" can have up to two entries each. e.g. if a polygon is about half logged, put both Mature and Clearcut. But ignore minor components, less than 20% or so. It's probably a good idea to mark the more abundant land use with a "1" or a double circle or something, so the data entry person can enter the primary/secondary entries as FC1 and FC2.

Bedrock - use the symbols from the legend I gave you for the "Bedrock formation" field.

On terrain card, Elev, Aspect, Slope av min max, %cf, dip, dip direct., road length ; and on landslide card, Elev, Aspect, Slope at above below, length, width, depth, %cf ; all these are NUMERIC fields! This means they have to be a SINGLE NUMBER (real or integer), i.e. things like <5%, 30-40%, etc are not allowed! However, av depth (terrain components), depth A-B (soil), approx age ; these are general fields and so can include text.

All depths, lengths, widths are in metres. Do not use cm. (You may have shown cm on the field card, but the data must be entered in the database as m.) All slopes are in %.

Text fields, including Remarks, Compact/hard/structure, Fate of debris, etc, can have up to 256 characters. Where "other" is used (Forest cover, Indicators, Contributing factors) it can be followed by a bunch of text up to 256 characters.

*****!!!!!! Backup !

Make photocopies of your work-in-progress and keep them somewhere safe.

Explanation of database - P Jordan, 2000-04-12
Landslide project, Arrow and Kootenay Lake Forest Districts

LSNUM - landslide number (key field)

MAP_SHEET, NUMBER

M_Elev - Elevation from inspection of map

M_Geol - Geology by category (as sent previously)

M_GeolSimple - Geology by simple category:

Q - Quaternary

g - granitic

n - gneiss

fs - fine sedimentary (Mesozoic - Slocan Group etc)

cs - coarse sedimentary (mostly Paleozoic - Hamill,

Badshot, etc)

ms - fine-textured metasediments (mostly Paleozoic -

Lardeau etc)

mv - metavolcanics (mostly Paleozoic - Kaslo etc)

v - volcanics (Mesozoic - Rossland Group etc)

p - Precambrian sediments and metasediments (Windermere

& Purcell)

A_Terrain - Terrain by category from air photo interpretation (by leading terrain type):

R - Rock

C1 - shallow colluvium (Cv, Cvb etc)

C2 - deep colluvium (Cb, Ck, Cc etc)

M1 - shallow morainal (Mv, Mvb etc)

M2 - deep morainal (Mb, Mbv, Mk etc)

G - glaciofluvial (FGt, FGs etc)

K - "Kame-type deposits", mixed FG and M

(the distinction between G and K is probably not

very meaningful)

L - glaciolacustrine

F - fluvial

D - decomposed rock

A - anthropogenic

A_Mod1, A_Mod2 - modifying processes on terrain symbol if present (-V etc)

Type - landslide type

DS debris slide/avalanche

DF debris flow

DSF combination debris slide --> debris flow

RF rock fall

RS rock slide

RFD rock fall or slide --> debris flow

SS slump, surficial

SR slump, bedrock
SE slump-earthflow
CF chronic failure (applied to retrogressing gully
headwalls etc (rare))

SIZE

1 0.02-0.05 ha
2 0.05-0.2 ha
3 0.2-1 ha
4 1-5 ha
5 > 5 ha

M_Slope - in percent

M_Aspect - by octant

A_Age - Age class (approx.):

1 1995-1999
2 1990-1994
3 1980's
4 1960's & 70's
5 1950's or older

Exact_Age - year if known

M_CurvH, M_CurvV - horizontal and vertical curvature

cv - concave, cx - convex, p - planar, ir - irregular,
g - gully, b - break or escarpment

A_Cause1, A_Cause2 - apparent cause (in order given; first one probably
takes precedent; this is the mappers's opinion)

N natural
RF road fill
RC road cut
DR drainage diversion, road
DS drainage diversion, skid trails
CC clearcut (ground disturbance, root strength,
enhanced snowmelt etc)

NB natural burn (wildfire)
MW mine waste
HW highway
RR railway
WL water line
PL pipeline (gas)
TL transmission line
DA deactivated road (if obviously recontoured)

A_Dev1, A_Dev2 - Land development associated with landslide (not an
opinion, a spatial relationship)

OR on road
BR below road
IC in cutblock
BC below cutblock

U unrelated to development
M on or below mine
Others - on or below other features, abbreviations as

above

Note - In general, M_ means a field obtained from maps by hand, and A_ means a field obtained from air photos. So I suggest that comparable information obtained from GIS should have the prefix G_.

APPENDIX B: BLANK LANDSLIDE PROFILE DATA CARD

BCMoF Landslide Profile Data Card:

<http://www.for.gov.bc.ca/isb/forms/lib/fs123-1.pdf>



LANDSLIDE PROFILE DATA CARD

DATE			PAGE		OF
Y	M	D			
FAILURE NO.					
RECORDED BY					

STARTING POINT OF PROFILE / COMMENTS _____

SEGMENT DISTANCE	SCOUR (m)			FILL (m)			PATH SLCPE (°)	PATH AZIMUTH (°)	SLOPE MORPH.	MATERIAL	FLOW DEPTH	GULLY FLOOR WIDTH / DEPTH	DEPOSIT TEXTURE	DEPOSIT MORPH.	STREAM CHANNEL		% REVEG.
	L	W	D	L	W	D									BANKFULL WIDTH	VALLEY FLOOR WIDTH	

STREAM CHANNELS: BANKFULL WIDTH @ P.O.E. _____ METRES

VALLEY FLOOR WIDTH @ P.O.E. _____ METRES

∠ = ANGLE OF ENTRY _____ °

FAILURE PATH
 STREAM CHANNEL

Note any stream channel degradation in the deposition zone as scour and note in Comments section.

APPENDIX C: BLUEBERRY CREEK DATA

Landslide profile data cards for Blueberry Creek event.

Note: Column numbers are consistent with Appendix B (BCMof) Landslide Profile data card

Aug. 20, 2002

Landslide #: **1 4 5 2 3**
 Drainage: **Blueberry Creek**

Reach (1-2)	Reach distance (m)	Average slope (%)	Average width (m)	degrees Aspect	Erosion (wxd) (m)	Deposition (wxd) (m)	Confinement	Material	Availability of material	Comments	
205 m	1-2	24	13	8	199°	—	3 x 0.2	S	F ₃	—	remnant area, standing trees, fluvial downcutting
	2-3	29	11	6	230°	—	4 x 0.3	S	F ₃	—	
	3-4	32	15	7	220°	—	3 x 0.2	S	F ₃	—	* photo; standing timber, sparse boundary, levees
215 m	4-5	31	20	10	195°	—	3 x 0.2	S	F ₃	—	
	5-6	49	16	15	195°	—	~80m ³	S	F ₃	—	widening of remnant, deeper lobes, ^{main} terminal deposition area
220 m	6-7	61	12	13	160°	—	10 x 0.5	S	F ₃	—	* photo; terminal lobe of boulders, logs
225 m	7-8	18	18	13	165°	—	10 x 0.5	S	F ₃	—	signs of older debris flows, noog return period
	8-9	109	18	22	155°	—	10 x 0.75	C	M _v /F ₃	Some	confined channel, some scouring
	9-10	40	18	25	155°	m2l. 15x2x40	S	M _v /F ₃	Some	* photo; 30% coarse gravel, 70% fines: 25G-70F-5silt	
	10-11	89	28	9	165°	4 x 0.5	—	G	C/R	Some	main deposition area; some scouring; levees on side
285 m	11-12	33	27	12	168°	3 x 0.5	2 x 0.5	C	M _v /C _v	abund.	* photo; slumping from oversteepened side slopes in M _v
295 m	12-13	71	22	10	160°	4 x 0.75	—	C	M _v /C _v	abund.	material slumping from side slopes
	13-14	73	22	10	174°	5 x 0.5	2 x 0.1	C	M _v	Some-abund.	
	14-15	43	23	7 (under) 166°	4 x 0.5	—	—	C	M _v	Some-abund.	
Reach break criteria			Availability of material (only erosional)			Confinement			General comments should include:		
slope gradient			abundant			canyon (>100%)			logged or unlogged		
erosion/deposit			some			gully (V-shaped)			levees and lobes (include dimensions)		
confined/unconfined			none (bedrock or compact till)			C confined			texture of deposit: %coarse gravel (>32mm),		
direction						S slightly confined			%fine gravel, %sand, silt, clay		
						U unconfined			notes on boulders (est. size), logs, past ls activity		
									diagram of entire slide with key points		
									photo #		
									10m ³ = 1 dump truck		
									30m ³ = 1 logging truck		

Peter Jordan
 Carol Wallace
 Marc Deschênes

Aug. 20, 2002

Landslide #:

Drainage: Pulasky Creek

L.V.

Reach (1-2)	Reach distance (m)	Average slope (%)	Average width (m)	Aspect	Erosion (max)	Deposition (max)	Confinement	Material	Availability of material	Comments
15-16	45	22	8	167°	4x0.5	-	C	M _b	some-abund.	
16-17	50	22	16	155°	2x0.5	6x1	S	M _b	abund.	* photo; depositional reach
17-18	185	25	9	160°	4x0.3	2x0.1	C	M _b	abund.	* photo; mainly erosional reach
18-19	64	28	9	166°	4x0.3	2x0.1	C	M _v	some	" " "
19-20	31	37	12	125°	5x0.2	2x0.2	C	M _v	some	some exposed bedrock
20-21	123	35	12	166°	5x0.5	4x0.1	C	M _v /R	some	" " "
21-22	60	35	13	180°	5x0.5	4x0.3	C	M _v /b _v	some	* photo; saprolite bedrock continuation of the creek gully and channeling
22-23	85	45	8	192°	6x0.5	meq.	C	b _v /M _v	some	shallow channel in slope below cutblock
23-24	105	50	6	216°	3x0.5	meq.	C	M _v /b _v	some	banking till; bottom edge of cutblock
24-25	21	50	8	235°	4x0.3	-	S	M _v	some	cutblock; flow of channel composed of saprolite
25-26	46	45	5	220°	3x0.5	-	S	M _v b	some	cutblock
26-27	35	48	10	226°	6x0.1	-	U	M _b	some	transitional zone
27-28	27	65	8 (0.5 deep)	225°	8x0.6	-	U	M _b		* photo; base of landslide scar
Reach break criteria		Availability of material			Confinement			General comments should include:		
slope gradient		abundant			canyon (>100%)			logged or unlogged		
erosion/deposit		some			gully (V-shaped)			leaves and lobes (include dimensions)		
confined/unconfined		none (bedrock or compact till)			confined			texture of deposit: %coarse gravel (>32mm),		
direction					slightly confined			%fine gravel, %sand, silt, clay		
					unconfined			notes on boulders (est. size), logs, past activity		
10m ³ = 1 dump truck								diagram of entire slide with key points		
30m ³ = 1 logging truck								photo #		

1465 m

15410 m

SKETCH
⇒

828
-120

708

Peter Jordan
Carol Wallace
Mark Aschens

APPENDIX D: HUMMINGBIRD CREEK DATA

Landslide profile data card for Hummingbird Creek debris avalanche.

Note: Column numbers are consistent with Appendix B (BCMoF) Landslide Profile data card

Name of DF: Hummingbird Creek Mapper: P. Jordan, J. Fannin, P. Kaley, M. Busslinger Date mapped: 14 July 2009 Path Geometry Card Page # 1 of 2

Reach	GPS W.P. = Pt		Path				Erosion		Deposition		Process	Conf.	Material			Vegetation sm	Comments	Photo #	taken from	
	Distance (m)	Average Slope (°)	Avg Flow Width (m)	Aspect Angle (°)	Avg Flow depth (m)	Width (m)	Depth (m)	Width (m)	Depth (m)	E/D*	UBCD Flow**	Terrain Symbol [†]	Availability							
1-2	35	1	57	27.5	10	323	-	10	0.3	-	-	E	u	zsMv	A	F	top of slide, Bedrock in failure plane	175 dwn.	top	
2-3			125	28.5	18	323	-	18	0.2	-	-	E	u	Mv/R	S	F	pt. 3 at bend, seepage water on surface, change from slide into avalanche behaviour, mostly eroded to bedrock	176 dwn.	pt. 2	
3-4			174	23.0	37	303	-	30 (+7)	0.3 (+0.6)	-	-	E	u	Mvb	A	F	erosion depth not constant in crosssection due to scoured channels --> two erosion depths, pt. 4 at high rock outcrop.	177 dwn.	mid reach	
4-5			80	29.0	94	316	-	79 (+15)	0.3 (+1.0)	-	-	E	u	Mvb	A	F	erosion depth not const. in crosssect. due to scoured channels, pt. 5 exposed rock to the right of tree stand, photos taken from pt. 4	178 up 179 dwn.	pt. 4	
5-6	36	5	79	34.0	115	332	-	115	0.3 *30%	-	-	E	u	Mvb	varying	F and none	pt. 6 at red rock Ø2m in creek (20m dwnstrm. from edge of slide), rock cliff in reach middle with steep rockfaces where erosion reached bedrock, mapping happened through right side of reach, because of cliffs to the left	180 dwn - 182 dwn	mid reach	
6-7	37	6	96	10.0		241						c					superelevation on opposite channel side where source material entered, deposition of logs along trimline	183 up 184 dwn. 185 left 186 left	6 upstrm 6 dwnst. in reach in reach	
7-8			49	13.5	"10"	231						c					pt. 8 end of ls source, pictures 188, 190, 189 show end of slide on left side of channel (in flow direction), note forest stand on upper end followed by cliff and edge of slide.	187 dwn. 188 l.u. 190 l.m. 189 l.d. 191 dwn.	pt. 7 in reach in reach in reach	
8-9			184	13.5	"10"	241						c						192 dwn. 193 up	pt. 8 pt. 9	
9-10			132	10.5	"15"	250		12	0.8			c					see cross-section for width,	194 dwn.	pt. 9	
10-11	39	10	43	9.5	"15"	272						c					pt. 10 is round boulder (3m into channel is waypoint 39)	195 dwn.	pt. 10	
11-12			34	13.0	9	215						c						196 dwn.	11 or 12?	
12-13			15	11.0	10	220						c						197 up	pt. 13	
13-14			32	13.0	11	276						c						198 dwn.	pt. 13	
14-15			38	15.0	10	322						c						199 dwn.	pt. 14	
15-16			34	10.0	12	256						c						200 dwn.	pt. 15?	
16-17	40	16	105	13.0	12	208						c						201 dwn.	pt. 16	
17-18			44	16.0	15	258						c								
18-19			171	16.0	19	240						c						bedrock cliff	202 dwn.	pt. 18

Evidence of volume change gone.

* Process
D = Deposition only
De = Deposition (minor erosion)
B = Both E and D
Ed = Erosion (minor Deposition)
E = Erosion only
T = Translation only (no E or D)
S = Slide source (erosion, top source)

**UBCDFlow
u = unconfined
c = confined
t = transition

† Terrain Classification System for British Columbia

* Vegetation
F = mature forest
I = immature for.
D = deciduous
L = logged

General Comments should include (on separate sheets)
Cross sectional area and form, flow depth, super-elevation
logged or unlogged
levees and lobes (include dimensions)
texture of deposit: %coarse gravel (>32mm)
%fine gravel, %sand, silt, clay
notes on boulders (est. Size), logs, past is activity
diagram of entire slide with key points

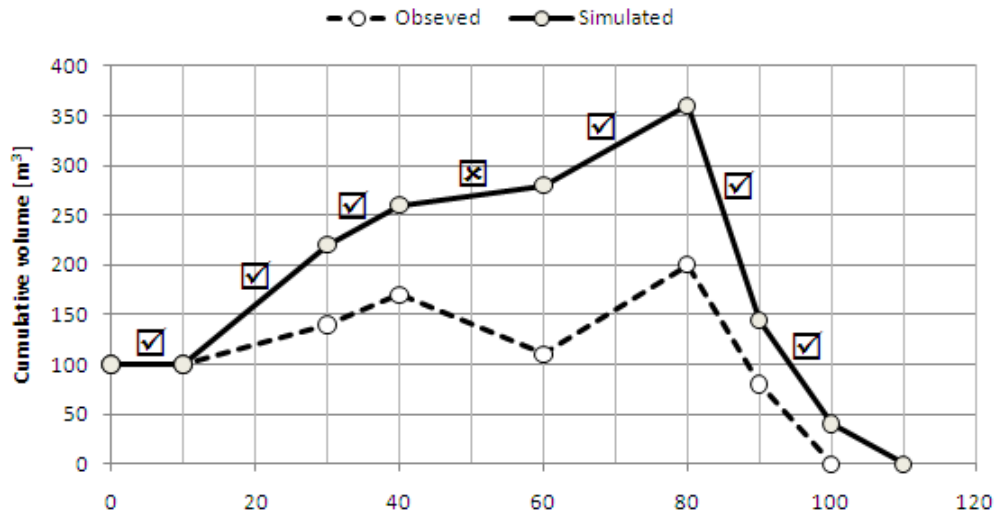
UBCDFlow Regression Eq. Domains

10.0°=17.6%	0sTHs18.5°	u (-dV)
18.5°=31.2%	18.5-THs55°	u (+dV)
20.5°=34.4%	30sTHs55°	c (+dV)
55.0°=142.8%	30sTHs55°	t (-dV)

APPENDIX E: SIMULATION SUCCESS INDICATORS

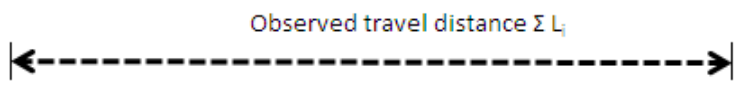
Process Indicator PI

Def: Sum of all reach lengths ($L_{i,p}$) where process (i.e. entrainment +dV, or deposition -dV) is correctly simulated, divided by the total observed length of an event path ($\sum L_i$).



Sim.	V_{init}	+dV	+dV	+dV	+dV	-dV	-dV	
Obs.	V_{init}	+dV	+dV	-dV	+dV	-dV	-dV	
	$L_{i,p}$	$L_{i,p}$	$L_{i,p}$	0	$L_{i,p}$	$L_{i,p}$	$L_{i,p}$	$\sum L_{i,p}$

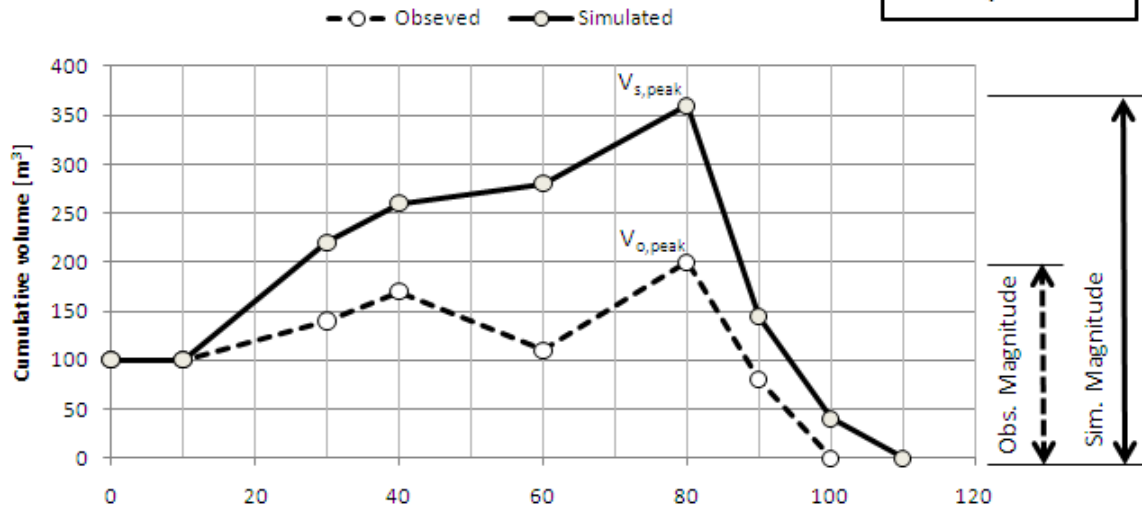
$$PI = \frac{\sum_{i=1}^n L_{i,p}}{\sum_{i=1}^n L_i} \cdot 100\%$$



Magnitude Indicator MI

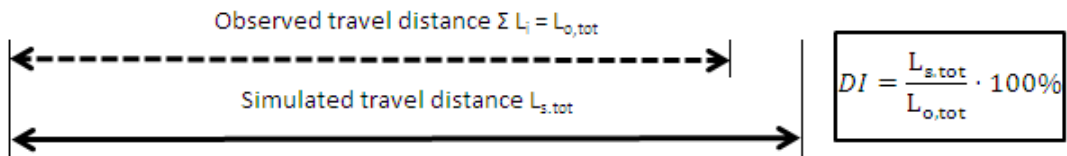
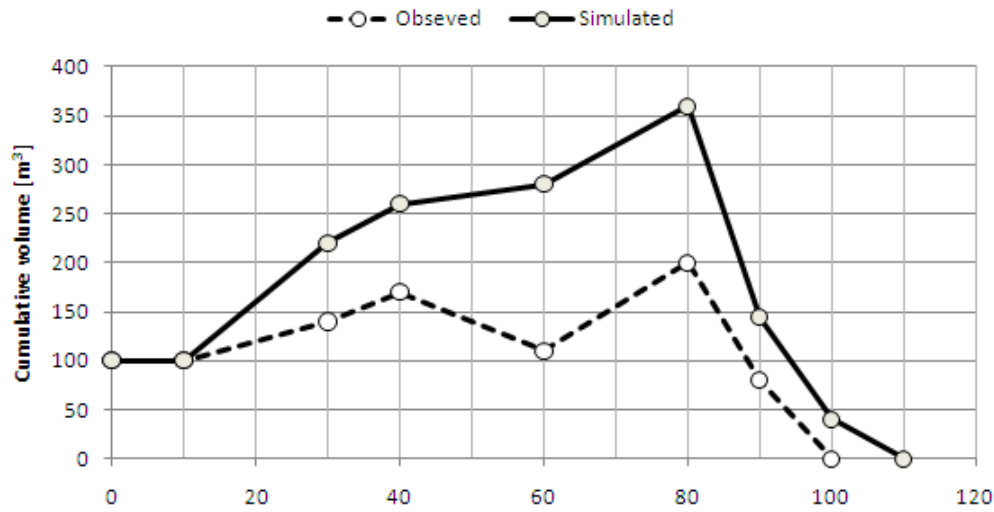
Def: The max. simulated value of the volume balance ($V_{s,peak}$) divided by the max. observed value of the volume balance ($V_{o,peak}$).

$$MI = \frac{V_{s,peak}}{V_{o,peak}} \cdot 100\%$$



Distance Indicator DI

Def: Travel distance is defined as the distance along the path from point of origin to the point where the volume becomes zero. The distance indicator is the ratio of simulated ($L_{s,tot}$) to observed ($L_{o,tot}$) travel distance.



APPENDIX F: DATA INTERPRETATION FOR SIMULATION

(Version 4)

Remarks

This is a guideline to process field observations from the Kootenay inventory into input data for UBCDFLOW modelling in a forensic manner. Sometimes the recommendations given here cannot be rigorously applied. In these cases it is suggested to consult all information available (data card, reach comments, photos, landslide card etc.) and make an informed judgement call.

Travel Distance

Travel distance is the total distance traveled along the path from head scarp to the end of deposition. It is divided into reach lengths. Simulated travel distances are inter-, or extrapolated based on the volume change gradient (dV_i/L_i) in the last reach, or reach of termination.

Initial Volume

For a forensic analysis the initial volume is known. If not reported otherwise, the initial volume is taken as the reported net volume exiting the first reach. Therefore, the model and the field observation have the same magnitude at the end of the first reach.

There are two ways to satisfy this condition:

1. either the reach width is set to zero and the observed volume is entered as V_{init} in UBCDFLOW (preferred approach)
2. or the volume that UBCDFLOW entrains in the first reach ($V_{(predicted) 1. Reach}$) is subtracted from the observed volume and the resulting volume is used as input.

$$V_{observed 1. Reach} - V_{(predicted) 1. Reach} = V_{init}$$

Width

As this is a forensic analysis, use reported flow widths w_e and w_d rather than reported average widths w , to get closer to field observation.

For reaches that are reported to have both w_e and w_d make a judgment call. Consider, that it is likely that the actual flow width is somewhere in the range of the reported flow widths. Consult reach comments and sketches and see if they indicate a flow width. Check photos, consider upper and lower reach.

For those reaches that have no reported flow width, consult the same sources as listed above. Maybe you can interpolate from adjacent reaches. Make sure you consider all information available. Then decide on a width.

Confinement

In general following conversion has been used:

Field Report	UBCDFLOW Input
Unconfined	Unconfined
Unconfined following confined	If $TH < 20.5^\circ \rightarrow$ Transition* If $TH > 20.5^\circ \rightarrow$ Unconfined
Slightly confined** Schematic Profiles: Slightly confined a)  b) 	There are two cases for which the class slightly confined was used for field mapping. a) An incised channel which is shallow and narrow, and can't accommodate the discharge of a large debris flow, which spills out onto gentler slopes on both sides. In this case a small event would be fully confined, but a large event would not. b) A channel which widens, so that the debris flow does not occupy the full channel width, and can spread out somewhat. In this case, a very large event might be fully confined by the valley sides, but a small event would not. Sometimes the small events become depositional in such reaches; in some other cases the smaller events become self-confined by depositing levees, but most of the volume flows through the reach. For these simulations the slightly confined reaches where often interpreted as confined, but could also be unconfined, especially in lower reaches where

	deposition occurs (note: in UBCDFLOW c would result in erosion only). If slightly confined was between c and u reaches; it was set as transition.
Confined	Confined
Gully	Confined
<p>* Do not use transition flow to account for energy loss or so. Transition is only used for unconfined following a confined reach. However if slightly confined follows a confined reach, and the following reach is also significantly wider, I would interpret it as transition.</p> <p>Roads that are below an unconfined reach can be set as transition.</p>	
<p>** check with reach comments, photos etc. If necessary make a judgment call keep also in mind that the idea behind c is to account for high pwp, no spreading, high velocity and therefore rel. mobile flow, compared to u where spreading is allowed the rheology is more granular, velocities generally lower and the flow is less mobile</p>	

This is a guideline for general procedure. UBCDFLOW is an empirical tool and it cannot be run without a critical assessment of the input. Better results are obtained if judgement is used rather than following a rigorous conversion. However assumptions have to be objective and based on facts reported from field.

For example Airy Creek 3017: Reaches 4-5; 3-4 and 2-3 are reported as slightly confined. I usually model these as confined. But the TH is reported to be smaller than 10° and therefore I expect some deposition to occur. However, UBCDFLOW would predict $-dV=0$, because it does not consider any deposition in confined reaches. So in this case I would use unconfined in order to account for deposition taking place at low gradients.

The same is true for example for Burton Creek 106.

APPENDIX G: UBCDFLOW: STEP-LIKE VOL. ESTIMATES

Sensitivity analysis of UBCDFLOW model: Investigation of volume change as a function of slope angle.

Within a confinement type, an UBCDFLOW regression equation applies only in a particular range of slope angles. Previous research raised concerns that volume change predictions might not be smooth around domain boundaries. The change from one equation to another might make the simulation very sensitive to slope angles.

Eq. type	Flow mode of flow	Regression equation	Range of slope angles
A	UF Deposition	$\ln(-dV_i) = -0.514 - 0.988 \ln(W_{d_i}) - 0.101(BAF_i) - 0.731 \ln(L_i) + 0.0155(TH_i)$	$0 \leq TH_i < 18.5^\circ$
B	UF Entrainment	$\ln(+dV_i) = 1.13 \ln(W_{e_i}) + 0.787 \ln(L_i) - 0.0636 \ln(dV_{i-1})$	$18.5 \leq TH_i < 29.5^\circ$
C	UF Entrainment	$\ln(+dV_i) = 0.728 + 1.31 \ln(W_{e_i}) + 0.742 \ln(L_i) - 0.0464(TH_i)$	$29.5 \leq TH_i < 55^\circ$
D	CF Entrainment	$\ln(+dV_i) = 0.344 + 0.851 \ln(W_{e_i}) + 0.898 \ln(L_i) - 0.0162(TH_i)$	$10.5 \leq TH_i < 55^\circ$
E	TF Deposition	$\ln(-dV_i) = -1.54 \ln(W_{d_i}) - 0.90 \ln(L_i) + 0.123(BAF_i)$	$0 \leq TH_i < 20.5^\circ$

$BAF_i = \cos(dTH_i) \cos(dAZ_i) \ln(\Sigma V_{i-1})$

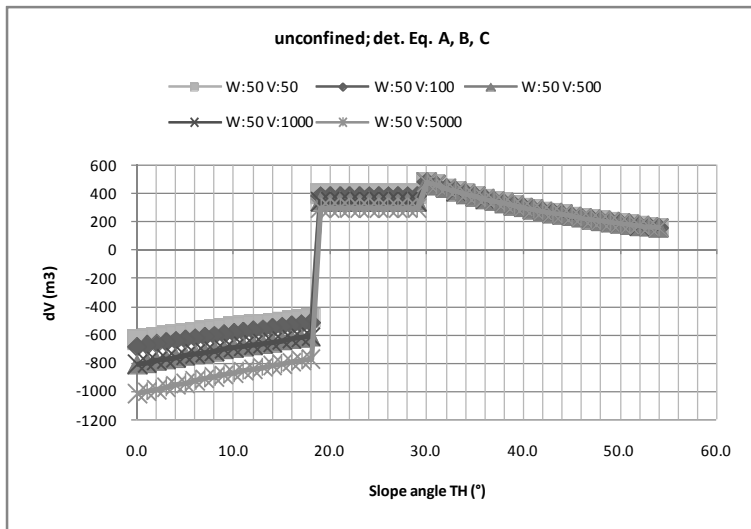
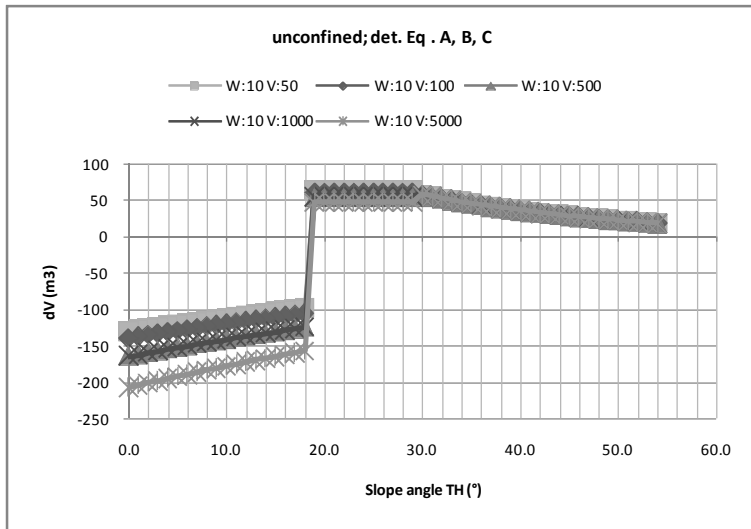
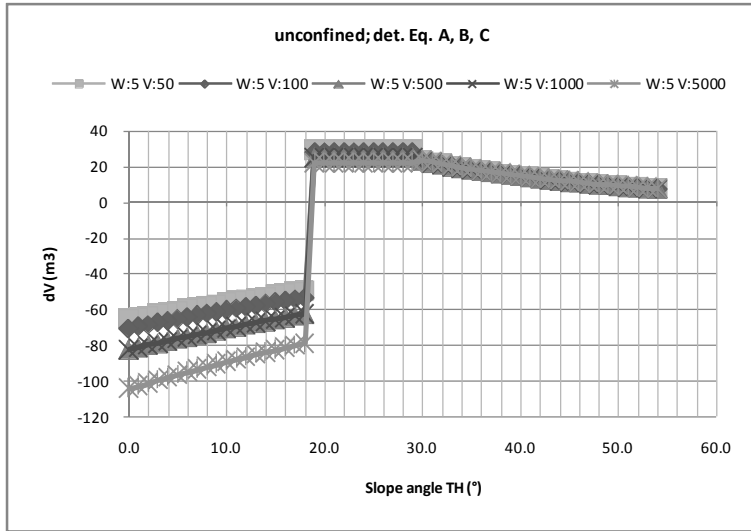
A sensitivity analysis was carried out to quantify the effect of slope angle on the computed volume changes. In order to quantify the UBCDFLOW volume change as a function of the slope angle, volume changes were calculated for virtual reaches. All variables were held constant except for slope angle. The virtual reach had 10m length. The bend angle function was neutralized by assuming a straight inflow direction (i.e. $dAZ_i=0$ and $dTH_i=0$). Incoming volumes (ΣV_{i-1}) were constant at 50, 100, 500 and 5000m³. Widths were constant at 5, 10 and 50m. The sensitivity analysis was performed for all three morphology types.

Analysis of the results showed that sensitive slope angles exist where the volume change calculations are step wise.

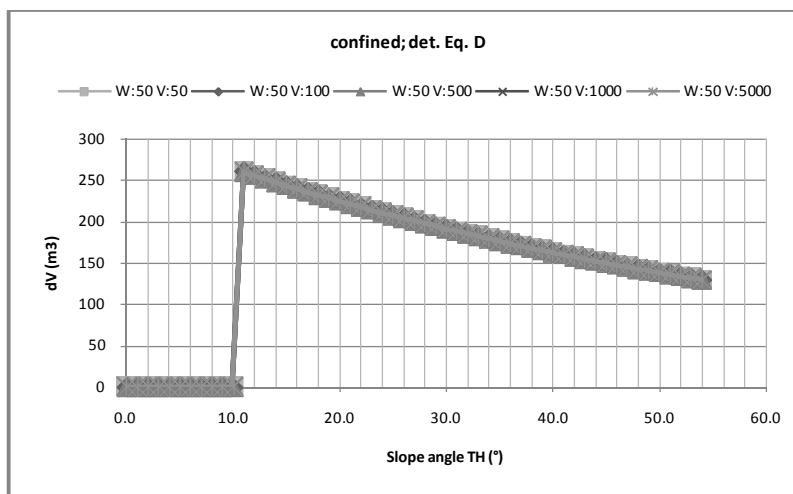
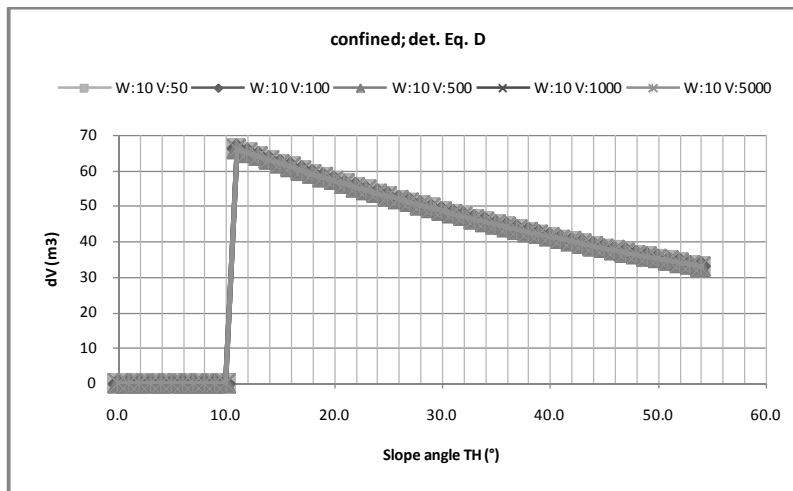
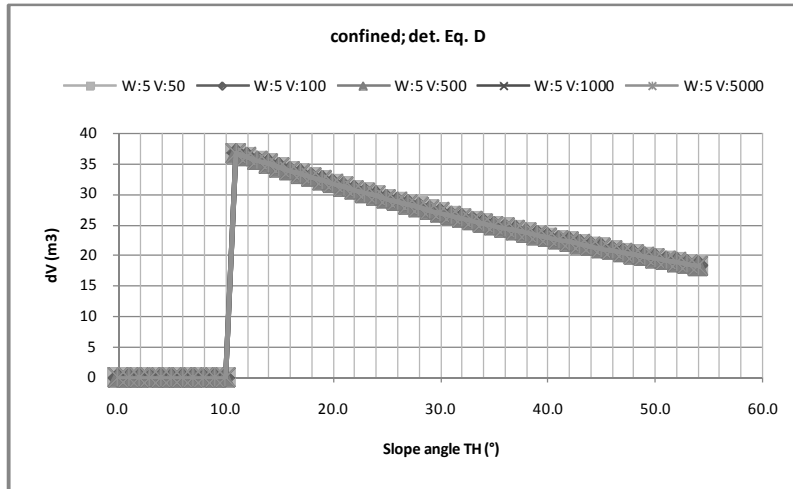
Morphology	Sensitive Slope Angle
Unconfined	18.5° (29.5°)
Confined	10.5°
Transition	20.5°

The following plots further show that magnitude of incoming volume plays a role in deposition of material. For unconfined flow higher inflow volumes result in more deposition. For transition flow higher inflow volumes yield in less deposition. It is also observed that volume change is not linearly related to width.

Unconfined flow sensitivity analysis results for equations A, B, and C



Confined flow sensitivity analysis results for equation D ($dV=0$ for $TH < 10.5^\circ$)



Transition flow sensitivity analysis results for equation E ($dV=0$ for $TH > 20.5^\circ$)

